Exploring Signaling Mechanisms regulating genetic and non-genetic Drug Resistance in Melanoma

PhD Thesis submitted by

Alberto Mattei

from **Onsernone TI**

for the degree of

PhD in Cell Biology

Supervisor
Prof. Dr. Olivier Pertz
Institute of Cell Biology
Faculty of Science of the University of Bern

Co-advisor
Prof. Dr. Mitchell P. Levesque
Department of Dermatology
University of Zürich

Accepted by the Faculty of Medicine, the Faculty of Science and the Vetsuisse Faculty of the University of Bern at the request of the Graduate School for Cellular and Biomedical Sciences

Bern,   Dean of the Faculty of Medicine

Bern,   Dean of the Faculty of Science

Bern,   Dean of the Vetsuisse Faculty Bern

Table of Contents

List of abbreviations

Abbreviation	Explanation
RAS	rat sarcoma
C/N Ratio	cytosolic/nuclear ratio
CDK4	cyclin-dependent kinase 4
CDKN2A	cyclin dependent kinase inhibitor 2A
DUSP	dual specificity phosphatases
ECM	extracellular matrix
EGF	epidermal growth factor
EGFR	epidermal growth factor receptor
EKAR	extracellular signal-regulated kinase activity reporter
ERK	extracellular signal-regulated kinase
FAK	focal adhesion kinase
FGFR	fibroblast growth factor receptors
FRET	Förster resonance energy transfer
GAPs	GTPase-activating proteins
GDP	guanosine diphosphate
GEFs	guanine nucleotide exchange factors
GFP	green fluorescent protein
GPCRs	G-protein-coupled receptors
GRB2	growth factor receptor-bound protein 2
GTP	guanosine triphosphate
HGF	hepatocyte growth factor
IEGs	immediate early genes
IGF-1R	insulin-like growth factor 1 (IGF-1) receptor
INPP4B	inositol polyphosphate 4-phosphatase type II
JNK	c-Jun N-terminal kinase
KD	knockdown
KTR	kinase translocation reporter
MAPK	mitogen-activated protein kinase
MITF	microphthalmia-associated transcription factor
MNKs	mitogen-activated protein kinase (MAPK) interacting protein kinases
mTOR	mechanistic target of rapamycin
NES	nuclear export signal or sequence
NF1	neurofibromatosis type 1
NLS	nuclear localization signal or sequence
OS	overall survival
PAK3	p21 activated kinase 3
pAkt	phosphorylated Akt
PDK1	phosphoinositide-dependent kinase-1

Continued

Abbreviation	Explanation
pERK	phosphorylated ERK
PH domain	pleckstrin homology domain
PHLPP1	PH domain leucine-rich repeat protein phosphatases 1
PI3K	phosphoinositide 3-kinase
PIP$_2$	phosphatidylinositol-biphosphate
PIP3	phosphatidylinositol-triphosphate
PLK4	polo-like kinase 4
PP2A	protein phosphatase 2A
PPPs	phosphoprotein phosphatases
PSPs	protein Serine/Threonine phosphatases
PTEN	phosphatase and tensin homolog
PTPs	protein Tyrosine phosphatases
RAF	rapidly accelerated fibrosarcoma
RFP	red fluorescent protein
ROI	region of interest
RSKs	ribosomal S6 kinases
RTK	receptor tyrosine kinase
SOS	son of sevenless
Src	proto-oncogene c-*Src*
UVR	ultraviolet radiation

Abstract

Melanoma is among the most heterogeneous and aggressive type of cancers. The BRAF^{V600E} mutation, found in over 50% of metastatic melanomas, drives aberrant MAPK-ERK pathway activation and tumor progression. Selective BRAF^{V600E} inhibitors lead to drug resistance and patient relapse in the clinic. A combination of BRAF^{V600E} and MEK inhibition only delays such drug resistance. Additional pro-survival signaling pathways, such as the PI3K-Akt cascade also contribute to tumorigenic progression. Here we use biosensors to study ERK/AKT activity dynamics at the single cell level in primary, patient-derived BRAF^{V600E}, as well as BRAF^{V600E}/NRAS^{Q61K} cells in which the secondary NRAS^{Q61K} mutation emerged upon treatment with a BRAF^{V600E} inhibitor. We find that BRAF^{V600E} cells display sustained ERK activity and Akt activity that fluctuates on timescales of hours. Dabrafenib-mediated BRAF^{V600E} inhibition leads to sustained Akt activity over timescales of hours. BRAF^{V600E}/NRAS^{Q61K} cells displayed both sustained ERK and Akt activity. Elevated Akt activity contributes to survival. We then performed siRNA kinome screens targeting each three oncogenic signaling paradigms. We find that BRAF^{V600E} cells are strongly resistant to kinome perturbations, with only a small number of kinases perturbations leading to decreased ERK activity. Surprisingly, BRAF^{V600E}/NRAS^{Q61K} cells were much more sensitive to kinome perturbations. We speculate that the NRAS^{Q61K} mutation restores RTK inputs and pathway crosstalks to the MAPK network, rendering it sensitive to these additional inputs. We found that the PI3K/Akt network is much more sensitive to kinome perturbations, with perturbation of RTKs, or kinases involved in nutrient sensing or cytoskeletal dynamics being able to inhibit aberrant Akt activity in the different cell systems. Our screens revealed signaling nodes for which drugs were available. Finally, we show that drug-mediated PLK4 or PAK3 inhibition, that were identified in our screens, leads to immediate decrease of aberrant Akt signaling in BRAF^{V600E} inhibited, BRAF^{V600E} cells, or in BRAF^{V600E}/NRAS^{Q61K} cells, implying a signaling crosstalk that involves direct protein interactions. Inhibition of these proteins leads to decreased survival. Our results provide new insights into the mechanisms of non-genetic and genetic origins of drug resistance, and identify new network vulnerabilities to intervene in drug resistance during targeted therapy.

1. Summary

Cutaneous melanoma is among the most heterogeneous and aggressive type of cancer and accounts for 80% of all skin cancer deaths. The RAS/MAPK (mitogen-activated protein kinase)-ERK signaling pathway is upregulated in 98% of melanomas. Under physiological conditions, the three-tiered MAPK cascade transduces extracellular signals from cell surface receptors to intracellular signals that promote cell growth and proliferation. In most cases, extracellular ligands such as growth factors bind and activate receptor tyrosine kinases (RTK) to activate the small GTPase RAS. RAS activation in turn recruits cytosolic serine-threonine RAF kinases (CRAF, BRAF, ARAF) to the membrane, promotes their dimerization and activation. This in turn leads to sequential MEK and ERK activation. A large number of ERK substrates can then enforce fate decisions such as proliferation, motility, death, survival or differentiation. Many ERK substrates are upstream components of the MAPK cascade such as RAF, SOS and other proteins. ERK activity also leads to the transcription of such upstream components such as DUSP and Sprouty proteins. This allows for feedback regulation that controls duration and amplitude of the ERK signaling output, as well as appropriate signal termination that is essential for cellular homeostasis. In the case of melanoma, this cellular homeostasis is often disrupted by a BRAF^{V600E} mutation that constitutively activates ERK and promotes tumor progression. In 2011, the BRAF^{V600E}-specific inhibitor vemurafenib revolutionized melanoma treatment. Despite strong effects in tumor reduction, together with low patient toxicity, vemurafenib-based targeted therapy leads to efficient responses in only ~ 50% of patients. However, in responsive patients drug-resistant tumors appear on a time scale of months. In 70% of melanoma patients that relapses on such targeted therapy, tumor cells reactivate the MAPK pathway via a BRAF-independent MEK activation triggered by a number of different mechanisms. This led to the rationale of combining BRAF^{V600E} inhibitors with MEK inhibitors, which nowadays remains the standard of care for melanomas with BRAF^{V600E} lesions. Unfortunately, short-term non-genetic resistance and acquired genetic resistance to targeted therapy invariably develop. Beside reactivation of the MAPK pathway, MAPK-independent resistance mechanisms that involve alternative signaling pathways e.g. the PI3K/Akt/mTOR signaling pathway also occur.

How cell subpopulations within a tumor rewire their kinome to reactivate aberrant oncogenic signaling during therapy remains poorly understood. We tackled this challenge by exploiting fluorescent biosensors to quantify ERK/Akt activity states in thousands of single living cells. We used patient-derived, primary melanoma cells that harbor a BRAF^{V600E} primary mutation from a drug naïve patient to study non-genetic origin of drug

resistance. We also used cells from a patient that harbored a primary BRAF^{V600E}, but hardwired a secondary NRAS^{Q61K} mutation upon treatment with a BRAF^{V600E}-specific inhibitor. These BRAF^{V600E}/NRAS^{Q61K} cells provide an opportunity to study genetic drug resistance. Our technology offered new insights into the mechanisms of non-genetic and genetic drug resistance. This also enabled us to carry several kinome-wide RNAi screens to identify potentially druggable kinases that contribute to oncogenic ERK and Akt signaling, and thus might provide new possibilities for combination therapies to tackle the problem of drug resistance in melanoma.

First, we show that BRAF^{V600E}-induced ERK activity is aberrantly sustained most likely due to insensitivity to a negative feedback from ERK to RAF in both cell lines. A kinome perturbation screen revealed that the MAPK network displays robustness against genetic perturbations as only 6 kinase knockdowns (KDs) led to loss of ERK activity in BRAF^{V600E} cells. In marked contrast, in BRAF^{V600E}/NRAS^{Q61K} cells we found that KD of 24 kinases, of which 5 were also present for BRAF^{V600E} cells, led to decreased ERK activity. This counterintuitive result, e.g. two mutations in the MAPK network might be more powerful at activating ERK than only one, suggests that the NRAS^{Q61K} mutation restores some signaling inputs and crosstalks to the MAPK cascade, making it more sensitive to perturbations.

Second, we observe heterogeneous single-cell Akt activity states that fluctuate on timescales of hours in BRAF^{V600E} cells, which then switch to sustained Akt activity upon BRAF^{V600E} inhibition with dabrafenib on a timescale of 6-24 hours. In BRAF^{V600E}/NRAS^{Q61K} cells, Akt activity is sustained both in presence and absence of dabrafenib. Sustained Akt activity enhances survival in both non-genetic (dabrafenib-treated BRAF^{V600E} cells), and genetic (BRAF^{V600E}/NRAS^{Q61K} cells) drug resistance cell systems. Kinome screens reveal that PI3K-Akt is much more sensitive than MAPK-ERK signaling to perturbations. KD of proteins that include RTKs, kinases that regulate cytoskeletal dynamics, as well as cellular metabolism can downregulate aberrant Akt signaling, with different kinases being important in BRAF^{V600E} versus BRAF^{V600E}/NRAS^{Q61K} cells. PI3K/Akt signaling is therefore also of central importance in the context of BRAF^{V600E} and NRAS^{Q61K} mutations that are mainly thought to be important for the MAPK pathway. This might involve constitutive activation of the PI3K pathway by NRAS^{Q61K}. The large number of kinases of which loss of function can affect aberrant Akt activity make them strong candidates for combination therapies to tackle drug resistance.

Finally, our kinome screens identify druggable kinases (PLK4 = polo-like kinase 4, and PAK3 = p21 activated kinase 3) that inhibit increased Akt activation upon BRAF^{V600E} inhibition or the secondary NRAS^{Q61K}. These kinases have not been extensively studied with respect to their interaction with the MAPK-ERK and PI3K/Akt pathways. We show that PLK4 or PAK3 inhibition reverts aberrant Akt activity on time scales of minutes, implying a direct crosstalk between PLK4 and PAK3 and oncogenic Akt activity. PLK4 or PAK3 inhibition in combination with dabrafenib decreases cell survival, and thus could provide a therapeutic benefit. This occurs in both BRAF^{V600E}, as well as BRAF^{V600E}/NRAS^{Q61K} cells. However, Akt activity can get activated again to some level in the BRAF^{V600E}/NRAS^{Q61K} cells on timescale of hours, further illustrating the remarkable plasticity of signaling networks, and showing the need of studying non-genetic mechanisms of drug resistance.

In summary, our single-cell measurements of ERK and Akt activities provide new insights into the pathological signaling network states that regulate genetic and non-genetic drug resistance. The ability to explore these signaling networks at scale identifies new vulnerabilities to tackle the problem of resistance to targeted therapy.

2. Introduction

2.1 Melanoma - overview

2.1.1 Incidence and mortality

Cutaneous melanoma is a malignancy that originates from transformed melanocytes and is among the most heterogeneous and aggressive type of cancer. The incidence of melanoma has been rising worldwide in fair-skinned populations over the last decades, and Switzerland registers the third highest incidence rates in the world after Australia and New Zealand[1,2]. In Switzerland, melanoma is the fourth most common cancer with nearly 2450 new diagnoses per year between 2008 and 2012, with deaths that reached an average of 180 men and 130 women per year in the same period[3]. With these numbers, melanoma accounts for 2% of all cancer deaths in our country. Melanoma is prevalently diagnosed in later stages of life for both sexes (Figure 1), with a median age at diagnosis of 67 years for men and 60 for women. Clinically, melanoma ranges between 2 very different clinical extremes. The first case is represented by thin primary lesions that can
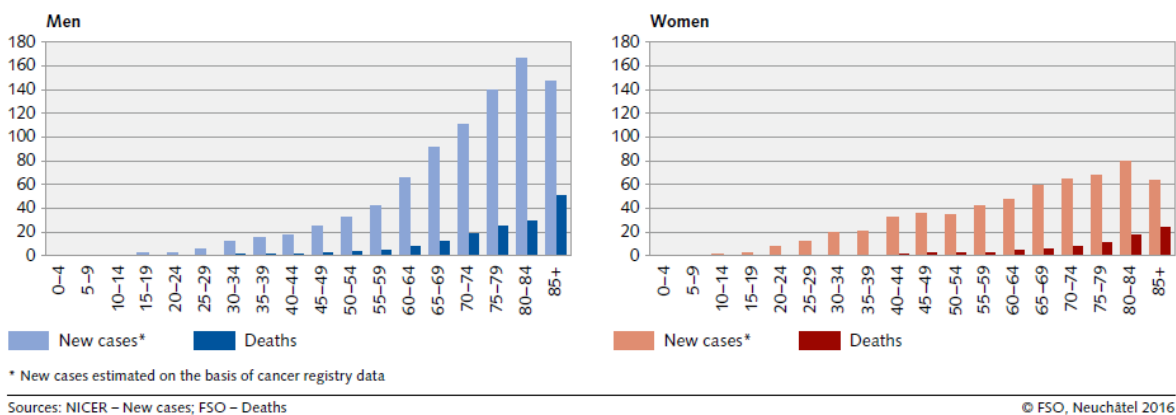
Figure 1 **Age/sex- specific incidence of melanoma per 100'000 inhabitants, 2008-2012.** (NICER)

be treated predominantly by surgical removal. Patients with thin melanomas, defined as being less than 1mm thick, have a high 5-year survival rate that exceeds 99% and that is favored by the increasing awareness in the population, which leads to diagnosis of early-stage diseases with a favorable prognosis. Conversely, the second case is the very aggressive metastatic unresectable melanoma, once considered untreatable, with a 5-year survival rate of ~27% in the US in the period 2010-2016[4]. Of note, melanoma is not

exclusively a skin cancer, but can be found in less than 5% of cases in sites such as the eye, the mucosae, the gastrointestinal tract, the genitourinary system.

2.1.2 Etiology

Within the basal layer of the epidermis, melanocytes have the important function to produce melanin pigments in organelles called melanosomes. Melanosomes are then transferred from melanocytes to neighboring keratinocytes via dendritic processes. The delivered melanin inside the melanosomes absorb ultraviolet radiation (UVR) and function also as potent antioxidants to neutralize UVR-generated free radicals[5], thereby protecting the keratinocytes of the skin from UVR-mediated genotoxic effect. Exposure to UVR is the most important risk factor for cutaneous melanoma; acute, strong, and intermittent exposure to sunlight in youth leads to higher risk of the disease. Sun avoidance when the intensity of UVR reaches its peak (between 10 am and 3 pm), and the use of sunscreens with elevated protection when exposed to strong sunlight, are encouraged. However, indoor tanning, insufficient sunscreen protection, and sun-seeking behaviors are common among young people[6]. Sunbeds among women younger than 40 increased 2.3- to 6-fold the likelihood of developing melanoma, with a stronger relationship among women in their 20s[7]. Sunburns in childhood are associated with the highest risk[8].

The major host risk factors are the number of melanocytic nevi, familiar history and genetic susceptibility[8]. A quarter of melanomas develops from a preexisting nevus and the number of nevi (>25 nevi), their size (> 5mm), and type (dysplastic) are positively correlated with melanoma risk[9,10]. About 5-12% of all melanomas have hereditary causes[11]. The study of families with inherited melanoma showed how mutations in cyclin dependent kinase inhibitor 2A (*CDKN2A*) were the most common genetic abnormalities (~40%), followed by the more rare cyclin-dependent kinase 4 (*CDK4*) mutations[12]. Finally, certain phenotypic traits increase the risk of developing melanoma by approximately 50% e.g. fair skin, light eyes, high freckle density, red hair, inability to tan[13].

2.1.3 Melanoma as a genetic disease

The last two decades have witnessed dramatic progress in understanding the molecular basis of melanoma. In 2002, a systematic genetic screen revealed how the majority of cutaneous melanoma harbors activating *BRAF* mutations[14]. Of these, in more than 85% of cases a point mutation in the *BRAF* gene results in a single amino acid substitution of valine for glutamic acid at the 600 position (*BRAF^V600E* mutation). Beside *BRAF*, activating

mutations in *RAS* genes were found in high proportions, in particular the isoform *NRAS* (20% of melanomas), over *KRAS* (2%) and *HRAS* (1%)[15]. According to the genomic classification of melanoma proposed by the Cancer Genome Atlas network (TCGA), 4 subtypes of melanoma have been defined based on the mutation of *BRAF*, *NRAS*, *NF1*, or none of these, indicated as triple-wild-type subtype[16]. *NF1* is the third most frequently mutated gene (14%) and encodes for the tumor suppressor neurofibromin, a negative regulator of RAS[17]. All three top hotspot mutations result in the activation of the RAS/MAPK (mitogen-activated protein kinase)-ERK signaling pathway, which promotes oncogenic cell growth and proliferation (Figure 2).

Today we know that *BRAF* and *NRAS* mutations are the two most common driver oncogenes in melanomas from intermittently sun-exposed skin. However, 70% to 80% of benign nevi carry the acquired *BRAF* mutation, but the majority of nevi will not turn to melanoma, which underscores the incomplete understanding of the relationship between melanocytic nevi and development of the tumor[18]. This means that while *BRAF* mutations drive melanoma growth and progression, melanomagenesis is a multistep process that involves the cooperation of additional genetic causes. For example, concurrent *BRAF*
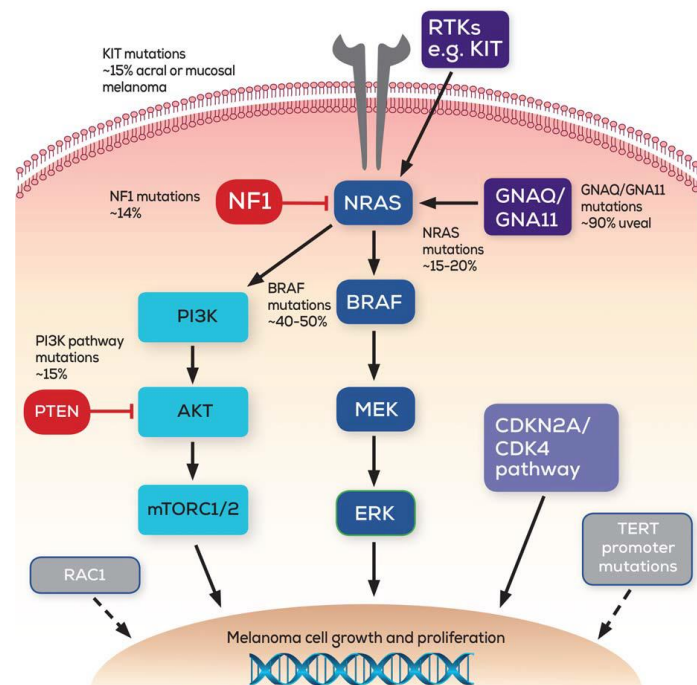

Figure 2 **Schematic of relevant cell signaling pathways and frequency of mutations.** (Davis et. al., 2018)

mutation and *PTEN* inactivating mutations result in melanoma formation in mouse models[19]. PTEN is a critical tumor suppressor in melanoma that negatively regulates the oncogenic phosphatidylinositol 3-kinase (PI3K)/protein kinase B (Akt) signaling pathway. Loss of PTEN function results in the overactivation of the pro-survival Akt pathway and is considered involved in tumor progression rather than in initiation[20].

2.1.4 Clinical therapy

A formal staging of melanoma is required to provide prognostic information. Staging systems are continuously refined upon identification of novel prognostic factors. The earliest stage is 0 (melanoma in situ), with the other stages ranging from I (1) to IV (4). In general, the higher the number, and the more the cancer has spread. Within a stage, subdivisions are made with capital letters (e.g. A, B, etc.) and an earlier letter means a lower stage. Despite high inter-patient variability in cancer-experience, similar stages have similar prognosis and similar associated therapy. According to the widely used staging system called TNM, developed by the American Joint Committee on Cancer (AJCC), three tumor conditions are evaluated for staging. The first condition to evaluate is the primary (main) tumor (T), in particular the thickness via the Breslow measurement, and the ulceration, which is a breakdown of the skin over the melanoma. Melanomas thicker than 1mm have greater chance of spreading, and ulceration worsens the outlook. The second condition to evaluate is the spread to nearby lymph nodes (N), and third the spread to distant sites (M for metastasis).

AJCC Stage	Melanoma Stage Description
0	The cancer is confined to the epidermis, the outermost skin layer (Tis). It has not spread to nearby lymph nodes (N0) or to distant parts of the body (M0). This stage is also known as *melanoma in situ*.
I	The tumor is no more than 2mm thick and might or might not be ulcerated (T1 or T2a). The cancer has not spread to nearby lymph nodes (N0) or to distant parts of the body (M0)
II	The tumor is more than 1 mm thick (T2b or T3) and may be thicker than 4 mm (T4). It might or might not be ulcerated. The cancer has not spread to nearby lymph nodes (N0) or to distant parts of the body (M0).
III (A,B,C,D)	Several subcategories, but characterized by spread to nearby lymph nodes. It has not spread to distant parts of the body (M0).

IV	The tumor can be any thickness and might or might not be ulcerated (any T). The cancer might or might not have spread to nearby lymph nodes (any N). It has spread to distant lymph nodes or to organs such as the lungs, liver or brain (M1).
Source: American Cancer Society	
Table 1 **Staging system of melanoma**	

Clinical therapy of early-stage localized melanoma is mostly surgical and in 80% of the cases is resolutive[21]. Conversely, disseminated stage IV melanoma was once considered untreatable, and chemotherapy with the alkylating agent dacarbazine, FDA-approved in 1975, was associated with partial responses and a historical median overall survival (OS) of 6-9 months from the diagnosis (and an overall 1-year survival of 27%)[22].

2011 was a landmark year for treatment of metastatic melanoma, with the approval of the immunotherapy agent anti-CTLA-4 antibody ipilimumab and the BRAF^{V600E}-specific targeted inhibitor vemurafenib. If the goal of cancer immunotherapy is to stimulate or activate immune responses against tumor cells, targeted therapy focuses in the selective inhibition of the oncogenic drivers of tumor progression. Over the last few years, the combined targeted inhibition of BRAF^{V600E} and its downstream substrate MEK in patients with BRAF(+) metastatic melanoma increased dramatically the median OS of patients over 33 months[23]. Unfortunately, intrinsic (primary) resistance to treatment occurs in 15-20% of melanomas, and acquired (secondary) resistance develops in most cases[24]. An overview of the current treatment options (in 2021) for BRAF(+) and BRAF wildtype melanomas is presented in Figure 3.
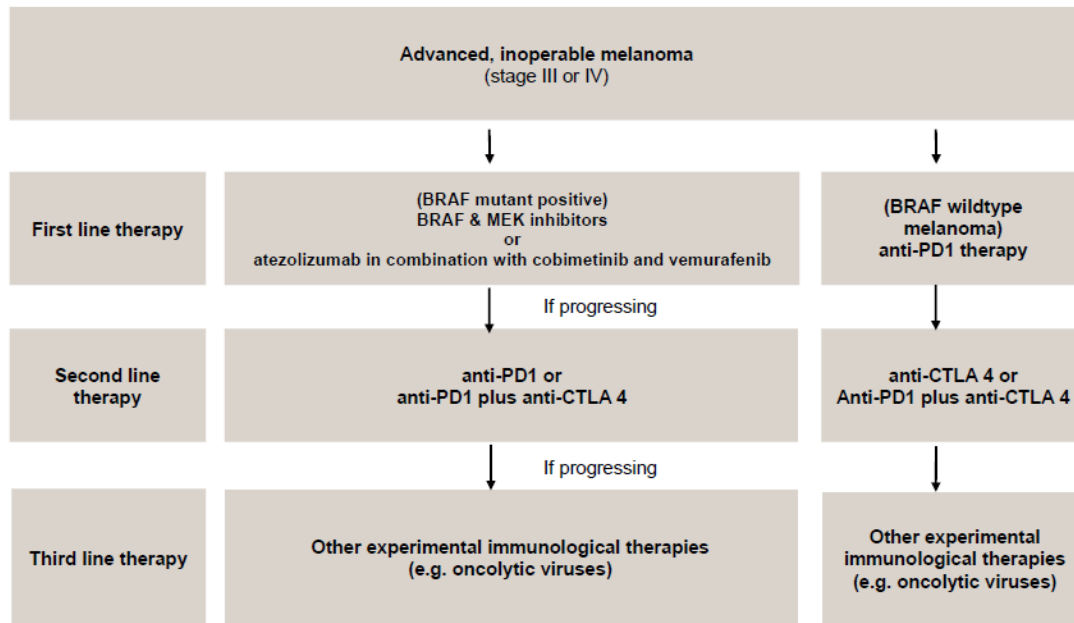
Figure 3 **Current treatment options for BRAF(+) and BRAF wildtype melanoma.**

(Kuryk et al., 2020)[21]

2.2 Cell signaling

2.2.1 Signaling cascades

Every cell has the essential ability to detect the extracellular environment and react in real time to signals from neighboring cells, from the extracellular matrix (ECM), and from other external but also internal sources. Extracellular signals range from physical agents such as temperature, pressure, light, voltage, to chemical agents (e.g. small endogenous or exogenous molecules). Upon detection, physical and chemical signals are transduced by complex cellular machineries, called signaling cascades, and propagated through the cell as a series of molecular events. Typically, such molecular events are protein phosphorylation catalyzed by protein kinases. Finally, signals are relied to downstream effectors which are responsible to generate cellular responses. The whole process is called cell signaling. Importantly, signaling cascades are not linear computing units that process signals only in one direction, but they have mechanisms to control the magnitude

and duration of the processed signals. These control mechanisms can reinforce or attenuate signals, and are termed positive and negative feedbacks, respectively. Signaling cascades can also interact with each other and modulate cellular responses in a coordinated fashion. Among crucial cellular responses, cell growth, proliferation, survival, and motility are particularly relevant in cancer biology. In fact, loss of control mechanisms can lead to aberrant signaling that promotes responses such as tumor initiation, progression, and metastatic dissemination.

2.2.2 Receptor tyrosine kinase signaling

Receptor tyrosine kinases (RTKs) are a subclass of tyrosine kinases that is integrated into the cell membrane and serves as first transducers of extracellular signals to intracellular signals, which are then propagated as a series of molecular events, typically phosphorylation. Of the 90 tyrosine kinases, 58 are RTKs, divided in 20 subfamilies. In general, RTKs are activated by a vast number of different receptor-specific ligands. Mainly, these ligands are secreted growth factors, typically proteins that are released in the extracellular space by neighboring cells and that mediate cell-cell communication. Upon ligand-receptor binding, the receptor dimerizes or oligomerizes, and the resultant conformational change causes trans-autophosphorylation within the dimer, which enables the RTKs to assume an active conformation[25]. The active RTK dimer recruits a variety of downstream proteins to the membrane, which then act as second messengers to initiate a signaling cascade of events that amplifies much fold the small signal first transduced by the ligand-receptor interaction. RTKs can also be activated by mechanosensory inputs mediated by cell-cell contacts and cell-ECM contacts, mainly via interaction with mechano-sensing integrins, which act as cell surface receptors activated by ECM components. RTKs can in turn control the mechano-sensing machinery, e.g. by phosphorylating the core cadherin complex components β-catenin, α-catenin, p120 catenin, or cadherin itself (essential components in mediating cell-cell adhesion), and modulate cell adhesion[26]. Several parallel pathways can be activated downstream of RTKs, most prominently multiple MAPK pathways and the PI3K-Akt pathway.

Given the important role to initiate cell signaling that regulates cellular processes such as growth, motility, metabolism, differentiation, cell death, the level of RTK activity is tightly balanced by several mechanisms, including by tyrosine phosphatases. Under normal physiologic conditions, such control mechanisms are crucial to prevent an aberrant activation of RTK signaling. In cancer, RTK activity is often dysregulated and

consequently the fine balance between cell growth and cell death is disrupted, and oncogenic signaling promotes tumor progression. Briefly, common mechanisms that increase RTK activity in cancer include gain-of-function mutations, overexpression and genomic amplification, chromosomal rearrangements, duplication of the kinase domain, and autocrine activation[25].

2.2.3 MAPK signaling

The mitogen-activated protein kinase (MAPK) cascades are intracellular signal transduction pathways activated by many extracellular signals and that control crucial cellular processes including growth, proliferation, differentiation, motility and apoptosis. Four different mammalian MAPK pathways have been identified and they share the same three-tiered structure that can propagate and amplify many folds the transmitted signal (Figure 4)[27]. The four MAPK pathways are named according to their downstream component: extracellular signal-regulated kinase 1 and 2 (ERK1/2), c-Jun N-terminal kinase (JNK), p38, and ERK5. Their structure is divided in three core kinases termed MAPKKK or MAP3K, MAPKK or MAP2K, and MAPK, that can be additionally complemented by an upstream MAP4K and a downstream MAPKAPK component[27]. Once the MAP3K is activated by upstream events, most of the time RTKs-mediated events, sequential phosphorylation and activation of the sequential kinases propagates the signal. Eventually, the downstream kinase of the MAPK pathway phosphorylates and modulates the activity of hundreds of regulatory proteins that enforce fate decisions such as proliferation, motility, death.

An important feature of the evolutionary conserved three-tiered structure is that it enables signal amplification through the cascade. In fact, concentrations of ligands in the extracellular compartment are often low and if the concentration of a kinase in the cascade is higher than its preceding activator, as previously documented in multiple pathways[28], amplification is achieved. Another crucial feature of the three-tiered structure is that it enables multiple opportunities for regulatory inputs to modulate, via negative and positive feedbacks, the overall activity output of the pathway. Of importance, the four MAPK pathways react to distinct, but overlapping, upstream signals, and enforce partially overlapping fate decisions. Growth factors for example can activate all MAPK cascades, but if ERKs react mainly to mitogenic stimuli, JNK and p38 react to stress stimuli from the environment. Similarly, the four MAPK pathways promote proliferation or differentiation, but if ERK is the only one associated with cell migration, JNK and p38 can instead
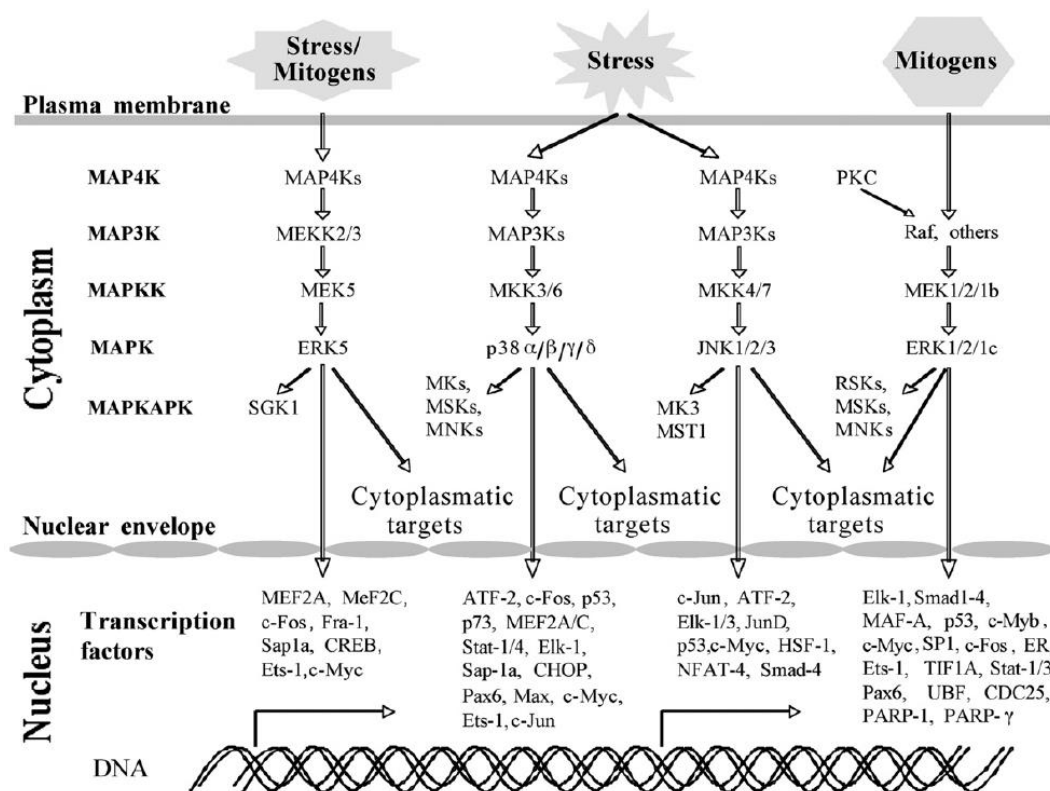
Figure 4 **Schematic representation of the MAPK cascades and their downstream targets.** The indicated stimulants are not exhaustive. (Plotnikov et al., 2011)[27]

promote inflammation or apoptosis[29]. Particularly in focus in this thesis, the ERK cascade is introduced in more detail in the next section.

2.2.4 The RAS-RAF-MEK-ERK/MAPK pathway

The ERK1/2 cascade was the first MAPK pathway elucidated and represents a prototype MAPK[27]. Under physiological conditions, ERK cascade transduces extracellular signals from cell surface receptors to intracellular signals that promote cell growth and proliferation. In most cases, extracellular ligands such as growth factors bind and activate receptor tyrosine kinases (RTK). Active RTKs (mostly dimers) recruit the adaptor protein GRB2 (growth factor receptor-bound protein 2), which then associate with SOS (son of sevenless) that has guanine nucleotide exchange (GEF) activity towards RAS. The small GTPase RAS is therefore induced by SOS to exchange its GDP with GTP, and the

resultant active membrane-localized RAS-GTP recruits the MAP3K tier of the cascade, namely the cytosolic serine-threonine RAF kinases (CRAF, BRAF, ARAF), to the membrane, and promotes their dimerization and activation with a mechanism not fully understood. This in turn leads to sequential MEK and ERK activation. Finally, the amplified signal continues to the MAPKAPK components (RSKs, MNKs and MSKs), and to a large number of ERK substrates which can then enforce fate decisions. Currently, as many as 200 substrates of ERK are identified[30]. Illustrative ERK targets that can affect cell fate are transcription factors such as Elk1, c-Fos, and c-Myc, or the potent pro-apoptotic protein BIM (found to be inhibited upon phosphorylation by several member of the MAPKs[31]). Importantly, ERK substrates can be located in the cytoplasm, in the nucleus, or in other organelles, and for ERK to exerts nuclear functions such as activation of transcription factors, or chromatin remodeling to enable transcription, a nuclear translocation is essential[27].

ERK-mediated transcriptional regulation occurs on several different timescales, but a hallmark of the response to mitogens is the rapid induction, within minutes after ERK activation, of many mRNAs of the so-called immediate early genes (IEGs), termed like this because they do not necessitate preceding *de novo* protein synthesis for their expression[29]. ERK rapidly phosphorylates Elk-1, one of the main regulators of IEGs[32], which in turn can induce IEGs like c-Fos, important for cellular processes such as proliferation and differentiation. Resting cells do not express the small protein c-Fos and, upon Elk1-mediated activation, c-Fos concentration rapidly increases. To stabilize c-Fos, otherwise rapidly degraded, phosphorylation by nuclear ERK and downstream RSKs is a crucial event. Additional IEGs like c-Myc and Fra1 seem to be stabilized by ERK1/2 phosphorylation[33]. As ERK regulates a myriad of downstream targets involved in many crucial cellular processes, the fine tuning of the specific cell fate caused by a stimulant might occur via integration of signals from other signaling pathways and, as explained in section 2.2.6, via decoding of signaling dynamics of the transduced signal.

2.2.5 The PI3K-Akt pathway

The highly conserved PI3K-Akt pathway is present in all cells of higher eukaryotes and is crucial to promote survival and growth in response to extracellular signals such as growth factors, cytokines, hormones, and other cellular stimuli[34]. Of importance, this pathway has been found activated in over 20% of melanoma patients that relapsed after targeted therapy against MAPK/ERK pathway, and therefore is the second most attractive target

in melanoma[35,16,36,37]. As for the RAS-RAF-MEK-ERK pathway, extracellular ligands bind and activate cell surface receptors, namely RTKs or G-protein-coupled receptors (GPCR), leading to recruitment and activation at the plasma membrane of one or more isoforms of the class I PI3K (phosphoinositide 3-kinase) family (Figure 5). In addition to RTKs and GPCRs, the third way to activate class I PI3Ks is via Ras-related GTPases[38]. At the membrane, and within seconds to minutes of growth factor stimulation, class I PI3K catalyses the phosphorylation of the inositol lipid PIP_2, mainly $P4,5P_2$ (phosphatidylinositol-4,5-biphosphate), to generate $P3,4,5P_3$, a PIP_3 inositol lipid[38]. Common in all PI3K effectors is a pleckstrin homology (PH) domain selective for $P3,4,5P_3$ and/or $P3,4P_2$. PIP_3 is therefore able to recruit specific proteins like Akt to the membrane via the PH domain. Several different families of PI3K effectors, such as serine/threonine kinases of the AGC family, guanine nucleotide exchange factors (GEFs), and GTPase-activating proteins (GAPs), control distinct enzymatic or signaling functions[39], underscoring the extremely pleiotropic effects that results from PI3K activation. As for the Akt sub-family of AGC kinases (Akt1, Akt2, Akt3), also the Akt activator PDK1 (phosphoinositide-dependent kinase-1) is recruited to the membrane via PH domain[38]. In close proximity at the membrane, the constitutively activated PDK1 phosphorylates the Akt activation loop (Thr 308 on Akt1), thereby activating Akt. To reach maximal activation however, Akt requires phosphorylation of Ser 473. The most important Akt S473 kinase is the mechanistic target of rapamycin (mTOR) complex 2 (mTORC2)[40]. After a peak in Akt activity generally in the first hour, signal termination is achieved primarily by the phosphatase PTEN, which dephosphorylates PIP_3 to PIP_2. Not discussed here, an additional way of recruiting Akt and PDK1 is via $PI3,4P_2$, which is then dephosphorylated by the phosphatase INPP4B. Beside PTEN, PP2A (protein phosphatase 2A) and PHLPP1/PHLPP2 (PH domain leucine-rich repeat protein phosphatases 1/2) can dephosphorylate the Akt residues T308 and S473 respectively, and terminate Akt signaling.

Over 100 AKT substrates have been reported in literature, with a wide repertoire of downstream effects e.g. cell survival, growth, proliferation, cell migration, angiogenesis, glucose metabolism.
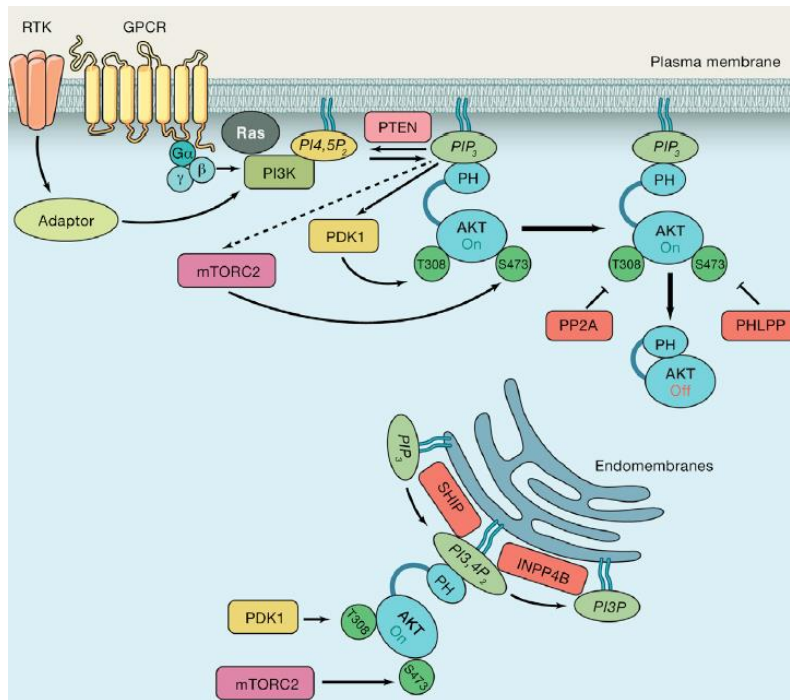
Figure 5 **Molecular mechanisms of Akt regulation.**

From Manning and Toker, 2017: Stimulation of RTKs or GPCRs leads to activation of PI3K, leading to PIP3 production at the plasma membrane. Cytosolic inactive AKT is recruited to the membrane and engages PIP3 through PH domain binding. This leads to phosphorylation of T308 and S473 by PDK1 and mTORC2, respectively, resulting in full activation. Signal termination is achieved by the PIP_3 phosphatase PTEN and the PP2A and PHLPP protein phosphatases. A separate endomembrane pool of active AKT likely exists that is activated through engagement of $PI3,4P_2$ through the action of the SHIP phosphatase and terminated by INPP4B. (Manning and Toker, 2017)[38].

2.2.6 Signaling dynamics

Cell fate decision results from the complex interplay of a relatively limited set of signaling mechanisms. Extracellular input signals are received by membrane receptors that can activate multiple downstream signaling cascades at the same time, and each cascade transduces the signal to effectors that in turn can promote specific or overlapping cellular processes. It is not obvious how every cell can enforce specific cell fates with the use of limited machineries and in noisy environments in which exposure to multiple input signals often occurs. Moreover, intrinsic cellular noise due to different expression of proteins,

21

different morphology, different cell-cycle stage, and many other factors, results in a considerable intercellular heterogeneity of responses even within isogenic cell populations, as demonstrated by recent single-cell analysis studies. The identity of the input signal is not sufficient to provide specific instructions, so that other mechanisms must be present to denoise the signal and enforce a cell fate decision.

The observation that many genetic and signaling circuits display spontaneous dynamic behaviour (pulsing) in the activity of key regulators and effectors provoked a series of fundamental questions on whether pulsatile behaviour carries information, how pulsatile behaviour is generated and regulated, and which cellular functions pulsing might enable. Today, pulsatile activity has been shown for many signaling pathways, including ERK pathway, which displays signaling dynamics in response to growth factors. The concept of signaling dynamics suggests that the topology of the signaling pathway, beyond the linear structure of the sequential core components, enables the cell to process different external signals and to internally represent their properties such as the identity, amplitude (concentration), and timing. Signaling pathways are now seen as complex machineries that, upon stimulation with an input signal, can regulate the signal transduction by the mean of positive and negative feedbacks on multiple levels. Such feedbacks can be mediated by the core components, but also from downstream effectors, and allow for complex modulation of the amplitude and duration of the target protein activity. Of importance, multi-level signalling network not only allows to incorporate positive and negative feedbacks, but also allows for additional regulation by integrating signals from other pathways via crosstalk connections.

Many ERK substrates are upstream components of the ERK cascade such as RAF, SOS and other proteins (Figure 6A). ERK activity also leads to the transcription of upstream regulatory components such as DUSP and Sprouty proteins. This allows for feedback regulation that controls the dynamics of ERK signaling output, as well as appropriate signal termination that is essential for cellular homeostasis (Figure 6B). Every cell then integrates ERK signaling dynamics together with signaling dynamics of all the active pathways. The resulting decoded information and the basal phenotype of the cell (due to intrinsic cellular noise) determine the cell fate (Figure 6C). Hence, dynamic signal processing greatly expands the capabilities of signaling pathways[41] to encode information and ultimately to specify a specific cell response.

Decades of research with traditional population-averaged assays such as Western Blot made it very difficult to observe unsynchronized pulsing of signals in cells, but recent
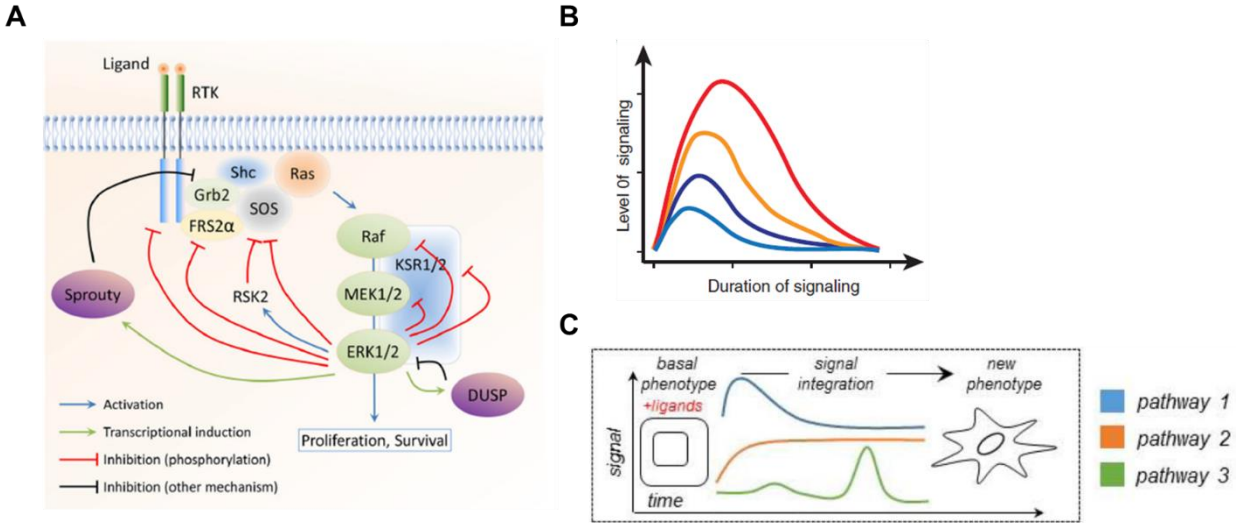
Figure 6 **Signaling dynamics are translated into a cell fate decision.** (A) Negative feedback regulation of the ERK pathway. Many negative feedback loops within the ERK pathway modulate ERK output activity. Direct phosphorylation by ERK and transcriptionally induced feedback regulators are indicated (Lake et al., 2016)[42]. (B) Pathway negative feedbacks convert different level of signaling intensity into distinct durations of pathway activity (Sagner and Briscoe, 2017)[43]. (C) Cell fate decision is a function of the basal phenotype of the cell and the integration of all the signaling dynamics from the activated pathways (Day et al., 2016)[44].

advances in live cell and in single-cell biosensor imaging for the quantitative exploration of biological processes enabled the investigation of signaling dynamics in individual living cells. Details on the single-cell imaging technology used in the present thesis can be found in section 2.3.4.

2.3 Targeted therapy

2.3.1 Current situation

As introduced in section 2.1, the three most common mutated proteins in melanoma, namely BRAF, NRAS, and NF1, result in the aberrant activation of ERK pathway, a central step in melanoma pathogenesis[45]. Indeed, the RAS/MAPK (mitogen-activated protein kinase)-ERK signaling pathway is upregulated in 98% of melanomas. Under physiological conditions, ERK is responsible for upstream negative feedbacks that control duration and

magnitude of the growth signaling output of the pathway[46], thus ensuring cellular homeostasis. In over 50% of metastatic melanomas, this cellular homeostasis is disrupted by a BRAF[V600E] mutation that constitutively activates ERK and promotes tumor progression. In 2011, the BRAF[V600E]-specific inhibitor vemurafenib revolutionized melanoma treatment. Despite strong effects in tumor reduction, together with low patient toxicity, vemurafenib-based targeted therapy leads to efficient responses in only ~ 50% of patients. Additionally, in responsive patients drug-resistant tumors appear on a timescale of months. In 70% of melanoma patients that relapses on such targeted therapy, tumor cells reactivate ERK pathway via a BRAF-independent MEK activation triggered by a number of different mechanisms. This led to the rationale of combining BRAF[V600E] inhibitors with MEK inhibitors, which nowadays remains the standard of care for melanomas with BRAF[V600E] lesions. Over the last few years, the combined targeted inhibition of BRAF and MEK in patients with BRAF(+) metastatic melanoma increased dramatically the median overall survival (OS) of patients from the historical 6-9 months (classical chemotherapy with dacarbazine) to 33.6 months[23]. From 2013 to 2016, mortality rate for metastatic melanoma dropped by a striking 17.9% (due to targeted therapy and immunotherapy), an unprecedented result in cancer medicine[47]. Unfortunately, short-term non-genetic resistance and acquired genetic resistance to targeted therapy invariably develop.

2.3.2 Non-genetic resistance to targeted therapy

Non-genetic mechanisms of resistance enable subpopulations of drug-sensitive melanoma cells to first evade drug-mediated cytotoxicity and proliferate again. Such mechanisms act on timescales of hours/days, and during the first weeks of targeted therapy they enable resistant cells to survive, to be selected, and to cause a tumor relapse. In later stages of the targeted therapy, non-genetic resistance can be hard-wired by the acquisition of a genetic mutation that lock cells back to a permanent oncogenic signaling state that is refractory to drugs.

In over 70% of BRAFi-treated melanomas that relapses, tumor cells reactivate MAPK pathway via a BRAF-independent MEK activation triggered by a plethora of different mechanisms[35], of which 37% occurs in a RAS-dependent manner[36]. Upon BRAF[V600E] inhibition, ERK activity sharply decreases and ERK-mediated upstream negative feedbacks to RTKs are relieved[48]. As a consequence, RTK-ligand-induced signaling becomes again an important activator of ERK pathway by promoting a RAS-dependent

activation of MEK that is BRAF-independent. Additionally, overexpression of *NRAS* or RTKs genes reinforces this mechanism. The BRAF-independency is achieved by the activation of different RAF proteins. A switch from BRAF^{V600E}-monomer autonomous signaling to a RAS-mediated CRAF dimer signaling has been long established as a mechanism of drug resistance[49]. Restricted literature showed also an intrinsic flexible switch from BRAF to ARAF[50], or mutations in ARAF[51], to mediate BRAFi resistance. Moreover, subpopulations of resistant cells were recently shown to escape the drug-induced cell-cycle arrest via pulsatile reactivation of MAPK pathway driven by RTKs-induced RAS activity[52].

Known resistance mechanisms mediated by MAPK reactivation are mostly cell-autonomous, but non-cell autonomous resistance mechanisms have been described. The complicated interplay of cancer cells with the tumor microenvironment modulated by stromal cells, in particular fibroblasts and macrophages, was shown to promote BRAFi resistance[53,54,55]. In particular, a spheroid model of subcutaneous tumor pieces embedded in collagen matrix exhibited adaptive tolerance to BRAFi via pulsatile reactivation of ERK activity within 12 hours from drug addition. This tolerance was caused by melanoma associated fibroblasts (MAFs) that remodeled the matrix, which in turn activated the integrin β1-FAK-Src signaling axis in melanoma cells and this reactivated ERK pathway[56]. Another short-term mechanism of resistance mediated by the tumor microenvironment involves the secretion of hepatocyte growth factor (HGF) by stromal cells. HGF leads to activation of MET, a receptor for HGF, which in turn can reactivate MAPK/ERK and PI3K/Akt thus promoting BRAF^{V600E} inhibition resistance[53].

MITF (microphthalmia-associated transcription factor) is a melanocytic lineage-specific transcription factor considered the master regulator of melanocyte development, function and survival[57]. In the last decade, the function of MITF was tightly connected to the phenotype switching ability of melanoma cells, which enables cells to reversibly switch between different cellular states, namely a proliferative, more epithelial, drug-sensitive phenotype, and an invasive, more mesenchymal, drug-resistant phenotype[58]. High MITF protein levels have been associated to the proliferative phenotype, while low MITF levels to the invasive one. This plasticity is suspected to enable a program of adaptive mechanisms that ultimately results in enhanced cell survival independent of MAPK pathway activation[59]. Although both extremely high levels and low levels of MITF have been shown to contribute to therapeutic resistance, this non-genetic MITF-centric resistance model does not provide any obvious drug target[60].

2.3.2 Genetic resistance to targeted therapy

Tumors are heterogeneous collection of cells that exhibit distinct phenotypic and molecular features, and that differ regarding their genomes, transcriptomes, epigenomes, proteomes, but also their motility, metabolism and their potential for angiogenesis, metastasis and other processes[61]. All these differences evolve over time and under targeted therapy treatment. The vast intratumor heterogeneity and intertumor heterogeneity within metastasis in a patient represent a major challenge in clinical therapy as the same drug regimen almost never works on all tumor cells. Conversely, drugs exert selective pressure on cells that are intrinsically resistant or that acquire resistance, a situation that creates the molecular basis for tumor relapse. Intrinsic resistance is clinically characterized by the lack of objective response to therapy, while acquired resistance arises after an initial period of drug efficacy. Genetic factors are an undeniable contributor of both intrinsic and acquired resistance, depending on whether mutations arose before or during treatment. Many genetic mechanisms of resistance have been described in melanoma, which are not exhaustively summarized in Figure 7.

Upon BRAF inhibition, genetic mechanisms that reactivate MAPK/ERK pathway often involve activating mutations in the NRAS protein or loss of NF1, a negative regulator of RAS. Of importance, RAS can activate not only the RAS-RAF-MEK-ERK axis, but also the PI3K/Akt pathway downstream of receptor tyrosine kinase (RTK) receptors such as IGF-R, FGFR or MET. The RAS-PI3K-AKT axis can limit the cytotoxicity mediated by RAF inhibition.[62,63] Moreover, genetic alterations of core components of this pathway (e.g. AKT1, AKT3, PIK3CA), of important phosphatase regulators (PHLPP1, PTEN), and alterations of the expression level of several receptor tyrosine kinases (RTKs) have been found in resistant melanomas.[64] At the level of RAFs, BRAF gene amplification, BRAF truncations resulting from alternative splicing, and CRAF overexpression, have been all reported to reactivate ERK pathway[35]. Furthermore, increased ERK activity might result from activating mutations of MEK itself or its additional activators, COT1 kinase (encoded by the *MAP3K8* gene)[35,65]. Finally, additional genetic deregulation of the tumor suppressor *CDKN2A*, that is able to induce cell growth arrest and senescence through INK4A/ARF[66], of the cell-cycle regulator CDK4, of Cyclin D1, might also lead to BRAF inhibition resistance.
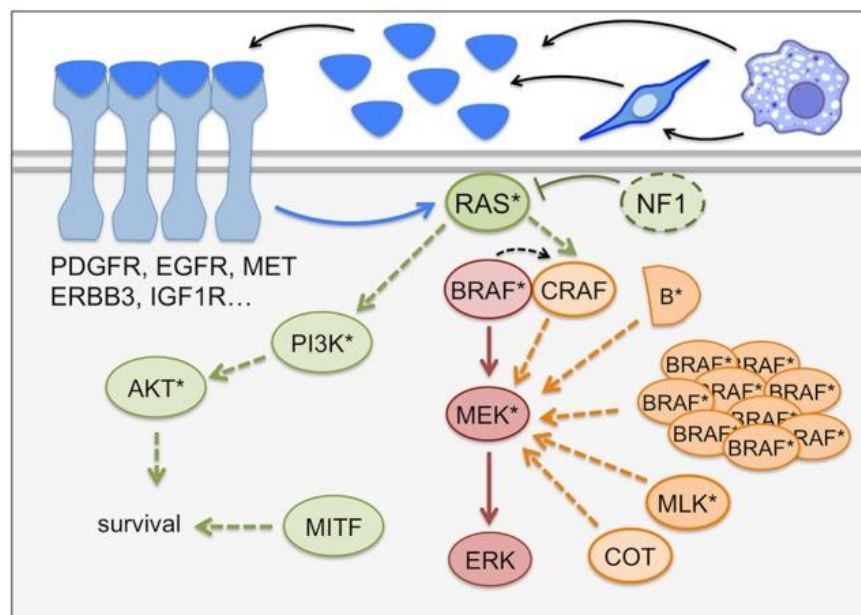
Figure 7 **Genetic mechanisms of resistance to BRAF inhibition.** Overexpression or mutations of the proteins RAS, BRAF, CRAF, MEK or its activators COT and MLK, can result in resistance to BRAF inhibitors. RTK-induced RAS-dependent reactivation of ERK pathway or the alternative PI3K-Akt pathway leads to enhanced tumor survival. Many ligands can induce RTKs activation, including HGF secreted by stromal cells (fibroblasts, macrophages) (Arozarena and Wellbrock, 2017)[35].

2.3.4 ERK-KTR and Akt-KTR biosensors

The complex intratumor and intertumor heterogeneity of melanoma remains a poorly understood reservoir of drug-refractory subpopulations of cells. As more and more studies demonstrated that signal transduction dynamics encode information and might determine cell fates[41,67,68], it became urgent the need to profile individual cells within tumors to understand how intrinsic drug resistance emerges in subpopulations of previously drug-naïve cells. Signaling dynamics have passed undetected with population-averaged assays such as Western Blot, but recent advances in live cell and in single-cell biosensor imaging for the quantitative exploration of biological processes enabled the investigation of signaling dynamics in individual living cells. Genetically-encoded fluorescent biosensors can be stably expressed in cells and allow for image-based quantification of the target kinase activity with high temporal resolution and in individual cells.

In 2008, the Förster resonance energy transfer (FRET) phenomenon was exploited to build the first widely used FRET-based ERK biosensor termed extracellular signal-regulated kinase activity reporter (EKAR). EKAR consists of 4 main elements: a donor fluorophore (green fluorescent protein GFP in its first implementation), an acceptor fluorophore (red fluorescent protein RFP), a substrate phosphorylation peptide from Cdc25C containing the consensus MAPK target sequence (PRTP), and the proline-directed WW phospho-binding domain[69]. Active ERK phosphorylates the substrate sequence, which is then bound by the WW phospho-binding domain (Figure 8A). The resulting conformational rearrangement brings into close proximity the two fluorophores and FRET phenomenon is observed: upon excitation with light, the donor fluorophore transfers energy to the acceptor fluorophores through a non-radiative process, thus shifting the emission profiles of the two fluorophores. The ratio, called FRET ratio, between the fluorescent intensity of the acceptor RFP over the donor GFP is then used as a proxy for ERK activity. Figure 8B shows ERK activity kinetics upon EGF stimulation at various concentrations. Phosphatases can finally revert the FRET sensor to its original conformation. Over the years several improvements increased specificity and dynamic
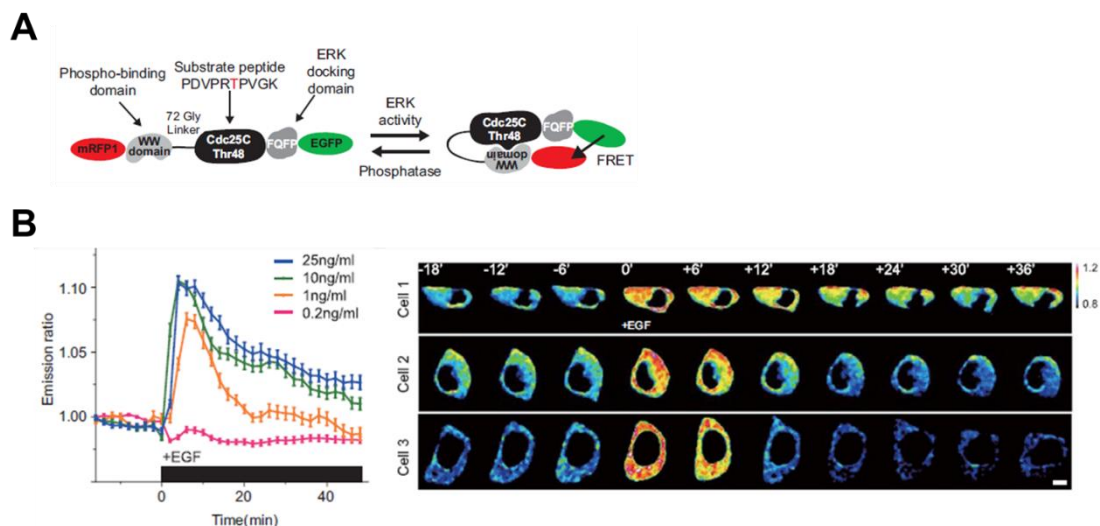
Figure 8 **EKAR biosensor.** (A) Schematic of the original EKAR (Harvey et al., 2008)[69]. (B) Average ERK activity kinetics measured by FRET ratio upon different EGF stimulations in a population of HEK293 cells stably expressing a modified version of EKAR. Stimuli introduced at 0′ (Ryu et al., 2018)[70]. (C) Three representative time series of cell from a single field of view. Each cell experienced ERK excitation by EGF stimulation, with diverse decaying kinetics (Ryu et al., 2018).

range of the EKAR sensor. The possibility to monitor kinase activity in single individual living cells led to exciting discoveries also in the cancer biology field. Successful use of FRET biosensors in intravital microscopy revealed a pervasive heterogeneity of ERK activity in melanoma cells of a tumor model in mice. ERK reactivation in single cells upon BRAF inhibition was then observed in vivo.[56] The same group also showed how a spheroid model of subcutaneous tumor pieces embedded in collagen matrix exhibited non-genetic adaptive tolerance to BRAFi via pulsatile reactivation of ERK activity within 12 hours from drug addition[56].

Recently, subpopulations of resistant melanoma cells were shown to escape the drug-induced cell-cycle arrest via pulsatile reactivation of MAPK pathway driven by RTKs-induced RAS activity[52]. This observation was enabled by a more recent ERK biosensor termed ERK-KTR[71]. The fluorescent ERK kinase translocation reporter (ERK KTR) was developed in 2014 and translates ERK kinase activity into a nucleo-cytoplasmic relocalization event of the biosensor. Active ERK recognizes the KTR sensor by utilizing a conserved docking site of a specific endogenous substrate (Elk1). Located in the nucleus at rest, the reporter translocates to the cytosol upon ERK phosphorylation on specific phosphorylation sites within NLS and NES sequences (Figure 9A-B). Dephosphorylation by phosphatases causes the biosensor to return into the nucleus. Hence, proxy for the kinase activity of ERK is the cellular localization of the fluorescent KTR sensor. Advantages of the KTR technology over FRET technology include the direct visual appreciation of changes in the target kinase activity without the need for prior image processing, increased dynamic range, but also the use of only one fluorophore that enables multiplexed fluorescent imaging (instead of the two fluorophores used by FRET sensors). KTR technology is generalizable to other kinases[72], with successful implementation of JNK-KTR, p38-KTR, and also an Akt-KTR. Akt-FoxO3A-KTR[73] was developed from the transcription factor and substrate of Akt FoxO3a. Same as in KTR technology, FoxO3a has a naturally occurring arrangement of NLS, NES, and phosphorylation sites of Akt in the central portion of Foxo3a. Like KTRs, FoxO3a shuttles between the nucleus and the cytosol upon Akt phosphorylation. A truncated version of FoxO3a (the first 1-402 aminoacids), fused with GFP and modified with a mutation in a key residue to eliminate the transcriptional activity of FoxO3a, displayed clear functionality in reporting Akt activity. These new technologies led to the realization that signaling dynamics encode information that cells use to determine cell fate. Thus, investigating single cell kinase activities with high temporal resolution becomes an essential tool to

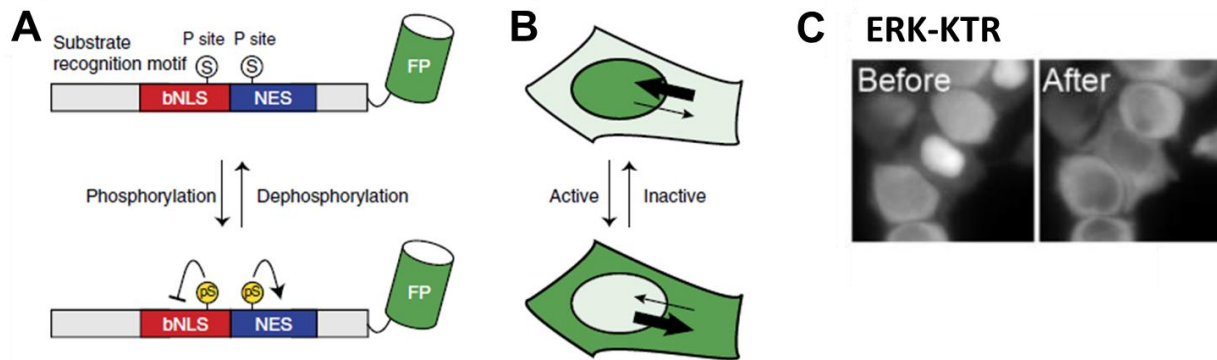Figure 9 **Schematic of KTR biosensors.** (A,B) Phosphorylation and dephosphorylation of P sites within bNLS and NES sites lead to nuclear-cytoplasmic shuttling (Kudo et al., 2018)[74]. (C) EGF-induced activation of ERK leads to phosphorylation of ERK-KTR and its relocation to the cytosol (Maryu et al., 2018)[75].

unravel the complexity of signal interpretation.

3.Hypothesis and Aim of the Thesis

The BRAF^{V600E} mutation is found in over 50% of metastatic melanomas. The consequent aberrant activation of the MAPK-ERK pathway drives tumor progression. Nowadays, the standard of care for melanomas with BRAF^{V600E} lesions is a combination therapy with a BRAF^{V600E} inhibitor and a MEK inhibitor. Unfortunately, short-term non-genetic resistance and acquired genetic resistance to targeted therapy invariably develop. In 70% of melanomas, these resistance mechanisms involve the reactivation of the MAPK pathway, and in the remaining cases involve the compensatory activation of alternative signaling pathways, such as the PI3K/Akt/mTOR signaling pathway.

Here, we analyze ERK/Akt activities in thousands of individual cells of a drug naïve versus a relapsed patient. We hypothesize that quantification of single cell ERK/Akt activities might provide insights on the aberrant evolution of drug-resistant signaling states. We used patient-derived, primary melanoma cells that harbor a BRAF^{V600E} primary mutation from a drug naïve patient to study non-genetic origin of drug resistance. We also used cells from a patient that harbored a primary BRAF^{V600E}, but hardwired a secondary NRAS Q61K mutation upon treatment with a BRAF^{V600E}-specific inhibitor. These BRAF^{V600E}/NRAS^{Q61K} cells provide an opportunity to study genetic drug resistance. We further hypothesize that aberrant signaling states associated to oncogenic growth in our cell models in absence or in presence of BRAF^{V600E} inhibition are promoted by the activity of hidden kinases in the context of a network of unknown crosstalks between signaling pathways. Such kinases that contribute to oncogenic ERK and Akt signaling might be druggable, which in turn might provide new possibilities for combination therapies to tackle the problem of drug resistance in melanoma. We aim to identify these hidden players in oncogenic signaling with an unbiased systemic approach: a kinome-wide RNAi screen that exploits our high-throughput technology. We finally aim to revert oncogenic signaling with novel combination therapies that target BRAF^{V600E} and the identified putative drug targets.

4.Main Results

Manuscript: **Exploring Signaling Mechanisms regulating genetic and non-genetic Drug Resistance in Melanoma**

In preparation

Contribution:

I am the lead author of this publication. I designed the study and the experiments together with O. Pertz. The RNAi screen expertise was provided by B. Neumann. I performed all the experiments and imaging. I performed all image analysis and data analysis, including of the RNAi screens. I prepared all figures. In the present form, I wrote all the manuscript with inputs from O. Pertz. In the next few months, O. Pertz and I are going to re-elaborate the manuscript for submission.

Exploring Signaling Mechanisms regulating genetic and non-genetic Drug Resistance in Melanoma

Alberto Mattei [1], Maciej Dobrzyński [1], Beate Neumann [2], Mitchell P. Levesque [3], Olivier Pertz [1,4*]

[1] Institute of Cell Biology, University of Bern, Baltzerstrasse 4, 3012 Bern, Switzerland

[2] EMBL Heidelberg, Meyerhofstrasse 1, 69117 Heidelberg, Germany

[3] Department of Dermatology, University of Zurich Hospital, Gloriastrasse 31, 8091 Zurich, Switzerland

[4] Lead contact

*Correspondence: olivier.pertz@izb.unibe.ch

ABSTRACT

Melanoma is among the most heterogeneous and aggressive type of cancers. The $BRAF^{V600E}$ mutation, found in over 50% of melanomas, drives aberrant MAPK-ERK pathway activation and tumor progression. Selective $BRAF^{V600E}$ inhibitors lead to drug resistance and patient relapse in the clinic. A combination of $BRAF^{V600E}$ and MEK inhibition only delays such drug resistance. Additional pro-survival signaling pathways, such as the PI3K-Akt cascade also contributes to tumorigenic progression. Here we use biosensors to study ERK/AKT activity dynamics at the single cell level in primary, patient-derived $BRAF^{V600E}$, as well as $BRAF^{V600E}/NRAS^{Q61K}$ cells in which the secondary $NRAS^{Q61K}$ mutation emerged upon treatment with a $BRAF^{V600E}$ inhibitor. We find that $BRAF^{V600E}$ cells display sustained ERK activity and Akt activity that fluctuates on timescales of hours. Dabrafenib-mediated $BRAF^{V600E}$ inhibition leads to sustained Akt activity over timescales of hours. $BRAF^{V600E}/NRAS^{Q61K}$ cells displayed both sustained ERK and Akt activity. Elevated Akt activity contributes to survival. We then performed siRNA kinome screens targeting each three oncogenic signaling paradigms. We find that $BRAF^{V600E}$ cells are strongly resistant to kinome perturbations, with only a small number of kinases perturbations leading to decreased ERK activity. Surprisingly, $BRAF^{V600E}/NRAS^{Q61K}$ were much more sensitive to kinome perturbations. We speculate that the $NRAS^{Q61K}$ mutations restores RTK inputs and pathway crosstalks to the MAPK network, rendering it sensitive to these additional inputs. We found that the PI3K/Akt network is much more sensitive to kinome perturbations, with perturbation of RTKs, or kinases involved in nutrient sensing or cytoskeletal dynamics being able to inhibit aberrant Akt activity in the different cell systems. Our screens revealed signaling nodes for which drugs were available. Finally, we show that drug-mediated PLK4 or PAK3 inhibition, that were identified in our screens, leads to immediate decrease of aberrant Akt signaling in $BRAF^{V600E}$ inhibited, $BRAF^{V600E}$ cells, or in $BRAF^{V600E}/NRAS^{Q61K}$ cells, implying a signaling crosstalk that involves direct protein interactions. Inhibition of these proteins leads to decreased survival. Our results provide new insights into the

mechanisms of non-genetic and genetic origins of drug resistance, and identify new network vulnerabilities to intervene in drug resistance during targeted therapy.

INTRODUCTION

Cutaneous melanoma is among the most heterogeneous and aggressive type of cancer. In melanoma, the RAS/MAPK (mitogen-activated protein kinase)-ERK signaling pathway is upregulated in 98% of the cases[1]. Under physiological conditions, the three-tiered ERK cascade transduces extracellular signals from cell surface receptors to intracellular signals that promote cell growth and proliferation. Several ligand-activated receptors, in particular growth factors activated receptor tyrosine kinases (RTK), participate in activating RAS (HRAS, KRAS, and NRAS) at the plasma membrane. In turn, the active RAS recruits cytosolic serine-threonine RAF kinases (CRAF, BRAF, ARAF) to the plasma membrane and promotes their dimerization and their catalytic activity[2]. This in turn leads to sequential MEK and ERK activation. A large number of ERK substrates can then enforce fate decisions such as proliferation, motility, death, survival or differentiation. Many ERK substrates are upstream components of the MAPK cascade such as RAF, SOS and other proteins. ERK activity also leads to the transcription of such upstream components such as DUSP and Sprouty proteins. This allows for feedback regulation that controls duration and amplitude of the ERK signaling output, as well as appropriate signal termination that is essential for cellular homeostasis. In more than 50% of melanomas, this cellular homeostasis is disrupted by a BRAF^{V600E} mutation that constitutively activates ERK and promotes tumor progression.

Over the last few years, the combined targeted inhibition of BRAF and MEK in patients with BRAF(+) metastatic melanoma increased dramatically the median overall survival (OS) of patients from the historical 6-9 months (classical chemotherapy) to 33.6 months[3]. Unfortunately, intrinsic (primary) resistance to treatment occurs in 15-20% of melanomas, and acquired (secondary) resistance develops in most of the cases[4]. In over 70% of BRAFi-treated melanomas that relapse, tumor cells reactivate MAPK pathway via a BRAF-independent MEK activation triggered by a plethora of different mechanisms[5], of which 37% occurs in a RAS-dependent manner[6]. RAS-dependent activation of MEK that is BRAF-independent stems from the activation of a different RAF protein. Upon BRAF inhibition, a switch from BRAF^{V600E-}monomer autonomous signaling to a RAS-mediated CRAF dimer signaling reactivates MAPK pathway and has been long established as a mechanism of drug resistance[7]. Restricted literature showed also an intrinsic flexible switch from BRAF to ARAF[8], or mutations in ARAF[9], to mediate BRAFi resistance. Recently, subpopulations of resistant cells were shown to escape the drug-induced cell-cycle arrest via pulsatile reactivation of MAPK pathway driven by RTKs-induced RAS activity[10].

Beside reactivation of MAPK pathway, MAPK-independent resistance mechanisms converge in the activation of alternative signaling pathways[6]. The pro-survival phosphatidylinositol 3-kinase

(PI3K)/AKT/mammalian target of the rapamycin (mTOR) signaling pathway is activated in over 20% of relapsed patients and therefore is the second most attractive target in melanoma[5,11,6,12]. Of importance, RAS does not only activate the RAS-RAF-MEK-ERK axis, but also the PI3K/Akt pathway downstream of receptor tyrosine kinases (RTKs) such as IGF-R, FGFR or MET. The RAS-PI3K-Akt axis can limit the cytotoxicity mediated by RAF inhibition[13,14]. Moreover, genetic alterations of core components of this pathway (e.g. RAS, AKT1, AKT3, PIK3CA), of important phosphatase regulators (PHLPP1, PTEN), and alterations of the expression level of several receptor tyrosine kinases (RTKs) have been found in resistant melanomas[15].

Despite the intense effort to elucidate the molecular events that underpin the onset of early drug resistance, the complex intratumor heterogeneity of melanoma remains a poorly understood reservoir of drug-refractory subpopulations of cells[16]. To tackle this complexity, single cell omic technologies are now an invaluable tool to investigate melanoma development and progression in single subclones[17,18]. Signaling activity is then inferred from gene expression data, an approach that however disregards the effect of intrinsic cellular noise (e.g. cellular metabolism, cell morphology, stochastic gene expression) which might promote aberrant signaling dynamics invisible to omic technologies. As more and more studies demonstrated that signal transduction dynamics encode information and might determine cell fates[19,20,21], it became urgent the need to profile individual cells within tumors to understand how intrinsic drug resistance emerges in subpopulations of previously drug-naïve cells. To date however, signaling dynamics that mediate intrinsic drug-refractory states in resistant subclones continue to elude us. Recently, advances in live cell and in single-cell biosensor imaging for the quantitative exploration of biological processes enabled the investigation of signaling dynamics in individual living cells.

Here, we analyze ERK/Akt activities in thousands of individual cells of a drug naïve versus a relapsed patient. We hypothesized that quantification of single cell ERK/Akt activities might provide insights on the aberrant evolution of drug-resistant signaling states.

To address this hypothesis, we used two primary patient-derived melanoma cell lines that are low passage, and that have been exome-sequenced and previously characterized[22]. Therefore, cells should have drifted less than common melanoma cell lines used in cell culture. Both M000921 and MM121224 cell lines harbor the BRAF[V600E] mutation. However, only in MM121224 a secondary NRAS[Q61K] mutation emerged after 4 months of targeted therapy of the patient with LGX818 (BRAFi). The two lines were genetically engineered to express both an ERK and an Akt fluorescent biosensor to report on ERK/Akt activities in living cells[23,24]. Remarkably, we showed that both cell lines exhibited sustained ERK activity. Interestingly, M000921 cells showed a heterogenous Akt activity that was homogeneously activated upon BRAF inhibition to increase pro-survival signals in a timescale of 6-24 hours. Conversely, MM121224 cells always showed a sustained

Akt activity. Our data suggest that the activation of Akt pathway mitigated the cytotoxicity of BRAF inhibition in our paradigm of non-genetic vs genetic drug resistance.

To tackle the challenge of reverting these aberrant signaling states in untreated and treated cells, we then hypothesized that loss of function kinome-wide siRNA screens might identify network vulnerabilities that lead to ERK and/or Akt inhibition. We found multiple kinases knockdowns that led to loss of ERK, Akt, or ERK/Akt activities. We finally showed that PLK4 and PAK3 share direct crosstalks with Akt network and that concomitant BRAF[V600E] and PLK4 or PAK3 inhibition provided additional cytotoxicity compared to BRAF[V600E] inhibition alone.

RESULTS

BRAF[V600E] vs. BRAF[V600E]/NRAS[Q61K] melanoma cells both exhibit sustained ERK activity, but a heterogeneous vs. sustained Akt activity, respectively.

To investigate melanoma-associated signaling states that fuel drug resistance, we first chose two primary patient-derived melanoma cell lines that are low passage and that have been previously characterized, exome-sequenced and extensively described before[22,25]. The M000921 cell line carries a BRAF[V600E] mutation and was isolated from a drug naïve patient. The MM121224 cell line harbors a BRAF[V600E] mutation and a secondary NRAS[Q61K] mutation that emerged in a subclonal population of cells isolated from a metastasis of a patient after 4 months of treatment with a BRAF inhibitor (LGX818) (Figure 1A). From now on we refer to these cell lines as BRAF[V600E] and BRAF[V600E]/NRAS[Q61K], respectively. BRAF[V600E] cells were reported to have a proliferative phenotype sensitive to BRAF inhibition, whereas BRAF[V600E]/NRAS[Q61K] cells showed a drug resistant phenotype[25]. Such secondary NRAS mutations are a prevalent cause of RAF inhibition resistance able to reactivate MAPK pathway in the context of polyclonal intratumor and intertumor heterogeneity[6,26]. At first glance, it can seem unintuitive that a NRAS mutation emerges in response to BRAF[V600E] drug treatment as NRAS is itself activating RAF proteins. Nevertheless, upon BRAF inhibition ARAF and CRAF isoforms are activated in a RAS-dependent manner and their increased activity has been shown to convey resistance. Furthermore, another logic behind a NRAS mutation might be the consequent activation of a parallel pathway, as RAS proteins are known activators of the RAS-PI3K-Akt axis. We speculate that BRAF[V600E] drug resistance in BRAF[V600E]/NRAS[Q61K] cells involved either of ERK or Akt pathway.

To monitor ERK/Akt signals in real-time, we stably transfected cells with two fluorescent biosensors that report on ERK and Akt activities (Figure 1B). These two biosensors, termed ERK-KTR[27] and Akt-KTR[28] (Kinase Translocation Reporter), tagged with mScarlet[29] and mNeonGreen[30] respectively, natively reside in the nucleus. Then, their cognate kinase recognizes the KTR sensor by utilizing a conserved docking site

of specific endogenous substrates (Elk1 for ERK and FoxO3a for Akt); upon ERK/Akt phosphorylation on specific phosphorylation sites within NLS and NES sequences, the reporters translocate to the cytosol. In particular, Akt-FoxO3A-KTR[28] was developed from the transcription factor and substrate of Akt FoxO3a. Same as in the synthetic KTR technology first developed to report ERK activity, FoxO3a has a naturally occurring arrangement of NLS, NES, and phosphorylation sites of Akt in the central portion of Foxo3a. As ERK-KTR, FoxO3a shuttles between the nucleus and the cytosol upon Akt phosphorylation. A truncated version of FoxO3a (the first 1-402 amino acids), fused with a fluorescent protein and modified with a mutation in a key residue to eliminate the transcriptional activity of FoxO3a, displayed clear functionality in reporting Akt activity. Dephosphorylation by phosphatases cause the biosensors to return into the nucleus. Hence, proxy for the kinase activity of ERK and Akt is the cellular localization of their respective KTR sensors.

Not surprisingly, we found that both starved cell lines had high ERK activity in most of the cells (Figure 1C), as evidenced by the cytosolic localization of the KTR reporter. A hyperactive ERK activity results from the BRAF V600E mutation[31]. Interestingly, BRAF^{V600E} cells showed heterogeneous localization of the Akt biosensor, which reflects heterogeneous Akt activities. Surprisingly instead, BRAF^{V600E}/NRAS^{Q61K} cells had high Akt activity in all cells. The two cell lines also displayed different morphologies: BRAF^{V600E} cells displayed a highly spread phenotype, while BRAF^{V600E}/NRAS^{Q61K} cells were much smaller and exhibited a spindly, highly prolonged shape. To validate our biosensor system, we used MEK and Akt inhibition. We observed that ERK and Akt biosensors relocated to the cytosol in an inhibitor specific manner, which could be quantified by decreased C/N ratios (Figure 1E-F). Quantification of steady-state untreated cells (Figure 1C) also confirmed the similarly high ERK activity phenotype between the two cell lines and the different Akt activity phenotype (Figure 1D). To extract ERK/Akt activities in single cells, we developed an automated image analysis pipeline that segments and tracks nuclei by exploiting the nuclear marker histone 2B (H2B)-miRFP703[32]. The pipeline then segments the cytosols and extracts cytosolic/nuclear fluorescence intensities ratios (C/N) of the biosensors that quantify ERK/Akt activities. Quantified steady-state signals confirmed the key difference in Akt activity between the two cell lines (Figure 1D). Moreover, normalized dose-response curves for two MEK inhibitors (U0126 and Cobimetinib; Figure 1G), and one Akt inhibitor (Figure S1B), resulted in similar results for biosensor measurements and phospho ERK (pERK) and phospho Akt (pAkt) immunostaining in the same cells. Specificity of the immunostaining of active pERK and active pAkt Ser473 was demonstrated upon MEK/Akt inhibition in BRAF^{V600E} cells not expressing the biosensors (Figure S1A). Finally, normalized dose-response curves of the allosteric Akt inhibitor MK2206 as extracted from KTR data or immunostaining data showed similar results (Figure S1B). We then used timelapse imaging to measure single-cell ERK and Akt activity dynamics over a period of about 24 hours. We observed sustained ERK activity during this period in both cell lines. In BRAF^{V600E} we observed

fluctuating levels of Akt activity that switched on and off on timescales of one to multiple hours (Figure 2A). This explains the heterogeneity of Akt activity levels at steady-state. In marked contrast, BRAF[V600E]/NRAS[Q61K] cells exhibited sustained Akt activity (Figure 2B). Thus, drug-tolerance that a secondary concomitant NRAS mutation provides in melanoma subclones might not be exerted exclusively via the reactivation of ERK pathway but also, at least in part, via activation of PI3K pathway. We then also quantified the migration speed of the cells (Figure S2D, upper panel) and we found a >50% higher velocity (µm/minute) in BRAF[V600E]/NRAS[Q61K] cells compared to BRAF[V600E] cells. This is consistent with previous studies that identified oncogenic RAS to promote cell motility in a PI3K/Akt- and PI3K-Rac1-dependent manner via remodeling of the cytoskeleton dynamics[33,34,35,36]. Akt inhibition decreased migration speed in both cell lines (Figure S2D, lower panel).
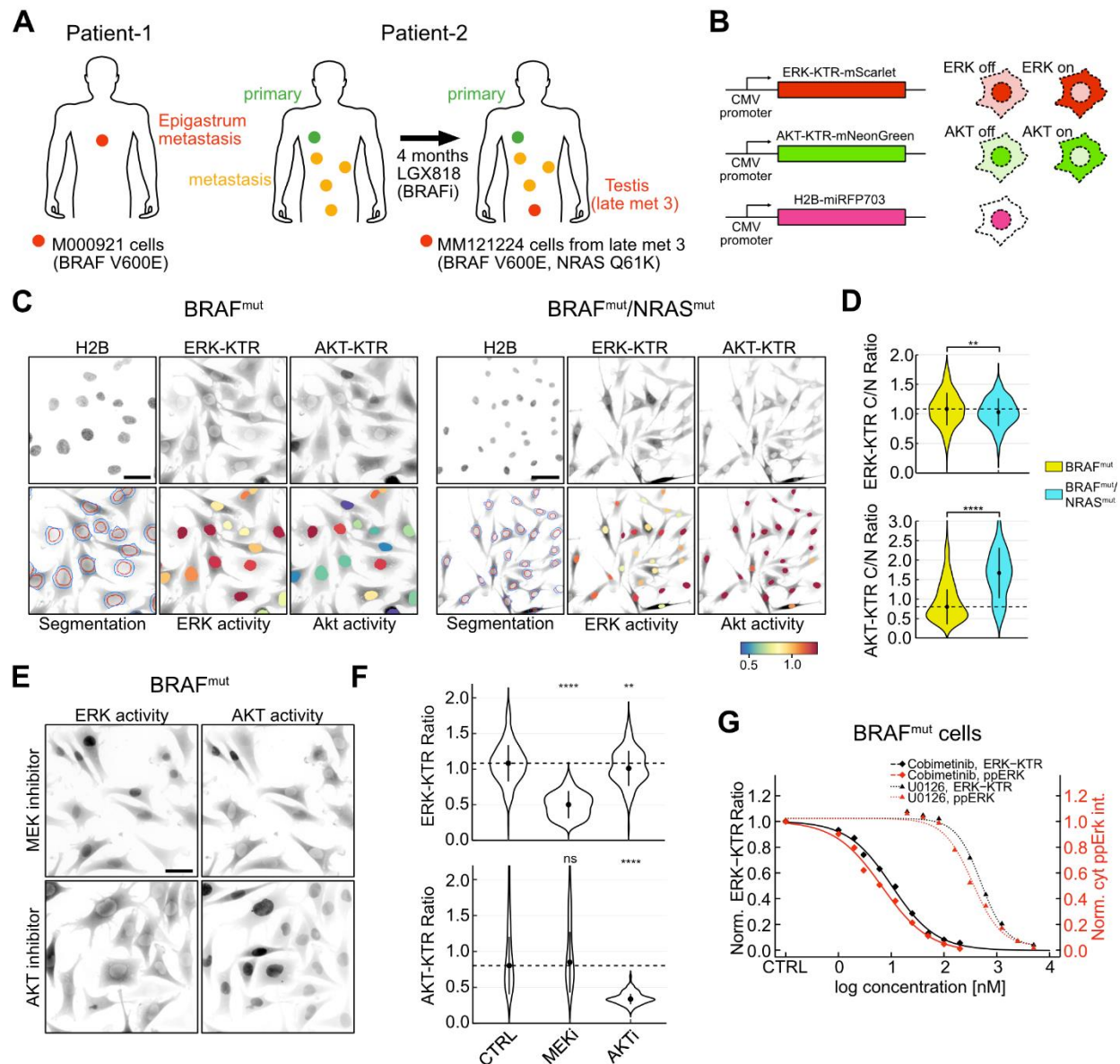
Figure 1 Validation of ERK/ Akt biosensor system in patient-derived melanoma cells. **(A)** Description of the two patient-derived cell lines used in our study. **(B)** Description of the multiplexed biosensor system to visualize ERK/ Akt activities. The genetically-encoded, stably-expressed ERK-KTR-mScarlet and Akt-KTR-mNeonGreen biosensors translocate from nucleus into cytosol upon phosphorylation-mediated activation by ERK or Akt respectively. H2B-miRFP703 is used for nuclear segmentation and tracking. Quantification of a ratio of fluorescence intensities in a cytosolic region of interest (ROI) over a nuclear ROI (C/N Ratio) serves as proxy for ERK/Akt activities. **(C)** Upper rows: Representative micrographs of ERK and Akt-KTR signals as well as H2B signals in starved BRAF[V600E]

and BRAF^{V600E}/NRAS^{Q61K} cells. Lower rows: segmentations used to compute C/N ratios as well as activity color-coded nuclei of ERK/ Akt C/N ratios. Note color scale bar for C/N ratios. Scale bar = 50 µm. **(D)** Violin plots that show ERK/Akt C/N ratios in starved single cell BRAF^{V600E} and BRAF^{V600E}/NRAS^{Q61K} cells. **(E)** Representative micrographs of ERK and Akt-KTR signals in starved BRAF^{V600E} cells in presence of Akt or MEK inhibition after 1 hour of treatment. **(F)** Violin plot of ERK and Akt C/N ratios in presence of Akt or MEK inhibition after 1 hour of treatment in BRAF^{V600E} cells. **(G)** Dose-response curves of two MEK inhibitors as fitted from biosensor measurements (black lines) and from average cytosolic intensities of pERK immunostaining data (red lines) measured in the same BRAF^{V600E} cells. Data were min-max normalized between the 3rd quartile of inhibited cells (value= 0) and the median of the control (value=1). Symbols indicate median values. **(D,G)** The black dot and bar represent the median and the interquartile range, respectively. N=200 obs per group. Significance was obtained with a non-parametric Mann-Whitney U test. *, P <0.05; ****, P < 0.0001.

Sustained Akt activity fuels non-genetic resistance to BRAF inhibition in BRAF[V600E] cells and genetic resistance in BRAF[V600E]/NRAS[Q61K] cells.

Beside genetic factors that contribute to drug tolerance, which have been extensively studied, short-term non-genetic drug resistance, often occurring in a subset of cells, have been more recently documented[37,38,39]. These have been shown to occur within hours/days of BRAF[V600E] inhibition, and mainly involve reactivation of the MAPK pathway. We did not observe ERK reactivation upon dabrafenib-mediated BRAF[V600E] inhibition in both BRAF[V600E] and BRAF[V600E]/NRAS[Q61K] cells, or with cobimetinib-mediated MEK inhibition, as shown also with representative single-cell trajectories (Figure 2C and Figure S2A-B). Remarkably, however, BRAF[V600E] inhibition led to an upshoot of Akt activity on a timescale of multiple hours at the population average level. At the single-cell level, this involved a transition from a fluctuating regime to a sustained regime of Akt activity (Figure S2E). MEK inhibition led to a milder Akt upshoot that tended to decrease after 24 hours. The sustained Akt activity of BRAF[V600E]/NRAS[Q61K] cells observed in absence of BRAF[V600E] inhibition was not affected by BRAF/MEK inhibition. We further verified that the BRAFi-triggered Akt upshoot in BRAF[V600E] cells was dose-dependent (Figure 2D) and reverted by MK2206-mediated Akt inhibition (Figure 2E). Immunostaining of pAkt Ser473 in cells not expressing biosensors validated the BRAFi-mediated Akt upshoot but not MEKi-mediated upshoot, possibly due to the reduced dynamic range of immunostaining to detect MEKi-mediated mild Akt upshoot after 24 hours of incubation (Figure S2F). We therefore focused on the BRAFi-mediated Akt upshoot.

BRAF[V600E] inhibition in BRAF[V600E] cells leads to rapid increase in Akt activity on timescales that involve signaling network rewiring. To test the hypothesis that the Akt upshoot increases survival, we tested the effect of BRAF[V600E], Akt inhibitors, and their combination, and evaluated cell survival. More specifically, we scored remaining cells after 72 hours of incubation. To fine tune this analysis, we developed an image analysis pipeline to recognize nuclei from living cells from nuclear debris from dead cells (Figure 2F, Figure S2G). We found that concomitant inhibition of BRAF and Akt in BRAF[V600E] cells decreased viability compared to inhibition of BRAF alone (Figure 2F). Of great interest, BRAF inhibition showed limited cytotoxicity in BRAF[V600E]/NRAS[Q61K] cells compared to BRAF[V600E] cells, as previously reported[22]. Yet, simultaneous BRAF and Akt inhibition reverted this resistant phenotype and reduced viability by more than 50% when dabrafenib was used at concentrations close to saturation of the ERK inhibition response (2-4 μM) (Figure 2F-G). Taken together, these findings provide evidence for the pro-survival role of Akt pathway in the rapid drug-induced intrinsic resistance in BRAF[V600E] cells, and in the acquired resistance in BRAF[V600E]/NRAS[Q61K] cells. Combined BRAF[V600E] and Akt inhibition is therefore a valid combination strategy to shut down survival signaling in both models of non-genetic (BRAF[V600E]) and genetic drug resistance (BRAF[V600E]/NRAS[Q61K]).
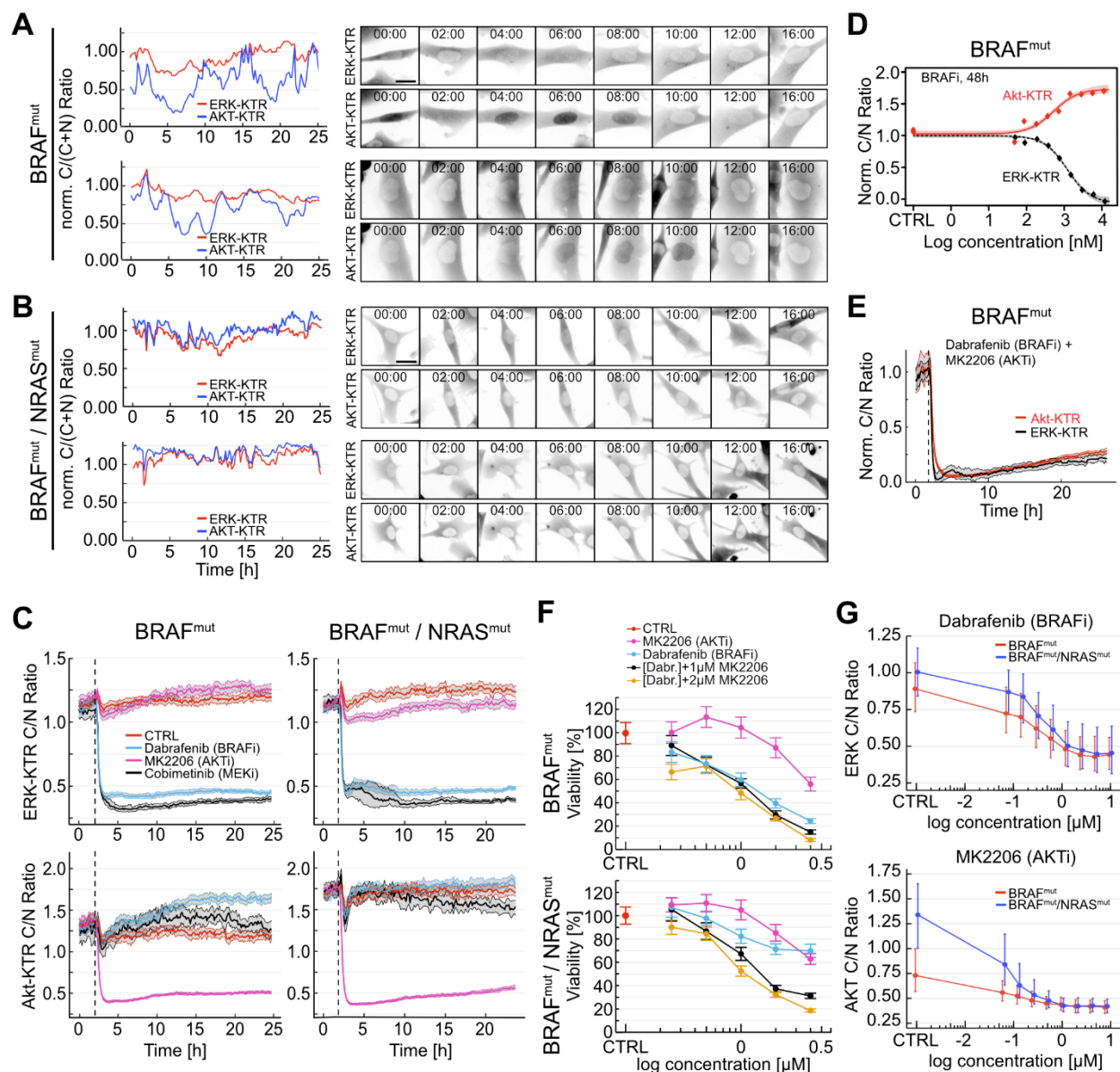
Figure 2 BRAF inhibition leads to compensatory Akt activation on timescales of hours leading to survival in BRAF^V600E cells. (A,B) Representative single-cell trajectories of ERK/Akt activities measured by min-max normalized cytosolic/(cytosolic+nuclear) fluorescence ratio of ERK/Akt biosensors in starved BRAF^V600E cells (A, left) and BRAF^V600E/NRAS^Q61K cells (B, left). C/(C+N) ratio avoids biased visual overestimation of the fluctuations of conventional C/N ratios when cells have very high activities (details in Methods). Both ERK and Akt-KTR C/N ratios are min-max normalized between a lower bound that corresponds to a maximal inhibition of BRAF^V600E cells (value= 0) and the median activity of all the BRAF^V600E cells (value = 1; n > 200 cells). Time-lapse micrographs (right) relative to the trajectories shown on the left are shown. T: hours:minutes ; scale bar = 25 μm. **(C)** Population medians of ERK and

Akt-KTR C/N ratios are shown for the indicated drugs. **(D)** Dose-response of normalized ERK activity inhibition and Akt activity upregulation in response to Dabrafenib (BRAFi) after 48 hours in fixed BRAF^{V600E} cells. Colored areas indicate the 95% confidence interval of the median. **(E)** Population medians of ERK and Akt-KTR C/N ratios are shown for the combination treatment of 4 µM Dabrafenib (BRAFi) and 2 µM MK2206 (Akti). **(F)** Viability measured as % of living cells in treatment response to indicated drugs against living cells in the control after 72 hours of drug incubation in BRAF^{V600E} cells (upper) and BRAF^{V600E}/NRAS^{Q61K} cells (lower). Viable cells were identified through detection of nuclei of living cells with a random forest-based imaging pipeline. **(G)** Dose-response of ERK and Akt activities after 1 hour of treatment with Dabrafenib (BRAFi) and MK2206 (Akti) in BRAF^{V600E} cells (upper) and BRAF^{V600E}/NRAS^{Q61K} cells (lower). Bars indicate the interquartile range. **(C, E)** Gray areas indicate the 95% confidence interval of the population medians (N > 200 cell trajectories). Vertical dashed lines indicate the drug treatment start (at 2 hours).

Kinome siRNA screens to identify MAPK/ERK – PI3K/Akt network vulnerabilities.

Having access to robust and scalable ERK/Akt measurements in BRAF^{V600E} and BRAF^{V600E}/NRAS^{Q61K} cells, we reasoned that we could perform loss of function screens to identify network vulnerabilities that lead to ERK and/or Akt inhibition. We performed kinome siRNA screens to identify new kinases that might crosstalk with oncogenic BRAF^{V600E} and/or NRAS^{Q61K} signaling. We performed kinome-wide siRNA screen in the three following experimental paradigms: ERK^{high}/Akt^{heterogeneous} phenotype in starved BRAF^{V600E} cells (screen 1); ERK^{high}/Akt^{high} status in BRAF^{V600E}/NRAS^{Q61K} cells (screen 2), and ERK^{high}/Akt^{high} status in BRAFi-treated BRAF^{V600E} cells (Figure 3A). The siRNA library targeted each kinase with three independent siRNAs, covering all the known and putative kinases. A previously established reverse solid-phase transfection procedure[40] (Figure S3A) was used to perturb our cells. Briefly, cells were seeded on siRNA/transfection mix-coated 384-well plates, cells were starved after 66 hours (screens 1 and 2), or treated with 3 μM dabrafenib after 52 hours (screen 3). 72 hours after seeding, cells were fixed, imaged, and processed with our image analysis pipeline to extract ERK/Akt activities. To quality control transfection efficiency, *AURKB* KD was evaluated to give the expected mitotic slippage phenotype (Figure S3B)[41]. Moreover, plate duplicates showed significant correlation ($R > 0.7$, $p <<< 0.001$; Figure S3C). To identify siRNA perturbations that inhibit ERK and/or Akt activity, we set up specific C/N ratio that were plate-normalized. This was in part because multiple siRNA perturbations affected cell numbers, precluding the use of statistical descriptors that depend on cell numbers. On the other hand, we applied stringent criteria for hit selection: 1) we used thresholds on normalized C/N ratios that give phenotypes that are visually self-explaining, 2) we selected hits only if at least two out of three siRNAs exhibited the phenotype, 3) the phenotype was present in both duplicates of the screens (details in the material and methods section). A visual representation of the hit selection for a given screen is provided (Figure 3B, S3D, S4A-C). Venn diagrams summarize the number of hits for each screen, as well as the hits that overlap between the different screens (Figure 3C). A number of penetrant phenotypes expected to lower ERK/Akt activities provided a sanity check for our screen (*BRAF* KD for ERK activity, as well as *PIK3CA*, *PIK3CB* and *PDK1* for Akt activity) (Figure 3D).

In screen 1, only a very small number of perturbations was found to affect ERK activity: *BRAF*, *CNKSR1*, *MAPK1*, *PACSIN2*, *STK11IP*, and *ULK3*. Representative micrographs and single-cell C/N distributions of selected "hit" siRNA perturbations provide an intuition of the phenotype penetrance (Figure 3E and 3F). A protein-protein interaction (ppi) network of the hit list of siRNA-perturbations that downregulate ERK activity in BRAF^{V600E} cells is depicted in Figure 4A (built with stringApp on Cytoscape, details in the material and methods section). Of these six kinases, all but *ULK3* were also found for the BRAF^{V600E}/NRAS^{Q61K} line
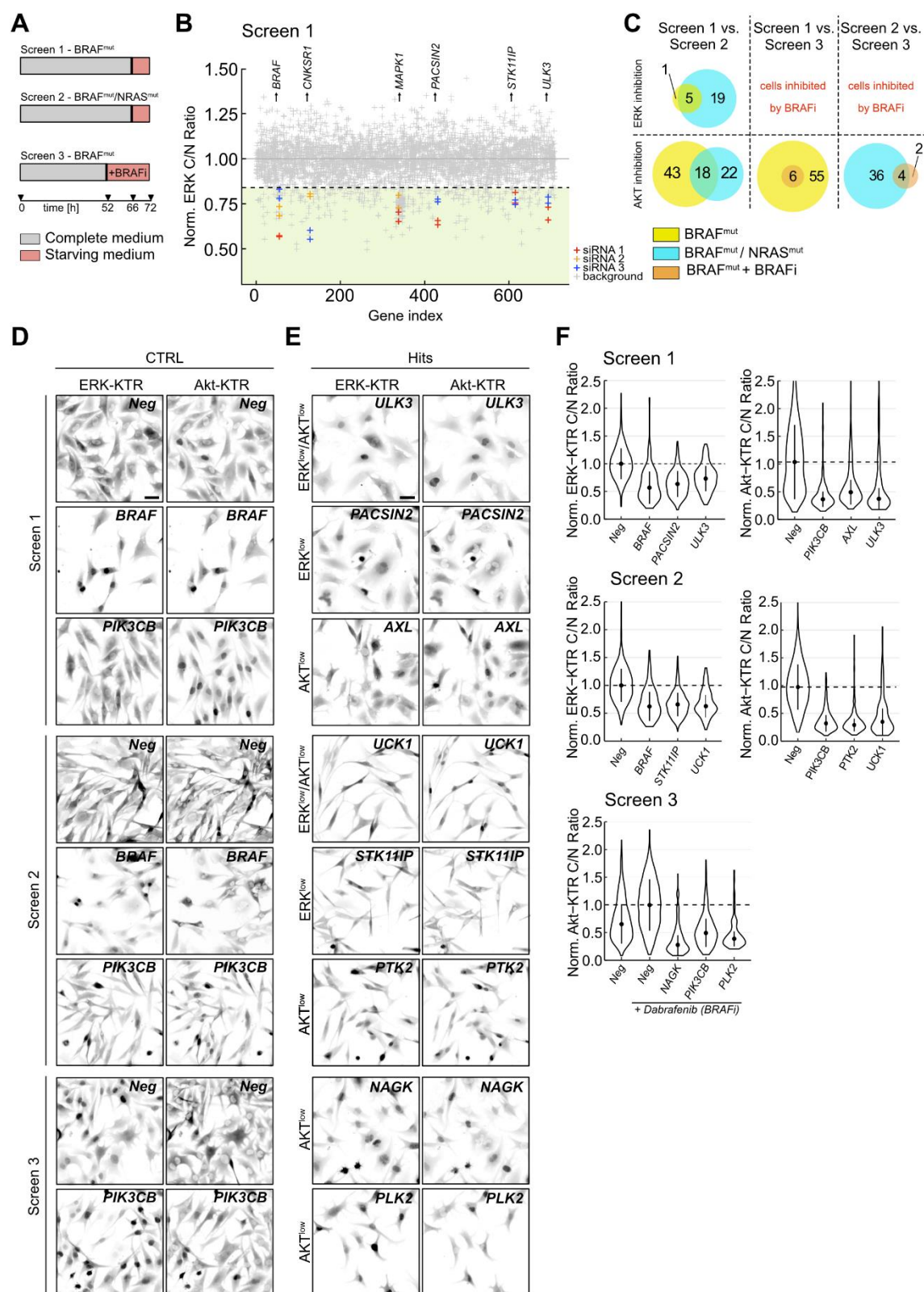
Figure 3 Overview of the kinome-wide siRNA screen on BRAF^{V600E} cells and BRAF^{V600E}/NRAS^{Q61K} cells. (A) Schematic of the three screening conditions. **(B)** Scatterplot that shows the effect of the hits identified in Screen 1 for KDs that downregulate ERK activity. X-axis is the index of the genes sorted in alphabetical order, and y-axis shows the magnitude of the effect on ERK activity as reported by normalized C/N ratios per plate. Red, orange, and blue crosses correspond to the first, second and third siRNA of a particular gene. Highlighted are siRNAs that showed the desired phenotype in both replicates. Grey crosses correspond to the siRNAs that do not display the desired phenotype. For details on the data processing and analysis of kinome siRNA screens refer to the material and methods section. Green area indicates the phenotype space beyond the threshold (at C/N ratio = 0.84). **(C)** Venn diagrams that depict the hit spaces for the 3 screens. **(D)** Representative micrographs of ERK/Akt KTR signals for non-targeting control siRNA (Neg) and for control hits for screen 1 (upper panels), screen 2 (middle panels) and screen 3 (lower panels). Control hits are *BRAF* for ERK activity and *PIK3CB* for Akt acvtivity. Scale bar = 50 μm. **(E)** Representative micrographs of ERK/Akt KTR signals for selected hits. Same distribution as in (D) Scale bar = 50 μm. **(F)** Violin plots of normalized ERK/Akt KTR C/N ratios for the siRNAs indicated in (E). The dot and the bar indicate the median and interquartile range.

(Figure S3D and Figure 4B), pinpointing the general impact of these nodes in ERK signaling across cell lines. *BRAF* and *CNKSR1* showed very penetrant phenotypes in both lines. *BRAF* but not *RAF1* or *ARAF* KD resulted in a robust ERK inhibition. The Connector Enhancer Of Kinase Suppressor Of Ras 1 (CNKSR1) is a pleckstrin homology (PH) domain-containing protein that act as a scaffold for the RAS/RAF/MEK/ERK cascade, thereby increasing their interaction and ultimately their activation[42]. CNKSR1 is also a regulator and binding partner of KSR1, a well-studied scaffolding protein of the MAPK pathway. This result suggests that, even in presence of BRAF^{V600E} activating mutation, a scaffold protein is still needed to efficiently activate ERK. *MAPK1* KD (the ERK2 isoform), but interestingly not *MAPK3* KD (the ERK1 isoform), caused a robust suppression of ERK activity, which suggests a more dominant role of *MAPK1* in BRAF^{V600E} cells that might compensate for the loss of the other isoform, a finding previously reported in BRAF V600E melanomas[43]. Conversely, *MAP2K1* and *MAP2K2* (MEK1/2) were not hits in any screen condition, which suggests that redundancy at the isoform level provide robustness against single perturbations.

Interestingly, *PACSIN2*, *STK11IP*, and *ULK3* represent non-trivial nodes that somehow modulate BRAF^{V600E} mediated ERK activation. Ppi-network identified only one interaction (edge) for *PACSIN2*, with *EGFR* (Figure 4A). PACSIN2 regulates the morphogenesis and endocytosis of caveolae[44], and EGF receptor internalization in the absence of stimulus[45]. Thus, PACSIN2 is a key regulator of growth factor signaling and, curiously, *PACSIN2* KD resulted in decreased activity of ERK rather than Akt, despite the presence of a BRAF^{V600E} mutation. The scaffolding protein STK11IP is functionally linked with LKB1 (STK11); STK11IP interacts with SMAD4, a TGFβ-regulated transcription factor, in a STK11IP-LKB1-SMAD4 ternary complex[46] that negatively regulate TGFβ gene responses[47]. Finally, *ULK3* KD decreased ERK activity but also Akt activity in BRAF^{V600E} cells (Figure S4A and Figure 4C). Very little is known about ULK3, but involvement in autophagy, cell division and execution of Sonic hedgehog pathway have been documented[48].

To our surprise, we found that more siRNA perturbations reduced ERK activity in BRAF^{V600E}/NRAS^{Q61K} cells compared to BRAF^{V600E} cells. BRAF^{V600E} and NRAS^{Q61K} combined mutations might intuitively make the MAPK network more robust to perturbations, since two constitutive inputs are feeding on MEK and ERK. This result therefore sounds rather unintuitive. Additional hits included *MAPK3* (ERK1), indicating that the additional NRAS^{Q61K} now makes cells sensitive to this perturbation, which is not the case in BRAF^{V600E} cells only. Additional hits included also the Akt-activator *PDPK1*. *ROCK1*, the well-known regulator of actin reorganization in cell migration and proliferation, and *PIP5K1C*, a subunit of one of the ROCK1 effectors in migration (PIP5K) were also hits. This suggests cross-talks between regulation of cell motility and the MAPK pathway in BRAF^{V600E}/NRAS^{Q61K} line. Then, we found cell surface receptor hits (*NTRK3* and *PLXNA2*), nucleoside salvage pathway related kinases (*DCK*, *UCK1*, *AK5*), and several disconnected nodes that have

not been previously reported to interact with ERK/Akt pathway (such as *PTK7*, *PRPF4B*, *WNK1*, and *CDKL1*).

The Neurotrophic Receptor Tyrosine Kinase 3 (*NTRK3)* gene encodes TrkC, a member of the Trk family of cell surface receptors, together with TrkA and TrkB. As an upstream activator of MAPK, PI3K, and PLCγ pathways upon neurotrophins ligand binding, *NTRK3* KD- mediated decrease of ERK activity in BRAF^{V600E}/NRAS^{Q61K} cells suggests that even in presence of two oncogenic mutations that activate this pathway, a certain growth factor responsiveness is conserved. Similarly, *PLXNA2* encodes plexin A2, a coreceptor for class A plexins which bind class 3 semaphorins. The sema/plexin system exhibits pleiotropic roles in axon guidance, invasive growth and cell migration, via a number of intracellular proteins and second messengers such as the kinases Pyk2, Syk, FAK, Fes and Src[49] (however *SRC* and *PTK2*/FAK KDs led to loss of Akt activity rather than ERK activity).

Interestingly, the deoxycytidine kinase *DCK*, the uridine-cytidine kinase *UCK1*, and the adenylate kinase *AK5*, formed a small cluster of connected hits (Figure 4B) involved in nucleoside salvage pathway, a pathway that recycles/salvages nucleotides from e.g. nucleic acid turnover as a complement to the de novo synthesis[50]. This finding suggests that impaired metabolic status of the cell might impact on ERK signaling in BRAF^{V600E}/NRAS^{Q61K} cells. Finally, several nodes disconnected from the well-studied ERK and Akt networks result from understudied kinase functions and insufficient ppi knowledge, the so called dark kinome[51]. Taken together, this data suggests that BRAF^{V600E}/NRAS^{Q61K} cells display a certain degree of plasticity of inputs that promote ERK activity - with hits involved in cell migration, in cell surface receptor signaling, and in nucleotide metabolism - and inputs from kinases with unknown relation to ERK pathway.

Perturbation of a large number of kinases lead to decreased Akt activity in BRAF^{V600E} and BRAF^{V600E}/NRAS^{Q61K} cells.

The PI3K-Akt-mTOR pathway regulates a wide range of key cellular processes such as metabolism, motility, survival, growth, and proliferation, involving over 100 Akt substrates[52]. The pleiotropic downstream effectors of Akt require this signaling network to integrate multiple growth signals e.g. from growth factor-activated receptors, from nutrient availability via feedback mechanisms exerted by mTOR - the master regulator of cellular metabolism - and other environmental signals[52]. In our kinome siRNA screens in starved cells, we found many KD perturbation of kinases that robustly downregulated Akt activity (Figure 4C-D). Beyond core nodes of the pathway itself (*PDPK1*, *PIK3CA*, and *PIK3CB* for both cell lines, *AKT2* and *AKT3* in BRAF^{V600E} line), several hits consisted of receptor tyrosine kinases, known to interact with Akt (*AXL*, *FLT4*/VGFR3, *PLXNA1* and *PLXNA2*, *NTRK3*), or from downstream signaling molecules (e.g. *SRC*, *KSR2*). *AXL* KD downregulated Akt activity in BRAF^{V600E} cells and is a member of the Tyro3, Axl, and Mer (TAM) family of RTKs. Cognate ligands such as Gas6 induce homo-dimerization of AXL and subsequent trans-

autophosphorylation within the intracellular kinase domain[53], an event followed by recruitment of adaptor and effector proteins of important downstream signaling cascades such as PI3K/Akt, JAK/STAT, NF-kB, and RAS/RAF/MEK/ERK. *AXL* KD had no effect on BRAF^{V600E}/NRAS^{Q61K} line, despite AXL have been associated to motile and invasive phenotype in multiple cancers, and the AXL/Akt axis to resistance in melanoma[54,55]. The NRAS^{Q61K} mutation downstream of RTKs might explain this fact. Another RTK siRNA perturbation that downregulated Akt activity in BRAF^{V600E} line but not BRAF^{V600E}/NRAS^{Q61K} line is *FLT4*, encoding for the vascular endothelial growth factor receptor VEGFR3. VEGFRs are known for their role in angiogenesis, a key process in tumor growth, and VEGFR3 has been shown to activate Akt pathway via a VEGFR3-VEGFR2-NRP1 (neuropilin 1) complex formation[56]. Overall, RTKs are not highly represented in Akt interactomes of the two cell lines, with BRAF^{V600E} line having some more hits than BRAF^{V600E}/NRAS^{Q61K} line. Additionally, *SRC* KD led to a robust loss of Akt activity in BRAF^{V600E} cells, and *KSR2* KD led to a more penetrant phenotype in BRAF^{V600E}/NRAS^{Q61K} cells than BRAF^{V600E} cells. SRC plays a major role in regulating the signal transduction of several surface receptors[57] and is object of intense studies in anti-cancer therapies, while KSR2 (Kinase suppressor of Ras 2) has a scaffolding function that promotes MAPK pathway downstream of RAS[58]. Curiously, *KSR2* KD downregulated Akt activity rather than ERK activity in both lines.

Our ppi networks show that more nodes connected to ERK and Akt networks were identified in BRAF^{V600E} line compared to BRAF^{V600E}/NRAS^{Q61K} line (42 vs 20), reflecting a more elusive biology in modulation of ERK and Akt networks in cells that carry an additional NRAS^{Q61K} mutation. We speculate that NRAS mutation reduces the sensitiveness of Akt network to inputs, although a consistent amount of siRNAs perturbations affected Akt signaling. Shared hits between the two cell lines included *PTK2*/FAK, *JAK1*, *MAGI2*, *ULK2*, *UCK1* and *CMPK1*, *TRAPP*, plus additional surprisingly robust phenotype from disconnected nodes such as *TTBK1* and *NAGK*. The Janus tyrosine kinase (JAK) family of proteins are crucial to mediate signal transduction initiated by several membrane receptors; among the downstream effectors of JAK proteins, the transcription factors STATs (Janus kinase/signal transducers and activators of transcription) regulate the expression of multiple proteins involved in induction or prevention of apoptosis[59]. JAKs play a pivotal role in intracellular signaling and in recent years crosstalks with RAS/ERK and PI3K/Akt network have been shown[60], although a mechanistic explanation remains elusive. It has been proposed that JAKs activate PI3K via IRS1/2 (Insulin Receptor Substrate 1/2)[61]. *JAK2* perturbation was also a hit in BRAF^{V600E} cells. The hit *PTK2* encodes for the non-receptor tyrosine kinase FAK (focal adhesion kinase) and has been linked to melanoma as a promising drug target that promotes invasion by regulating focal-adhesion mediated cell motility at sites of integrin clustering[62]. The integrin β1/Src/FAK axis was shown to activate ERK pathway[63] and Akt pathway[64]. *PAK3* (p21-activated kinase 3) KD led to a robust Akt activity decrease in BRAF^{V600E} cells. PAK3 has been previously shown to activate ERK pathway via direct

phosphorylation of CRAF and MEK, and to promote MAPK inhibition resistance in BRAF-mutant melanomas[65]. PAK (p21-activated kinase) family of kinases acts as downstream effector of the Rho family GTPases Rac and CDC42, thus playing a role in cell motility. PAK3 (and in general PAKs) input to Akt network is however not elucidated.

The additional hits *UCK1*, *CMPK1*, *NME6*, and *GUK1* (the first two shared between the two cell lines, the last two were found only in BRAF^{V600E} cells) are connected in the networks by consecutive edges either to *SRC*, or to *PTEN* (network interactor) via *MAGI2*. These four hits are involved in nucleotide metabolism and finally, via the guanylate kinase GUK1, to the catalysis of GMP to GDP. This result suggests that an impaired cellular metabolism decreases Akt activity, further corroborated by the presence of the *NAGK* perturbation across all screens and with a penetrant phenotype (Figure 3D, Figure 4C-D). The acetylglutamate kinase NAGK is an essential enzyme of the controlling step of arginine biosynthesis and therefore needed to make proteins[66]. Hence, these results suggest the potential role of metabolic strategies to target cellular pro-survival signaling via Akt pathway. Another striking observation is that several kinases involved in cell-cycle regulation were identified to downregulate Akt pathway upon KD in BRAF^{V600E} cells but not in BRAF^{V600E}/NRAS^{Q61K} cells (CDK4, CDK7, PLK2, and PLK4). However, constitutively active Akt in BRAF^{V600E}/NRAS^{Q61K} cells might have masked this Akt phenotype.

Of interest, the KD of *TPD52L3* caused a strong Akt activity reduction in screen 2 and screen 3, and less in screen 1. *TPD52L3* is one of four paralogous mammalian genes (i.e. with *TPD52*, *TPD52L1*, *TPD52L2*) and forms homo- and heteromeric complexes with other tumor protein D52-like proteins[67]. TPD52 overexpression has been described in melanoma and many other cancer types, which led to consider this family of proteins as a potential oncogene to target[68]. However, TPD52 biology is largely unknown, with some reports that implicated TPD52 in tumorigenesis and progression to metastasis.[68]

To mention, screen 3 was technically difficult to perform and less robust compared to screen 1 and screen 2 due to the additional effect of dabrafenib on the cells and the prolonged starvation associated to the treatment. However, we point out that our stringent criteria of hit selection identified also *MAP4K2* KD as perturbation that decreased Akt activity in the ERK^{high}/Akt^{high} signaling state in dabrafenib-treated BRAF^{V600E} cells. The biological functions of *MAP4K2* are poorly elucidated, but MAP4Ks have been reported to activate JNK via the MAP3K-MAP2K cascade[69].

In summary, the pleiotropic inputs and outputs of the PI3K/Akt pathway resulted in many KDs that affected Akt activity, revealing a complex wiring that has potentially many unknown mechanisms of regulation via positive/negative feedbacks and crosstalks. Overall, kinome siRNA screens revealed the robustness of ERK network compared to Akt network in BRAF^{V600E} cells, and a less robust ERK network in BRAF^{V600E}/NRAS^{Q61K} cells compared to BRAF^{V600E} cells.

A ERK inhibition in BRAF^{mut}

B ERK inhibition in BRAF^{mut}/NRAS^{mut}

C AKT inhibition in BRAF^{mut}

D AKT inhibition in BRAF^{mut}/NRAS^{mut}

E AKT inhibition in BRAF^{mut} + BRAFi

Legend:
- BRAF^{mut} hit
- BRAF^{mut}/NRAS^{mut} hit
- Both lines shared hit
- Screen 1 vs Screen 3 shared hit
- ERK/Akt paths nodes
- STRING interactors
- +++ ++ + penetrance phenotype
- Edge to BRAF or NRAS

54

Figure 4 Hit spaces shown as protein-protein interaction networks. (A-E) Hit spaces are shown as protein-protein interaction networks for the indicated screen condition and phenotype. Networks were generated with stringApp on Cytoscape and network visualizations were created using Cytoscape via the RCy3 package which interacts with Cytoscape via its REST API from within R (https://git.bioconductor.org/packages/RCy3). Interaction knowledge was sorted to include curated databases, experiments, and text mining, with edge (interaction) scores at medium confidence. The core elements of the ERK/Akt pathways are depicted as grey nodes with a thick black outline, or as colored nodes if such elements are also hits. Grey nodes with regular outline are string interactors. Edges (interactions) that connect hit nodes to either BRAF or NRAS nodes are indicated in red color, whereas all the other edges are indicated in black color. BRAF node is not presented as colored hit in (A,B) to keep a recognizable layout. Node size matches the penetrance of the phenotype across siRNAs and duplicates (big node ~ top 1st quartile of the hits, medium node ~ 2nd quartile, small node ~ 3rd and 4th quartile).

Akt pathway is resilient against pharmacological inhibition of protein targets identified in the RNAi screening.

We chose to pharmacologically inhibit selected kinases found in the RNAi screens to validate them as hits. A drug mining analysis to identify druggable kinases was performed (data not shown). Results were manually inspected to select the most specific, potent, and, when applicable, clinically advanced, small molecule inhibitors for a panel of protein targets. Inhibitors that target kinases found in ERK interactomes were not identified, except for NTRK3 and ROCK1 inhibitors, which failed to show any ERK inhibition (not shown). We reasoned that a kinase KD results in a great decrease of the protein content, while pharmacological inhibition of that kinase activity might not impair additional non-catalytic functions such as scaffolding functions, which might explain different phenotypes observed upon KD or drug inhibition. We identified AXL, FAK, JAK1, PAK3, and PLK4 as protein targets to validate their phenotype of loss in Akt activity upon siRNA perturbation, and to be investigated as putative drug combination therapies with dabrafenib (5A). Not shown, drug concentrations chosen for timelapse experiments were evaluated in previous literature and adjusted with pilot experiments that did not measure the inhibition of the primary target of the drugs, but that evaluated Akt signaling and absence of signs of acute toxicity.

Interestingly, we found that Akt activity was resistant against inhibition of these targets, especially in BRAF^{V600E}/NRAS^{Q61K} cells. In fact, if dabrafenib-mediated BRAF inhibition and MK2206-mediated Akt inhibition caused an expected durable decrease of ERK and Akt activities over 24 hours respectively (Figure 5B), inhibition of our targets often decreased Akt activity only transiently (Figure 5C). At the population level, AXL inhibition with bemcentinib (2 µM) caused a very modest decrease of Akt activity in BRAF^{V600E}/NRAS^{Q61K} cells (considered high overall), consistently with the kinome screen in which AXL was not a hit. In BRAF^{V600E} cells instead, bemcentinib caused an acute inhibition of Akt activity with an effect comparable to MK2206. This inhibition was transient and Akt activity rebounded after 4-6 hours, which illustrates the remarkable plasticity of Akt network. Of note, in the RNAi screening *AXL* KD decreased Akt activity 72 hours post transfection. FAK inhibition with defactinib (24 µM) in BRAF^{V600E} cells also resulted in acute decrease of Akt activity followed by a rebound over 6-10 hours. In BRAF^{V600E}/NRAS^{Q61K} cells, the inhibition was less pronounced. Also here, rebound occurred and appeared to be faster than in BRAF^{V600E} cells. Differently, JAK1 inhibition with ruxolitinib (24 µM) resulted in a more prolonged Akt inhibition in both cell lines. Interestingly, ruxolitinib also mildly decreased ERK activity. Of note, in the RNAi screens JAK1 was not identified as a hit in the ERK interactomes. Unfortunately, ruxolitinib was used with the caveat that it targets also JAK2 with a comparable potency; a JAK1 specific inhibitor is not available. FRAX486-mediate inhibition of PAK3 (3 µM) also caused a transient Akt inhibition in both lines, with a very fast and complete rebound in BRAF^{V600E}/NRAS^{Q61K} cells and a partial and slower rebound in BRAF^{V600E} cells. As for JAK1,

A

Kinase	Drug	Phenotype
AXL	Bemcentinib	AKT inhibition (1)
FAK	Defactinib	AKT inhibition (1, 2)
JAK1	Ruxolitinib	AKT inhibition (1, 2)
PAK3	FRAX486	AKT inhibition (1)
PLK4	Centrinone	AKT inhibition (1)

1 = Screen 1, BRAF^{mut}
2 = Screen 2, BRAF^{mut} / NRAS^{mut}
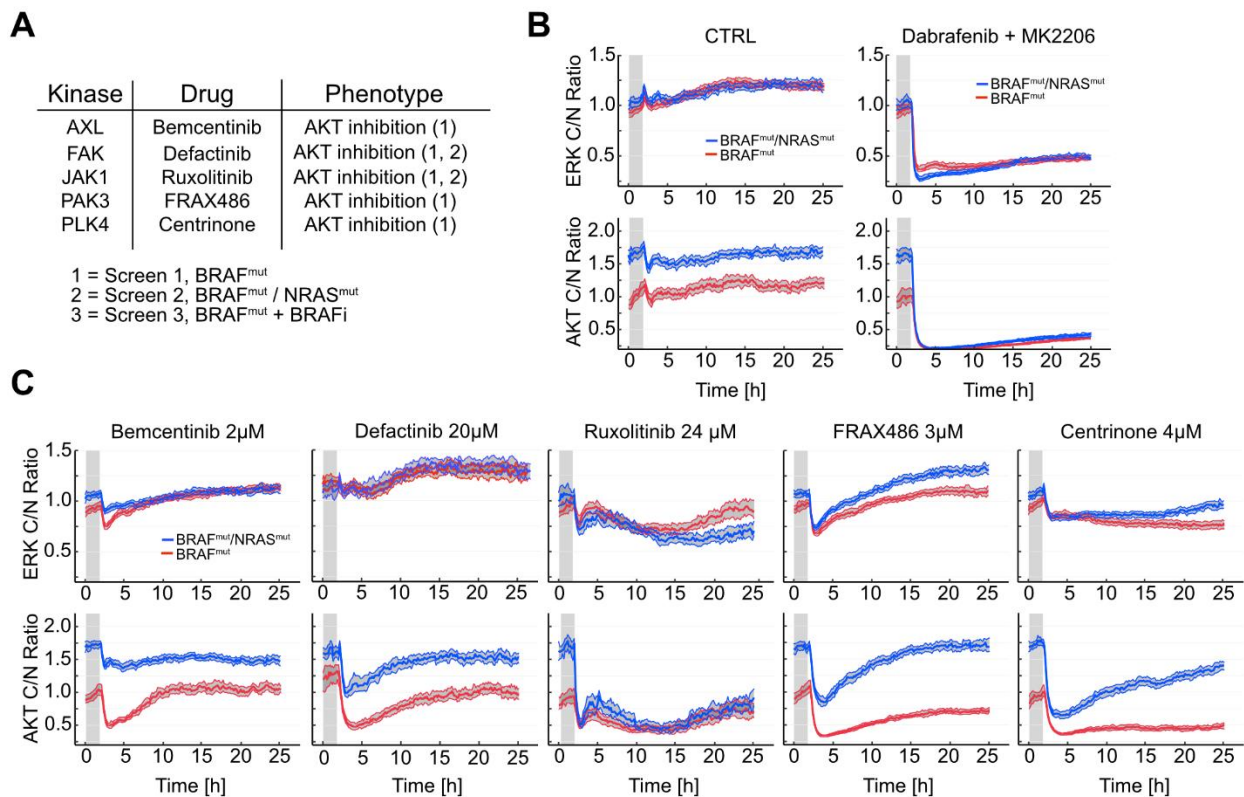3 = Screen 3, BRAF^{mut} + BRAFi

Figure 5 Small-molecule inhibitors of selected kinase targets cause heterogeneity of Akt signaling responses. (A) Overview of the drugs chosen to inhibit the kinase targets identified in the kinome screens. **(B)** Population medians of ERK and Akt KTR C/N ratios are shown for the indicated drug treatments. Gray areas indicate the 95% confidence interval of the population medians (N > 115 cell trajectories). Grey vertical areas indicate the first 2 hours of baseline before drug addition.

PAK3 specific inhibitors are not available; FRAX486 targets also PAK1 and PAK2 with similar potency as for PAK3. PAK1 has been shown to phosphorylate and activate CRAF and MEK1[70]. The small observable ERK inhibition in both cell lines was therefore not surprising using FRAX486, although it suggests that inputs to ERK pathway downstream of BRAF[V600E] play a small role in activating ERK. A rebound of ERK activity followed the FRAX486-mediated small ERK activity inhibition. Interestingly, PAK1-dependent phosphorylation of MEK on Ser298 was shown to be negatively regulated by ERK. ERK phosphorylation of MEK1 on Thr292 impairs the ability of PAK1 to activate MEK1[70]. FRAX486 might have caused an initial inhibition of ERK activity via decrease of MEK1 output, followed however by the partial relief of the negative feedback of ERK on MEK1, which might have caused a rebound of MEK1 activity. Furthermore, PAK1 was also found as a scaffold to facilitate Akt activation by PDK1 and to aid the recruitment of Akt to the membrane[71]. Even if the scaffolding function might not be affected by small molecule inhibition, this possibility is not excluded. With this caveat, we still point out the evidence from the siRNA screen that *PAK3* KD, but not *PAK1* or *PAK2*, led to loss of Akt activity in BRAF[V600E] cells. This interpretation is further corroborated by the same result observed with genetic silencing in a pancreatic cancer cell line[72].

Finally, PLK4 (polo-like kinase 4) inhibition with centrinone (4 µM) decreased Akt activity in BRAF[V600E] cells, whereas an Akt inhibition followed by a steady Akt activity rebound over 24 hours was observed in BRAF[V600E]/NRAS[Q61K] cells. Partial ERK inhibition was observed in both lines, with a steady effect on BRAF[V600E] cells. PLK4 is an essential regulator of the cell cycle and is considered the master regulator of centriole duplication. Besides the pivotal role in cell cycle, PLK4 has been documented to have an important anti-apoptotic activity in cancer cells[73] and to play a role in cancer invasion and metastasis via an activating phosphorylation of Arp2, an essential protein to generate branched actin networks important for cell motility[74]. Recently, *PLK4* KD was demonstrated to reduce epithelial-mesenchymal transition (EMT) of neuroblastoma cells through inhibition of PI3K/Akt pathway[75]; melanoma cells can undergo a reversible process like EMT called phenotype-switch that can mediate resistance to targeted therapy[76]. We consider very unlikely that a degradation of the drugs over time justifies a rebound effect on Akt activity as this rebound occurs with different timescales and amplitudes in the two cell lines (PAKi and PLK4i), and in general a degradation within 8 hours of drugs in phase 1-3 clinical trial appears unlikely. Nonetheless, further assessment might be required.

Taken together, these results validated the Akt inhibition phenotype upon KD of *AXL*, *FAK*, *JAK1*, *PAK3,* and *PLK4* in BRAF[V600E] cells, further confirmed by the reduction of pAkt Ser473 within 1 hour of treatment in cells that do not express the biosensors (Figure S5A, left). Our results also provided a rational for the absence of AXL, PAK3, and PLK4 in the Akt interactome of BRAF[V600E]/NRAS[Q61K] cell line. Here in fact, PAK3i and PLK4i decreased Akt activity within 1 hour of drug addition (with a stronger effect compared to AXLi and FAKi), further confirmed with the immunostaining of pAkt Ser473 (Figure S5A, right), but Akt

activity almost completely rebounded within 24 hours. In contrast however, defactinib-mediated FAK inhibition resulted in a rapid rebound of Akt activity, while in the RNAi screening was found as a hit.

Co-inhibition of BRAF with PLK4 or PAK3 provide additional cytotoxicity compared to BRAF inhibition alone in both BRAF^{V600E} and BRAF^{V600E}/NRAS^{Q61K}.

We then asked whether pharmacological inhibition of our putative drug targets, that we showed to rapidly interact with Akt network, in combination with BRAF inhibition might constitute novel therapeutical opportunities. To explore that, we performed a viability assay in which cells were treated for 72 hours with increasing concentration of bemcentinib, centrinone, FRAX486, ruxolitinib and defactinib alone, or in combination therapies with dabrafenib (4 µM). We reasoned that ERK pathway inhibition remains a cornerstone in the clinical targeted treatment of BRAF mutated melanoma, therefore we used a concentration of dabrafenib that saturates ERK activity response (4 µM). We then benchmarked whether the proposed combination therapies provided additional cytotoxicity to BRAF inhibition. In more details, 20-25 images per treatment were acquired (N = 4 replicates for BRAF^{V600E} line; N=3 replicates for BRAF^{V600E}/NRAS^{Q61K} line) and the number of surviving cells per image was normalized on a plate-by-plate base. Importantly, to score the overall percent survival rate, drug monotherapies were normalized against the median of DMSO control, whereas drug combinations were normalized against dabrafenib 4 µM monotherapy. We first found that the combination of BRAFi with MEKi or Akti were the most effective combination therapies in our in vitro setting, in both cell lines (Figure 6A). Not surprisingly, this result suggests that the targeted inhibition of ERK and Akt pathway in our cell model systems is the most effective strategy to reduce viability of the cells, and might be explained by the documented central importance of these two signaling pathways in survival and proliferation of melanoma.

We then found that the combination treatment of BRAFi with either PAK3i or PLK4i decreased cell viability of ~50% compared to BRAFi alone in both lines when used at the maximal concentration that we tried (Figure 6A-B). The concomitant BRAFi and PAK3i was particularly effective in BRAF^{V600E}/NRAS^{Q61K} cells (~ 70 % decrease of viability). Strikingly here, PAK3i monotherapy resulted in a potent cytotoxicity in BRAF^{V600E}/NRAS^{Q61K} cells. As survival curves of the combination therapies of PAK3i and PLK4i were not clearly steeper than their monotherapy counterparts, we reasoned that an additive cytotoxicity occurred. Additive cytotoxicity was not always achieved. In fact, combination therapies of BRAFi with JAK1i or FAKi did not increase cytotoxicity compared to BRAFi alone. In the case of BRAFi+JAK1i in BRAF^{V600E} cells, at smaller concentrations of ruxolitinib we observed an even enhanced viability of the cells. This tendency is only marginally observable in BRAF^{V600E}/NRAS^{Q61K} cells, but overall, this result suggests an antiapoptotic effect of JAK1/JAK2 inhibition in combination with BRAF inhibition. This finding is even more striking as JAK1/2 inhibition robustly decreased Akt activity (Figure 5C). Both FAKi and JAK1i monotherapy reduced
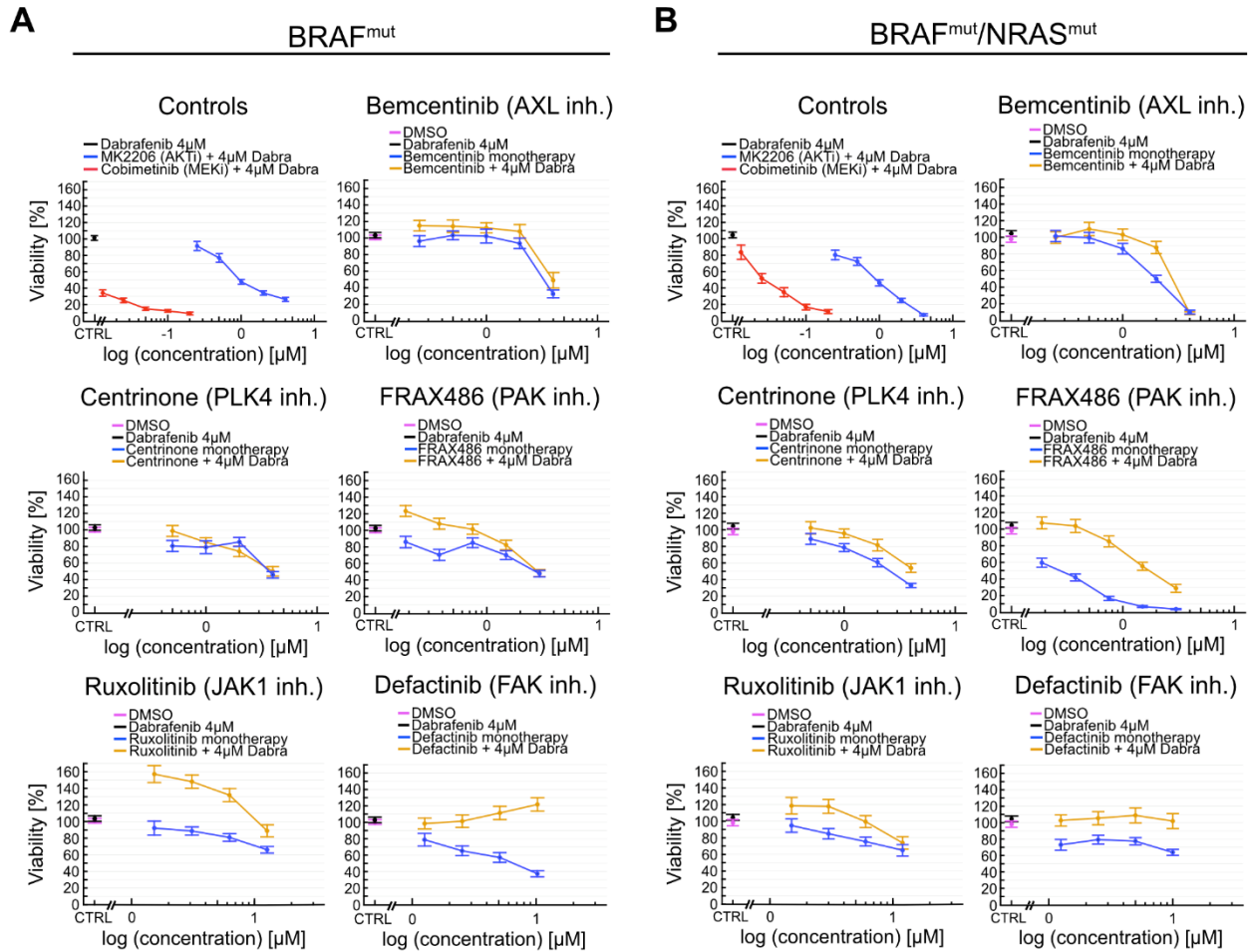
Figure 6 PLK4 and PAK3 inhibition, but not FAK and JAK1 inhibition, provided additional cytotoxicity in combination with BRAF inhibition in both cell lines. (A,B) Viability measured as normalized number of living cells per image in treatment condition against the median of living cells per image in control condition after 72 hours of treatment for the indicated drugs and drug combinations in $BRAF^{V600E}$ line (A) and $BRAF^{V600E}/NRAS^{Q61K}$ line (B). Control corresponds to DMSO treatment for drug monotherapies, whereas for combination therapies (with Dabrafenib 4µM) control corresponds to Dabrafenib 4 µM monotherapy. Data were pooled from 4 replicates in (A) and 3 replicates in (B); for every replicate, between 20 and 25 field-of-views per treatment were imaged. Normalized number of living cells/FOV is shown as median and 95% confidence interval of the mean.

viability compared to control, but this anti-proliferative activity was not observable when in combination with dabrafenib. Finally, AXLi in monotherapy exhibited a dose-dependent decrease of viability in BRAF^{V600E}/NRAS^{Q61K} cells, even if AXL was not identified as a hit in screen 2. This observation clearly shows that AXL reduced viability in an Akt-independent manner, as Akt activity was not decreased by AXL inhibition in BRAF^{V600E}/NRAS^{Q61K} cells. The combination of AXLi and BRAFi reduced viability only at the highest dose of 4 µM bemcentinib (by over 90%). This result suggests that in presence of BRAFi-mediated cytotoxicity, a strong inhibition of AXL is needed to provide additional cytotoxicity. In BRAF^{V600E} cells only 4 µM bemcentinib reduced viability in both mono- and combination therapy, which corroborates the idea that only a strong inhibition of AXL provides cytotoxicity and in an Akt-independent manner, as AXL-mediated decrease of Akt activity was transient (in monotherapy at least). However, higher doses than 4 µM bemcentinib resulted in early cytotoxicity that might be attributable to off-target effects.

Taken together, we demonstrate that our kinome screens identified druggable kinases (PLK4 and PAK3) that inhibited oncogenic Akt activity on time scales of minutes, implying a direct crosstalk between PLK4 and PAK3 and oncogenic Akt activity, and that their inhibition in combination with dabrafenib provided additional cytotoxicity compared to dabrafenib alone. However, Akt activity rebounded to some level in the BRAF^{V600E}/NRAS^{Q61K} cells on timescale of hours, further illustrating the remarkable plasticity of signaling networks, and showing the need of studying non-genetic mechanisms of drug resistance.

DISCUSSION

In this study, we show that the measurement of ERK/Akt activities in individual BRAF^{V600E} melanoma cells from a drug naïve patient versus BRAF^{V600E}/NRAS^{Q61K} cells from a relapsed patient that had received a BRAF^{V600E} inhibitor display aberrantly sustained ERK activity in both lines that is insensitive to negative feedback. Single cell monitoring also enabled us to identify heterogeneous Akt activity that fluctuates on timescales of hours in BRAF^{V600E} cells, while in BRAF^{V600E}/NRAS^{Q61K} cells Akt activity was homogeneously sustained. Upon BRAF^{V600E} inhibition with dabrafenib, Akt activity in BRAF^{V600E} cells turned to sustained on a timescale of 6-24 hours and remained sustained in BRAF^{V600E}/NRAS^{Q61K} cells. Sustained Akt activity promoted survival in intrinsic and acquired resistance to BRAF^{V600E} inhibition. We show that a kinome-wide RNAi screen performed with a scalable assay to measure single-cell ERK/Akt activities identifies new drug targets that allow us to inhibit resistant signaling states. We finally demonstrate that concomitant PLK4 and PAK3 inhibition partially reverts pathological Akt activity in our short-term (dabrafenib-treated BRAF^{V600E} cells), and genetic (BRAF^{V600E}/NRAS^{Q61K} cells) drug resistance cell systems. The rapid Akt activity downregulation of both implies a direct crosstalk between PLK4 and PAK3 and oncogenic Akt activity. Our unbiased approach illustrates the discovery of non-intuitive protein interactions in drug resistance.

ERK network is built for robustness against perturbations

Decades of research that focused on population-averaged assays such as Western Blot have been extremely important to identify signaling network nodes and their hierarchies, but with live single cells measurements of ERK activity we now show that ERK activity in our system of patient-derived cells that harbor a BRAF^{V600E} mutation is sustained over time. In 2009, Rosen's lab proposed BRAF^{V600E} to be insensitive to negative feedback regulation[77] as measured from steady-state pERK and pMEK levels as proxies for ERK activity and BRAF activity. In 2012, the same lab concluded that while levels of active RAS-GTP are likely too low in BRAF^{V600E} to promote RAS-dependent RAF dimerization and downstream signaling, MAPK pathway inhibition relieves strong ERK-mediated negative feedback of receptor signaling, and RTKs-mediated activation of RAS increases, as measured active GTP-loaded RAS.[39] Increased RAS-GTP levels were followed by a rebound of ERK pathway activity, as measured by the increase of induced CRAF, pMEK, and pERK (rebound), but additionally also pAkt. Both studies relied on population average assays and whether these steady state behaviors stemmed from any form of dynamic regulation of ERK activity at the single cell level was unanswered at the time. Sustained ERK activity at the single cell level now reveals how BRAF^{V600E} is truly insensitive to negative feedback regulation, a stricking finding that underscore the ability of BRAF^{V600E} to completely rewire the ERK output in melanoma and promote tumor progression. In physiological conditions, almost every component of the ERK cascade is regulated through negative feedback phosphorylation by downstream kinases[78]. ERK-mediated negative feedback to RTKs,

RAFs, and MEKs, confer robustness to the ERK output by buffering against noise in expression levels of the signaling network components[79]. In our BRAF[V600E] cell model system, BRAF[V600E] escapes negative feedback regulation but the MAPK network nonetheless exhibits a robust ERK activity against genetic perturbations in the RNAi screen. In fact, we found here that only six kinase knockdowns, namely *BRAF*, *MAPK1/ERK2*, *CNKSR1*, *PACSIN2*, *STK11IP* and *ULK3* led to loss of ERK activity according to our stringent criteria of hit selection (Figure 4A). All of them but *ULK3* were found also in BRAF[V600E]/NRAS[Q61K] line. First, the very penetrant *BRAF* KD-mediated reduction of ERK activity, not observed with *ARAF* or *CRAF* KDs, confirmed that sustained ERK activity is primarily driven by BRAF[V600E], and that the network plasticity to switch RAF isoforms to activate downstream MEK was not sufficient to restore loss of ERK activity mediated by *BRAF* KD. We speculate that *BRAF* KD results in physiological levels of ERK activation driven by ARAF and CRAF. Second, *ERK2* KD, as one of the two downstream nodes of BRAF, led to ERK activity decrease. Interestingly in BRAF[V600E] cells, *MAPK3/ERK1* was not a hit, which suggests redundancy of function within ERK1 and ERK2 compensated for the ERK1 knockdown, a finding previously described in melanoma[43]. On the same page, ongoing work in our research group showed that single knockdown of ERK1 or ERK2 in mouse fibroblasts only slightly affected the ERK output in response to and RTK input, whereas simultaneous *ERK1* and *ERK2* KD resulted in loss of ERK activation. The aberrant ERK signaling state mediated by the BRAF[V600E] mutation might favor ERK2 activity over ERK1, possibly through poorly understood non redundant functions between the two isoforms. Again, a similar finding results from the absence of MAP2K1/MEK1 and MAP2K2/MEK2 from the hitlist of both cell lines. Loss of one MEK isoform might be compensated for by the unperturbed isoform, which is corroborated by their high degree of homology and the identical substrate specificity[80]. An alternative hypothesis is that residual protein levels upon an incomplete isoform knockdown are still sufficient to maintain ERK output.

In this context it appears surprising that *CNKSR1*, *PACSIN2,* and *STK11IP* led to a loss of ERK activity in both lines. Our screen suggests that the scaffold protein CNKSR1 appear to have a central role in regulating the MAPK pathway. CNKSR1 is a regulator and binding partner of KSR1, a well-characterized scaffold protein that is recruited to the membrane and brings the three components of the MAPK cascade together, facilitating their interaction[42]. Additional vulnerabilities represented by STK11IP and PACSIN2 are poorly studied in melanoma. PACSIN2 interacts with PTRF through EHD2 in caveolae biogenesis[81]. PTRF was identified as a major contributor in a 15 proteins signature that differentiated a panel of primary melanoma cell lines that were sensitive to MAPK inhibition from drug-resistant primary lines[25]. Another intriguing finding is that *ULK3* KD led to loss of both ERK and Akt activity in BRAF[V600E] cells. If confirmed, such a network node might represent an attractive target to drug the ERK/Akt pathways simultaneously with a single therapeutical agent. A selective small molecule inhibitor against ULK3 is not available, which prevents further characterization of this hit from a signaling network perspective. Clarifying whether ULK3

inhibition leads to an acute decrease of ERK and Akt activities due to direct crosstalk, or rather to an activity decrease on the timescale of hours due to transcriptional adaptations, is pivotal to understand ULK3 interaction with these pathways.

Unexpected, more kinase KDs reduced ERK activity in BRAF^{V600E}/NRAS^{Q61K} cells compared to BRAF^{V600E} cells (24 genes vs 6 genes). We might think that the logic of a secondary NRAS mutation is to sustain ERK output even more robustly against perturbations. This systemic result needs be validated on additional double BRAF/NRAS mutated cell lines, but we hypothesize that an acquired NRAS mutation promotes the formation of active RAF dimers, which contribute to sustain ERK output. This hypothesis is corroborated by the abovementioned study[39] that showed how low levels of active RAS-GTP in BRAF^{V600E} cells are insufficient to activate CRAF in normal conditions, but upon relief of ERK-mediated feedback inhibition to RTKs, active RAS-GTPs forms and reactivates ERK pathway. A mutated NRAS that is locked in a GTP-active configuration might sustain ERK output, and this additional branch of ERK cascade activation might be influenced by upstream regulators of RAS subcellular localization, such as farnesyltransferase[82], or by negative feedbacks and crosstalks at the level of RAFs. For example, Akt has been shown to phosphorylate and negatively regulate CRAF[83]. Additionally, PAK1 phosphorylates CRAF at Ser338, a critical residue for activation, and also MEK1 at Ser298, a residue that enhances RAF-mediated MEK activation[84]. As PAK1 is a major downstream effector of the Rho GTPases Rac1 and CDC42[85], NRAS mutation might couple ERK output to cell motility cues. To support this scenario, the hit NTRK3 was previously shown to promote podocyte migration via ERK-mediated activation of WAVE2, a protein required for directed cell migration[86,87]; plexins, such as the hit PLXNA2, are known for their pleiotropic roles in processes such as invasive growth and cell migration via a number of intracellular proteins and second messengers such as the kinases Pyk2, Syk, FAK, Fes and Src[49], some of which might feed signals to ERK. Finally, *DCK*, *AK5*, and *UCK1* LD led to marked loss of ERK activity. These three hits formed a cluster and are involved in the nucleoside salvage pathway. This cluster highlight the important metabolic role of nucleosides to sustain ERK signaling. A depletion of nucleoside triphosphates might have affected the activity of many GTP-dependent proteins like RAS. Reduction of RAS-GTP might explain the loss of ERK activity in BRAF^{V600E}/NRAS^{Q61K} cells but not BRAF^{V600E} cells. Interestingly in that sense, Akt interactomes in both cell lines included multiple kinases related to the nucleoside metabolism, which underscores the tight connection of Akt pathway with the cellular metabolism.

Taken together, we provide evidence for increased sensitiveness to inputs of ERK network in BRAF^{V600E}/NRAS^{Q61K} cells. If confirmed in multiple cell lines and settings, this plasticity might represent an invaluable network property to explore novel combination therapies in double mutated melanoma tumors.

Different Akt activity patterns between BRAF^V600E and BRAF^V600E/NRAS^Q61K lines

We learned from single cell measurements that Akt activity is heterogeneous and fluctuates in BRAF[V600E] cells on timescales of multiple hours, while it is sustained in BRAF[V600E]/NRAS[Q61K] cells (Figure 2A-B and Figure S2A-B). We hypothesize that this striking difference is caused by the secondary NRAS mutation, which is likely to activate PI3K/Akt[8,14]. The sustained Akt activity in BRAF[V600E]/NRAS[Q61K] cells was associated with enhanced cellular motility (Figure S2D, upper panel), consistent with previous studies that identified oncogenic RAS to promote cell motility in a PI3K/Akt- and PI3K-Rac1-dependent manner[33,34,35,36]. Additionally, high Akt activity was shown to promote melanoma metastases in vivo[88]. The motile phenotype of BRAF[V600E]/NRAS[Q61K] cells was compromised upon Akt inhibition (Figure S2D, lower panel). We think that Akt activity fluctuations in BRAF[V600E] cells depend not only on the plethora of inputs that Akt network integrates (e.g. nutrient availability, cellular metabolism, growth factors), but also on motility cues, for example from the integrin β1-FAK-Src axis upstream of PI3K/Akt[89]. *FAK* and *SRC* were found as hits in both cell lines.

With great surprise, we found that exposure to the BRAF[V600E] inhibitor dabrafenib led to the upshoot of Akt activity in all BRAF[V600E] cells starting from 4-8 hours after drug addition, and reaching steady-state levels after 24 hours. This timescale excludes direct crosstalks between ERK and Akt networks to be the cause of the Akt upshoot. It has been previously shown that RAS-dependent rebound of ERK output upon BRAF inhibition in several BRAF[V600E] melanoma lines occurs on a similar timescale[39]. It has been shown that the ERK-dependent elevated expression of the RTK negative regulator Spry2 in untreated BRAF[V600E] cell lines markedly diminished 4-8 hours after exposure to the BRAF[V600E] inhibitor vemurafenib. Spry2-mediated negative feedback of RTKs decreased, and RTKs-induced activation of RAS increased within 24 hours of drug addition. Consequently, the restored sensitivity to RTK-induced, RAS-mediated activation of ERK network led to rebound of ERK activity. Similar processes upon dabrafenib treatment in BRAF[V600E] cells might have led to RTKs-induced RAS activation, and this caused Akt pathway activation rather than ERK pathway.

Sustained Akt activity increases survival in both non-genetic and genetic drug resistance against BRAF^V600E inhibition

Sustained Akt activity in both cell lines exposed to dabrafenib promoted survival (Figure 2E), as concomitant dabrafenib-mediated BRAF[V600E] inhibition and MK2206-mediated Akt inhibition enhanced cytotoxicity compared to dabrafenib alone. BRAF[V600E]/NRAS[Q61K] cells were more resistant to dabrafenib monotherapy compared to BRAF[V600E] cells, but simultaneous Akt inhibition reverted this phenotype. Importantly, dabrafenib-tolerance promoted by the acquired NRAS mutation in melanoma subclones might not exclusively result from ERK pathway reactivation, but also from activation of the parallel PI3K/Akt pathway.

In BRAF^{V600E} cells the short-term Akt activity upshoot upon BRAF^{V600E} inhibition is an intrinsic non-genetic mechanism of resistance that we speculate to be RAS-dependent. Our model systems of non-genetic and genetic drug resistance against BRAF^{V600E} inhibition both involved sustained Akt activity, which underscores how kinome remodeling led qualitatively to the same outcome. Of importance, the single-cell measurements enabled us to observe that this sustained Akt activity is a homogeneous population behavior. A recent study provided a different perspective on the role of compensatory Akt activation in BRAF^{V600E} melanoma cell lines. It has been shown that increased PI3K/Akt signaling upon BRAF inhibition (via tetracycline-inducible oncogenic *PIK3CA* or *AKT3* mutants) enables a dormant subpopulation of MAPK-inhibited cells to survive and be selected for their ability to reactivate MAPK signaling. Only afterwards, resistant cells with relapsed ERK activity proliferate independently from Akt activity[14]. This model of a step-wise evolution of intrinsic resistance moves beyond our findings. However, drugging simultaneously MAPK/ERK pathway and alternative survival pathways that display early mechanisms of compensatory activation induced by MAPK inhibition - here PI3K/Akt pathway - might improve the therapeutical efficacy. This benefit might be lost in later stages of adaptive and acquired drug resistance. A potential caveat of such a strategy is the selective pressure on drug-refractory subclones, which might promote an aggressive rebound of the cancer that might be even more challenging to treat. A more systemic knowledge is needed to uncover how pro-survival signaling pathways interact with RAS-ERK and RAS-Akt pathways to sustain ERK/Akt output in physiological and drug-treated condition. This systemic knowledge might enable to identify novel kinase vulnerabilities and therefore putative drug targets. In the future, understanding how drug-induced kinome remodeling shapes spatial and temporal regulation of these interactions in single cells might provide insights on how to permanently switch off tumorigenic signaling.

siRNA screens as a systemic approach to identify novel vulnerabilities of oncogenic ERK/Akt activities
The essential role of kinases in transducing signals warrants the choice of a kinome library to identify novel drug targets to revert aberrant signaling states. Kinases also represent one of the pharma industry's most important class of drug targets and a main research focus[90]. We developed a scalable pipeline for image-based screenings that can identify systemically which kinase KDs impact on ERK and Akt output. This assay can be reoriented to larger siRNAs libraries, to drug screenings, and to monitor the activity of other kinases.

We identified novel network vulnerabilities that lead to ERK and/or Akt inhibition. Although the nature of the interactions that we unveiled is not addressed in our study, we speculate that targeting even indirect interactions that result in loss of ERK or Akt activity might be a worth therapeutical approach. Indirect interactions are e.g. transcriptional changes in the expression level of regulators and interactors of the ERK/Akt pathways, or unspecific cytostatic effects that only subsequently affect ERK/Akt output.

A large number of upstream regulators and downstream effectors interact with PI3K/Akt pathway. We found many kinase KDs that led to loss of Akt activity. As depicted on the ppi networks (Figure 4A-D), many of the hits are disconnected from the core body of the ERK and Akt pathway nodes and edges. Some of these disconnected nodes were found for both cell lines (*NAGK*, *TTBK1*, *TPD52L3*, *TRRAP*, *FGFRL1*). Akt ppi networks included more hits that are core elements of the cascade (PDPK1, PIK3CA, PIK3CB), which suggests that Akt output is less robust compared to ERK output, in which only the upstream *BRAF* KD and *MAPK1* (ERK2) KD decreased ERK activity in both cell lines.

KD of the scaffolding proteins SRC and KSR2 led to robust Akt inhibition. SRC integrates and regulates RTK signaling and transduces signals to effectors such as PI3Ks[91]. Decades of pre-clinical research warranted targeting SRC as a promising therapeutic target, and our approach rediscovered SRC as an important contributor of Akt output that might be a sensitive node to target. KSR2 is prevalently known as a scaffolding protein that brings RAS, RAF, MEK and ERK in close proximity at the plasma membrane. Curiously, we found *KSR2* KD to inhibit Akt activity rather than ERK activity. Our findings highlight how drug targeting scaffolding proteins is a valuable strategy to target oncogenic Akt activity. However, small-molecule inhibition of scaffolding proteins might target catalytic activity and it is less clear how scaffolding functions might be affected.

We also found membrane receptors hits. We identified only a few RTKs for BRAF^{V600E} line (*AXL*, *FLT4*/VEGFR3) and BRAF^{V600E}/NRAS^{Q61K} line (*NTRK3*/TrkC). Plexin receptors (PLXNA1 for both lines, and PLXNA2 for BRAF^{V600E} line) were the only additional membrane receptors that we identified. Surprisingly, key RTKs in cancer biology such as the ones of the ErbB receptor family were not identified as hits. This might result from the redundance and plasticity of signaling due to promiscuous heterodimerization of ErbBs between them and with other membrane receptors[92]. If in BRAF^{V600E}/NRAS^{Q61K} cells the NRAS mutation might confer some independency from RTKs signaling, in BRAF^{V600E} we reasoned that beside receptor promiscuity, also the ERK-mediated negative feedbacks might play a role in desensitizing cells from ligand-dependent stimulation of RTKs and activation of Akt pathway. In view of these considerations, we expected to find RTKs in screen 3 as BRAF^{V600E} inhibition was speculated to sensitize cells to RTK signaling. In particular we expected hits of the ErbB family as ErbB receptors have been shown to promote drug resistance in melanoma[37] and other BRAF^{V600E} driven cancers[93]. However, screen 3 had technical limits and given our stringent criteria of hit selection, only very few hits were found (*PI3CB*, *PDPK1*, *NAGK*, *TPD52L3*, *MAP4K2*, *PLK2*).

Furthermore, hits of the nucleoside metabolism found for both cell lines (*UCK1*, *CMPK1*) or only in BRAF^{V600E} line (*NME6*, *GUK1*), and hits involved in cell-cycle regulation (*CDK4*, *CDK7*, *PLK2*, *PLK4* in

BRAF^{V600E} line), warrant the strategy to drug such kinases to hit highly proliferative cancer cells more specifically than non-transformed cells. Remarkably, *NAGK* and *TPD52L3* KD led to loss of Akt activity in all three screens. NAGK has an essential role in the carbohydrate metabolism, and a recent study identified NAGK-dependent hexosamine salvage as a key mechanism of tumor growth in pancreatic cancer cells, particularly under glutamine limitation[94]. NAGK might be a promising drug target to hit energy-hungry cancer cells. In summary, we identified several kinases previously known or not known to interact with ERK and Akt pathways.

PAK3 and PLK4 share direct crosstalks with Akt network that can be drugged

Most of kinases are still drug orphan and this results in the limited capacity to validate multiple nodes found in our siRNA screens. Of great importance, the pharmacological inhibition of selected hits affecting Akt pathway resulted in a very rapid inhibition of Akt activity. AXLi, PAK3i, FAKi, PLK4i and JAK1i all led to acute inhibition of Akt activity in BRAF^{V600E} cells within 1 hour of drug addition (Figure 5C). The magnitude of this inhibition was slightly variable but in general intense, with PAK3i and PLK4i resulting in the strongest and most prolonged Akt activity inhibition. Such a rapid Akt activity decrease suggests direct crosstalks that do not depend on transcriptional reprogramming, which instead occur on timescales of several hours. Intriguingly, with AXL and FAK inhibition Akt activity rebounded within hours. This finding might conversely be explained by transcriptional regulation, with overexpression of RTKs or reduced expression of negative feedback regulators as possible causes. As PAK3 and PLK4 rapid mechanisms of interaction with Akt pathway are unknown or insufficiently documented, we provided here evidence for their possible moonlighting functions. To the best of our knowledge, PAK3 and PLK4 have been reported to interact with Akt pathway in two studies. The first study proposed PAK3 as a Ser473-Akt kinase that activates the Akt-GSK3β-β-catenin signaling in several pancreatic cell lines and in a cell line dependent context[72]. The second study indicated PLK4 to promote epithelial-mesenchymal transition via PI3K/Akt signaling in neuroblastoma cells[75]. However, mechanistic insights on how PLK4 and PI3K/Akt pathway interact remain unknown. In BRAF^{V600E}/NRAS^{Q61K} cells, the acute inhibition of Akt activity with our panel of inhibitors was in general less strong, and negligible for AXLi. Here, a rebound of Akt activity was observed not only for FAKi, but also for PAK3i and PLK4i. We speculate that this robustness against Akt inhibition is driven by the NRAS mutation; we think RAS-independent mechanisms of PI3K-Akt activation to cause the immediate Akt activity decrease upon drug addition, and the rebound to be mediated by RAS activity in a context of remodeled feedback regulations.

Finally, the combined BRAF^{V600E} inhibition and PAK3 or PLK4 inhibition led to additional cytotoxicity in both cell lines compared to BRAF^{V600E} inhibition alone (Figure 6), but this promising result does not seem to depend on reduced Akt output. In fact, BRAF^{V600E}/NRAS^{Q61K} cells rebounded Akt activity but they

experienced the additional cytotoxicity provided by PAK3i or PLK4i. Moreover, JAK1 inhibition led to a more durable Akt inhibition in both cell lines, associated with a mild reduction of viability when used in monotherapy compared to untreated cells, but the combination therapy with BRAF^{V600E} inhibition resulted in an enhanced survival of the cells at lower doses of JAK1i. This result might be influenced by the simultaneous JAK1/JAK2 inhibition exerted by ruxolinib, and the "Yin and Yang" functions of these two kinases in the regulation of cancer cell survival[95]. Despite the loss of ERK and/or Akt activity with the associated pro-survival signaling was a strong rational to identify kinases as putative drug targets to be explored in novel combination therapies, the complex balance between primary and moonlighting functions of these drug targets must be further investigated to understand their effect on survival of cancer cells. A combination of BRAF^{V600E}/MEK inhibition, or BRAF^{V600E}/Akt inhibition, still remains the most effective treatment in our model systems in vitro, but we speculate that triple combination therapies with novel drug targets might enable to lower drug doses (with consequent improvement of toxicity profiles) and improve treatment efficacy. In the future, validation of our putative drug targets in more advanced animal models might reveal their potential in combination therapies.

Conclusion

In summary, we report novel insights on ERK and Akt aberrant signaling in primary patient-derived melanoma cells enabled by live single cells measurements of ERK and Akt activity. Our findings show that sustained Akt activity is a key mechanism of resistance in our paradigm of intrinsic vs acquired resistance to BRAF^{V600E} inhibition and this mechanism was observed homogeneously across the population of cells. Despite the simultaneous inhibition of BRAF^{V600E} and Akt resulted in increased cytotoxicity, the reason behind the intrinsic resistance of a subpopulation of cells to combination therapy remains unclear. A more systemic knowledge of the network of kinase interactions is essential to discover novel drug targets that can increase the efficacy of combination therapies of two or more targeted drugs. Our study provides evidence for a moonlighting function of PAK3 and PLK4 that might be of great interest to be further explored in the context of improved combination therapy. Finally, we have not explored single-cell responses to inhibition of our candidate drug targets, as our monoclonal cell lines exhibited strong population behaviors. However, single-cell technology enabled us to observe population behaviors. Drug-refractory signaling states might evolve over time in subpopulations of cells and we envision that with the development of novel and more specific drugs we might be able to identify resistant cells by their signaling activity. The integration of high-throughput single cell genetic approaches and signaling data represents a big challenge for the future that we hope to shine some light on the complex wiring of the cellular kinome, and unveil hidden mechanism of resistances that are now overlooked.

Limitations of the study

We provided a rational for identifying putative molecular targets to inhibit in a combination therapy with BRAF inhibitors. At the present time, however, only 62 FDA-approved small molecule protein kinase inhibitors are available to target about two dozen different protein kinases[96]. Most of the kinome is understudied and far from being targeted by developing drugs[90]. Therefore, most of the hits found in our siRNA screens cannot be validated with small molecule inhibitors. Moreover, one of the main hurdles in early-stage kinase inhibitor projects remain the selectivity required for pharmacological target validation[97], which might have blurred also our findings.

AUTHOR CONTRIBUTION

AM and OP designed the study. AM performed the experiments and analyzed data. BN provided the RNAi expertise and support to run the RNAi screen at the ALMF facility in EMBL, Heidelberg. In the present form, AM wrote the manuscript.

DECLARATION OF INTERESTS

The authors declare that they have no competing interests.

REFERENCES

1. Craig, S., Earnshaw, C. H. & Virós, A. Ultraviolet light and melanoma: Ultraviolet light and melanoma. *J. Pathol* **244**, 578–585 (2018).

2. Lavoie, H. & Therrien, M. Regulation of RAF protein kinases in ERK signalling. *Nature Reviews Molecular Cell Biology* **16**, 281–298 (2015).

3. Ascierto, P. A. *et al.* Update on tolerability and overall survival in COLUMBUS: landmark analysis of a randomised phase 3 trial of encorafenib plus binimetinib vs vemurafenib or encorafenib in patients with BRAF V600–mutant melanoma. *European Journal of Cancer* **126**, 33–44 (2020).

4. Wang, L. *et al.* An Acquired Vulnerability of Drug-Resistant Melanoma with Therapeutic Potential. *Cell* **173**, 1413-1425.e14 (2018).

5. Arozarena, I. & Wellbrock, C. Overcoming resistance to BRAF inhibitors. *Ann. Transl. Med.* **5**, 387–387 (2017).

6. Shi, H. *et al.* Acquired Resistance and Clonal Evolution in Melanoma during BRAF Inhibitor Therapy. *Cancer Discovery* **4**, 80–93 (2014).

7. Montagut, C. *et al.* Elevated CRAF as a Potential Mechanism of Acquired Resistance to BRAF Inhibition in Melanoma. *Cancer Res* **68**, 4853–4861 (2008).

8. Villanueva, J. *et al.* Acquired Resistance to BRAF Inhibitors Mediated by a RAF Kinase Switch in Melanoma Can Be Overcome by Cotargeting MEK and IGF-1R/PI3K. *Cancer Cell* **18**, 683–695 (2010).

9. Yen, I. *et al.* ARAF mutations confer resistance to the RAF inhibitor belvarafenib in melanoma. *Nature* **594**, 418–423 (2021).

10. Gerosa, L. *et al.* Receptor-Driven ERK Pulses Reconfigure MAPK Signaling and Enable Persistence of Drug-Adapted BRAF-Mutant Melanoma Cells. *Cell Systems* S2405471220303707 (2020) doi:10.1016/j.cels.2020.10.002.

11. Akbani, R. *et al.* Genomic Classification of Cutaneous Melanoma. *Cell* **161**, 1681–1696 (2015).

12. Allen, E. M. V. *et al.* The Genetic Landscape of Clinical Resistance to RAF Inhibition in Metastatic Melanoma. 17.

13. Villanueva, J. *et al.* Acquired Resistance to BRAF Inhibitors Mediated by a RAF Kinase Switch in Melanoma Can Be Overcome by Cotargeting MEK and IGF-1R/PI3K. *Cancer Cell* **18**, 683–695 (2010).

14. Irvine, M. *et al.* Oncogenic PI3K/AKT promotes the step-wise evolution of combination BRAF/MEK inhibitor resistance in melanoma. *Oncogenesis* **7**, 72 (2018).

15. Caporali, S. *et al.* Targeting the PI3K/AKT/mTOR pathway overcomes the stimulating effect of dabrafenib on the invasive behavior of melanoma cells with acquired resistance to the BRAF inhibitor. *International Journal of Oncology* **49**, 1164–1174 (2016).

16. Grzywa, T. M., Paskal, W. & Włodarski, P. K. Intratumor and Intertumor Heterogeneity in Melanoma. *Translational Oncology* **10**, 956–975 (2017).

17. Junker, J. P. & van Oudenaarden, A. Every Cell Is Special: Genome-wide Studies Add a New Dimension to Single-Cell Biology. *Cell* **157**, 8–11 (2014).

18. Fattore, L., Ruggiero, C. F., Liguoro, D., Mancini, R. & Ciliberto, G. Single cell analysis to dissect molecular heterogeneity and disease evolution in metastatic melanoma. *Cell Death Dis* **10**, 827 (2019).

19. Levine, J. H., Lin, Y. & Elowitz, M. B. Functional Roles of Pulsing in Genetic Circuits. *Science* **342**, 1193–1200 (2013).

20. Ryu, H. *et al.* Frequency modulation of ERK activation dynamics rewires cell fate. *Mol Syst Biol* **11**, 838 (2015).

21. Rosenbloom, A. B. *et al.* β-Catenin signaling dynamics regulate cell fate in differentiating neural stem cells. *Proc Natl Acad Sci USA* **117**, 28828–28837 (2020).

22. Raaijmakers, M. I. *et al.* Co-existence of BRAF and NRAS driver mutations in the same melanoma cells results in heterogeneity of targeted therapy resistance. *Oncotarget* **7**, 77163 (2016).

23. Regot, S., Hughey, J. J., Bajar, B. T., Carrasco, S. & Covert, M. W. High-Sensitivity Measurements of Multiple Kinase Activities in Live Single Cells. *Cell* **157**, 1724–1734 (2014).

24. Multiplexed fluorescence imaging of ERK and Akt activities and cell-cycle progression.pdf.

25. Paulitschke, V. *et al.* Proteomic identification of a marker signature for MAPK i resistance in melanoma. *EMBO J* **38**, (2019).

26. Allen et al. - The Genetic Landscape of Clinical Resistance to RA.pdf.

27.   Regot, S., Hughey, J. J., Bajar, B. T., Carrasco, S. & Covert, M. W. High-Sensitivity Measurements of Multiple Kinase Activities in Live Single Cells. *Cell* **157**, 1724–1734 (2014).

28.   Maryu, G., Matsuda, M. & Aoki, K. Multiplexed Fluorescence Imaging of ERK and Akt Activities and Cell-cycle Progression. *Cell Struct. Funct.* **41**, 81–92 (2016).

29.   Bindels, D. S. *et al.* mScarlet: a bright monomeric red fluorescent protein for cellular imaging. *Nat Methods* **14**, 53–56 (2017).

30.   Shaner, N. C. *et al.* A bright monomeric green fluorescent protein derived from Branchiostoma lanceolatum. *Nat Methods* **10**, 407–409 (2013).

31.   Wan, P. T. C. *et al.* Mechanism of Activation of the RAF-ERK Signaling Pathway by Oncogenic Mutations of B-RAF. *Cell* **116**, 855–867 (2004).

32.   Shcherbakova, D. M. *et al.* Bright monomeric near-infrared fluorescent proteins as tags and biosensors for multiscale imaging. *Nature Communications* **7**, 12405 (2016).

33.   Pollock, C. B., Shirasawa, S., Sasazuki, T., Kolch, W. & Dhillon, A. S. Oncogenic *K-RAS* Is Required to Maintain Changes in Cytoskeletal Organization, Adhesion, and Motility in Colon Cancer Cells. *Cancer Res* **65**, 1244–1250 (2005).

34.   Campbell, P. M. & Der, C. J. Oncogenic Ras and its role in tumor cell invasion and metastasis. *Seminars in Cancer Biology* **14**, 105–114 (2004).

35.   Campa, C. C., Ciraolo, E., Ghigo, A., Germena, G. & Hirsch, E. Crossroads of PI3K and Rac pathways. *Small GTPases* **6**, 71–80 (2015).

36.   Castellano, E. *et al.* RAS signalling through PI3-Kinase controls cell migration via modulation of Reelin expression. *NATURE COMMUNICATIONS* 13.

37.   Nazarian, R. *et al.* Melanomas acquire resistance to B-RAF(V600E) inhibition by RTK or N-RAS upregulation. *Nature* **468**, 973–977 (2010).

38.   Johannessen, C. M. *et al.* COT drives resistance to RAF inhibition through MAP kinase pathway reactivation. *Nature* **468**, 968–972 (2010).

39.   Lito, P. *et al.* Relief of Profound Feedback Inhibition of Mitogenic Signaling by RAF Inhibitors Attenuates Their Activity in BRAFV600E Melanomas. *Cancer Cell* **22**, 668–682 (2012).

40.   Erfle, H. *et al.* Work Flow for Multiplexing siRNA Assays by Solid-Phase Reverse Transfection in Multiwell Plates. *J Biomol Screen* **13**, 575–580 (2008).

41.   Neumann, B. *et al.* Phenotypic profiling of the human genome by time-lapse microscopy reveals cell division genes. *Nature* **464**, 721–727 (2010).

42.   Quadri, H. S. *et al.* Expression of the scaffold connector enhancer of kinase suppressor of Ras 1 (CNKSR1) is correlated with clinical outcome in pancreatic cancer. *BMC Cancer* **17**, 495 (2017).

43.   Crowe, M. S. *et al.* RAF-Mutant Melanomas Differentially Depend on ERK2 Over ERK1 to Support Aberrant MAPK Pathway Activation and Cell Proliferation. *Mol Cancer Res* **19**, 1063 (2021).

44.   Hansen, C. G., Howard, G. & Nichols, B. J. Pacsin 2 is recruited to caveolae and functions in caveolar biogenesis. *Journal of Cell Science* **124**, 2777–2785 (2011).

45.   de Kreuk, B.-J., Anthony, E. C., Geerts, D. & Hordijk, P. L. The F-BAR Protein PACSIN2 Regulates Epidermal Growth Factor Receptor Internalization. *Journal of Biological Chemistry* **287**, 43438–43453 (2012).

46.   Smith, D. P. LIP1, a cytoplasmic protein functionally linked to the Peutz-Jeghers syndrome kinase LKB1. *Human Molecular Genetics* **10**, 2869–2877 (2001).

47.   Morén, A., Raja, E., Heldin, C.-H. & Moustakas, A. Negative Regulation of TGFβ Signaling by the Kinase LKB1 and the Scaffolding Protein LIP1. *Journal of Biological Chemistry* **286**, 341–353 (2011).

48.   Kasak, L. *et al.* Characterization of Protein Kinase ULK3 Regulation by Phosphorylation and Inhibition by Small Molecule SU6668. *Biochemistry* **57**, 5456–5465 (2018).

49.   Alto, L. T. & Terman, J. R. Semaphorins and their Signaling Mechanisms. in *Semaphorin Signaling* (ed. Terman, J. R.) vol. 1493 1–25 (Springer New York, 2017).

50.   Ohler, L., Niopek-Witz, S., Mainguet, S. E. & Möhlmann, T. Pyrimidine Salvage: Physiological Functions and Interaction with Chloroplast Biogenesis. *Plant Physiol.* **180**, 1816–1828 (2019).

51.   Moret, N. *et al.* Exploring the understudied human kinome for research and therapeutic opportunities. *bioRxiv* 2020.04.02.022277 (2020) doi:10.1101/2020.04.02.022277.

52.   Manning, B. D. & Toker, A. AKT/PKB Signaling: Navigating the Network. *Cell* **169**, 381–405 (2017).

53.   Zhu, C., Wei, Y. & Wei, X. AXL receptor tyrosine kinase as a promising anti-cancer approach: functions, molecular mechanisms and clinical applications. *Mol Cancer* **18**, 153 (2019).

54.   Lemke, G. Biology of the TAM Receptors. *Cold Spring Harbor Perspectives in Biology* **5**, a009076–a009076 (2013).

55.   Zuo, Q. *et al.* AXL/AKT axis mediated-resistance to BRAF inhibitor depends on PTEN status in melanoma. *Oncogene* **37**, 3275–3289 (2018).

56.   Simons, M., Gordon, E. & Claesson-Welsh, L. Mechanisms and regulation of endothelial VEGF receptor signalling. *Nat Rev Mol Cell Biol* **17**, 611–625 (2016).

57.   Parsons, S. J. & Parsons, J. T. Src family kinases, key regulators of signal transduction. *Oncogene* **23**, 7906–7909 (2004).

58.   Dougherty, M. K. *et al.* KSR2 Is a Calcineurin Substrate that Promotes ERK Cascade Activation in Response to Calcium Signals. *Molecular Cell* **34**, 652–662 (2009).

59.   Bousoik, E. & Montazeri Aliabadi, H. "Do We Know Jack" About JAK? A Closer Look at JAK/STAT Signaling Pathway. *Front. Oncol.* **8**, 287 (2018).

60.   Levine, R. L., Pardanani, A., Tefferi, A. & Gilliland, D. G. Role of JAK2 in the pathogenesis and therapy of myeloproliferative disorders. *Nat Rev Cancer* **7**, 673–683 (2007).

61.   VanSaun, M. N. Molecular Pathways: Adiponectin and Leptin Signaling in Cancer. *Clin Cancer Res* **19**, 1926–1932 (2013).

62.   Mousson, A. *et al.* Inhibiting FAK–Paxillin Interaction Reduces Migration and Invadopodia-Mediated Matrix Degradation in Metastatic Melanoma Cells. *Cancers* **13**, 1871 (2021).

63.   Hirata, E. *et al.* Intravital Imaging Reveals How BRAF Inhibition Generates Drug-Tolerant Microenvironments with High Integrin β1/FAK Signaling. *Cancer Cell* **27**, 574–588 (2015).

64.   Xia, H., Nho, R. S., Kahm, J., Kleidon, J. & Henke, C. A. Focal Adhesion Kinase Is Upstream of Phosphatidylinositol 3-Kinase/Akt in Regulating Fibroblast Survival in Response to Contraction of Type I Collagen Matrices via a β1 Integrin Viability Signaling Pathway. *Journal of Biological Chemistry* **279**, 33024–33034 (2004).

65.   Lu, H. *et al.* PAK signalling drives acquired drug resistance to MAPK inhibitors in BRAF-mutant melanomas. *Nature* **550**, 133–136 (2017).

66.   Ramón-Maiques, S., Marina, A., Gil-Ortiz, F., Fita, I. & Rubio, V. Structure of Acetylglutamate Kinase, a Key Enzyme for Arginine Biosynthesis and a Prototype for the Amino Acid Kinase Enzyme Family, during Catalysis. *Structure* **10**, 329–342 (2002).

67.   N M Weijers, R. Identification of The Downregulation of TPD52-Like3 Gene and NKX2-1 Gene in Type 2 Diabetes Mellitus Via RNA Sequencing. *ADO* **3**, (2020).

68.   Tennstedt, P. *et al.* Patterns of TPD52 overexpression in multiple human solid tumor types analyzed by quantitative PCR. *International Journal of Oncology* **44**, 609–615 (2014).

69.   Chuang, H.-C., Wang, X. & Tan, T.-H. MAP4K Family Kinases in Immunity and Inflammation. in *Advances in Immunology* vol. 129 277–314 (Elsevier, 2016).

70.   Shaul, Y. D. & Seger, R. The MEK/ERK cascade: From signaling specificity to diverse functions. *Biochimica et Biophysica Acta (BBA) - Molecular Cell Research* **1773**, 1213–1226 (2007).

71.   Higuchi, M., Onishi, K., Kikuchi, C. & Gotoh, Y. Scaffolding function of PAK in the PDK1–Akt pathway. *Nat Cell Biol* **10**, 1356–1364 (2008).

72.   Wu, H.-Y., Yang, M.-C., Ding, L.-Y., Chen, C. S. & Chu, P.-C. p21-Activated kinase 3 promotes cancer stem cell phenotypes through activating the Akt-GSK3β-β-catenin signaling pathway in pancreatic cancer cells. *Cancer Letters* **456**, 13–22 (2019).

73.   Zhang, X., Wei, C., Liang, H. & Han, L. Polo-Like Kinase 4's Critical Role in Cancer Development and Strategies for Plk4-Targeted Therapy. *Front. Oncol.* **11**, 587554 (2021).

74.   Kazazian, K. *et al.* Plk4 Promotes Cancer Invasion and Metastasis through Arp2/3 Complex Regulation of the Actin Cytoskeleton. *Cancer Res* **77**, 434–447 (2017).

75.   Tian, X. *et al.* Polo-like kinase 4 mediates epithelial–mesenchymal transition in neuroblastoma via PI3K/Akt signaling pathway. *Cell Death Dis* **9**, 54 (2018).

76.   Arozarena, I. & Wellbrock, C. Phenotype plasticity as enabler of melanoma progression and therapy resistance. *Nat Rev Cancer* **19**, 377–391 (2019).

77.   Pratilas, C. A. *et al.* V600EBRAF is associated with disabled feedback inhibition of RAF-MEK signaling and elevated transcriptional output of the pathway. *Proceedings of the National Academy of Sciences* **106**, 4519–4524 (2009).

78.   Lake, D., Corrêa, S. A. L. & Müller, J. Negative feedback regulation of the ERK1/2 MAPK pathway. *Cell. Mol. Life Sci.* **73**, 4397–4413 (2016).

79.   Fritsche-Guenther, R. *et al.* Strong negative feedback from Erk to Raf confers robustness to MAPK signalling. *Mol Syst Biol* **7**, 489 (2011).

80.   Caunt, C. J., Sale, M. J., Smith, P. D. & Cook, S. J. MEK1 and MEK2 inhibitors and cancer therapy: the long and winding road. *Nat Rev Cancer* **15**, 577–592 (2015).

81.   Senju, Y. *et al.* Protein kinase C (PKC)-mediated phosphorylation of PACSIN2 triggers the removal of caveolae from the plasma membrane. *Journal of Cell Science* jcs.167775 (2015) doi:10.1242/jcs.167775.

82.   Simanshu, D. K., Nissley, D. V. & McCormick, F. RAS Proteins and Their Regulators in Human Disease. *Cell* **170**, 17–33 (2017).

83.   Zimmermann, S. Phosphorylation and Regulation of Raf by Akt (Protein Kinase B). *Science* **286**, 1741–1744 (1999).

84.   Ong, C. C. *et al.* P21-Activated Kinase 1 (PAK1) as a Therapeutic Target in BRAF Wild-Type Melanoma. *JNCI: Journal of the National Cancer Institute* **105**, 606–607 (2013).

85.   Chong, C., Tan, L., Lim, L. & Manser, E. The Mechanism of PAK Activation. *Journal of Biological Chemistry* **276**, 17347–17353 (2001).

86.   Gromnitza, S. *et al.* Tropomyosin-related kinase C (TrkC) enhances podocyte migration by ERK-mediated WAVE2 activation. *FASEB j.* **32**, 1665–1676 (2018).

87.   Yamazaki, D. *et al.* WAVE2 is required for directed cell migration and cardiovascular development. *Nature* **424**, 452–456 (2003).

88.   Cho, J. H. *et al.* AKT1 Activation Promotes Development of Melanoma Metastases. *Cell Reports* **13**, 898–905 (2015).

89.	Xia, H., Nho, R. S., Kahm, J., Kleidon, J. & Henke, C. A. Focal Adhesion Kinase Is Upstream of Phosphatidylinositol 3-Kinase/Akt in Regulating Fibroblast Survival in Response to Contraction of Type I Collagen Matrices via a β1 Integrin Viability Signaling Pathway. *Journal of Biological Chemistry* **279**, 33024–33034 (2004).

90.	Fabbro, D., Cowan-Jacob, S. W. & Moebitz, H. Ten things you should know about protein kinases: IUPHAR Review 14: Ten things you should know about protein kinases. *Br J Pharmacol* **172**, 2675–2700 (2015).

91.	Zhang, S. & Yu, D. Targeting Src family kinases in anti-cancer therapies: turning promise into triumph. *Trends in Pharmacological Sciences* **33**, 122–128 (2012).

92.	Kennedy, S. P., Hastings, J. F., Han, J. Z. R. & Croucher, D. R. The Under-Appreciated Promiscuity of the Epidermal Growth Factor Receptor Family. *Front. Cell Dev. Biol.* **4**, (2016).

93.	Herr, R. *et al.* BRAF inhibition upregulates a variety of receptor tyrosine kinases and their downstream effector Gab2 in colorectal cancer cell lines. *Oncogene* **37**, 1576–1593 (2018).

94.	Campbell, S. L. *et al. Glutamine deprivation triggers NAGK-dependent hexosamine salvage.* http://biorxiv.org/lookup/doi/10.1101/2020.09.13.294116 (2020) doi:10.1101/2020.09.13.294116.

95.	Wu, Q. *et al.* JNK signaling in cancer cell survival. *Med Res Rev* **39**, 2082–2104 (2019).

96.	Roskoski, R. Properties of FDA-approved small molecule protein kinase inhibitors: A 2021 update. *Pharmacological Research* **165**, 105463 (2021).

97.	Ferguson, F. M. & Gray, N. S. Kinase inhibitors: the road ahead. *Nat Rev Drug Discov* **17**, 353–377 (2018).

98.	McQuin, C. *et al.* CellProfiler 3.0: Next-generation image processing for biology. *PLoS Biol* **16**, e2005970 (2018).

99.	Berg, S. *et al.* ilastik: interactive machine learning for (bio)image analysis. *Nat Methods* **16**, 1226–1232 (2019).

100.	Dobrzyński, M., Jacques, M.-A. & Pertz, O. Mining single-cell time-series datasets with Time Course Inspector. *Bioinformatics* **36**, 1968–1969 (2020).

101. Otasek, D., Morris, J. H., Bouças, J., Pico, A. R. & Demchak, B. Cytoscape Automation: empowering workflow-based network analysis. *Genome Biol* **20**, 185 (2019).

102. Raaijmakers, M. I. G. *et al.* A new live-cell biobank workflow efficiently recovers heterogeneous melanoma cells from native biopsies. *Exp Dermatol* **24**, 377–380 (2015).

103. Gagliardi, P. A. *et al.* Collective ERK/Akt activity waves orchestrate epithelial homeostasis by driving apoptosis-induced survival. *Developmental Cell* S1534580721004366 (2021) doi:10.1016/j.devcel.2021.05.007.

104. Shcherbakova, D. M. *et al.* Bright monomeric near-infrared fluorescent proteins as tags and biosensors for multiscale imaging. *Nat Commun* **7**, 12405 (2016).

105. Balasubramanian, S., Wurm, F. M. & Hacker, D. L. Multigene expression in stable CHO cell pools generated with the piggyBac transposon system. *Biotechnol Progress* **32**, 1308–1317 (2016).

106. Yusa, K., Zhou, L., Li, M. A., Bradley, A. & Craig, N. L. A hyperactive piggyBac transposase for mammalian applications. *Proceedings of the National Academy of Sciences* **108**, 1531–1536 (2011).

107. Doncheva, N. T., Morris, J. H., Gorodkin, J. & Jensen, L. J. Cytoscape StringApp: Network Analysis and Visualization of Proteomics Data. *J. Proteome Res.* **18**, 623–632 (2019).

METHODS

KEY RESOURCES TABLE

REAGENT or RESOURCE	SOURCE	IDENTIFIER
Antibodies		
Monoclonal Anti-MAP Kinase, Activated (Diphosphorylated ERK-1&2)	Sigma-Aldrich	M8159
Phospho-Akt (Ser473)	Cell Signaling Technology	9271
Chemicals		
Hygromycin B solution	Santa Cruz biotechnology	sc-29067
Blasticidin S HCL	Tocris Bioscience	5502
Puromycin dihydrochloride	Sigma-Aldrich	P7255
FuGENE® HD Transfection Reagent	Promega	E2311
Dabrafenib	Selleckchem	S2807
Cobimetinib	Selleckchem	S8041
MK2206	MedChem Express	HY-108232
SCH772984	MedChem Express	HY-50846
Centrinone	MedChem Express	HY-18682
Defactinib	MedChem Express	HY-12289
Ruxolitinib	MedChem Express	HY-50856
Bemcentinib	MedChem Express	HY-101977
FRAX486	MedChem Express	HY-15542B
DAPI		
Lipofectamine™2000 Transfection Reagent	invitrogen	12566014
Deposited data		
Raw and analyzed data	This paper	
Experimental models: Cell lines		
M000921 (Homo Sapiens)	URPP Biobank, University of Zurich; Zurich; Switzerland	CVCL_S808
MM121224 (Homo Sapiens)	URPP Biobank, University of Zurich; Zurich; Switzerland	10.18632/oncotarget.12848
Oligonucleotides		
Primer forward for cloning ERK-KTR-mScarlet in pPB: TCAGGGATCCACTAGTGCCAC CATGAAGGGAAGA	This paper	N/A
Primer reverse for cloning ERK-KTR-mScarlet in pPB: CATGCTCGAGCGGCCGCTTA TCTAGATCCGGTGGATC	This paper	N/A

Continued

REAGENT or RESOURCE	SOURCE	IDENTIFIER
Recombinant DNA		
pMB-PB-FoxO3A-mNeonGreen	Laboratory of Olivier Pertz, University of Bern, Switzerland	N/A
H2B-miRFP703	Laboratory of Vladislav Verkhusha Lab, Albert Einstein College of Medicine	Addgene #80001
pBrHygro-ERK-KTR-mScarlet	Laboratory of Olivier Pertz, University of Bern, Switzerland	N/A
pPBbSr2-miRFP703	Laboratory of Olivier Pertz, University of Bern, Switzerland	N/A
Software and algorithms		
Cell Profiler 2.2.0 and Cell Profiler 3.0	McQuin et al., 2018[98]	https://cellprofiler.org/
Ilastik 1.3.3	Berg et al., 2018[99]	https://www.ilastik.org/
ImageJ	Schneider et al., 2012	https://imagej.nih.gov/ij/
R 4.0	R Core Team, 2017	https://www.R-project.org/
RStudio-1.4.1106	RStudio	https://rstudio.com/
Time Course Inspector (TCI)	Dobrzynski et al., 2020[100]	https://github.com/pertzlab/shinytimecourse-inspector
Cytoscape 3.8	Otasek et al., 2019[101]	https://cytoscape.org/
shinyHTM	Botelho and Tischer, github	http://doi.org/10.5281/zenodo.2594651
stringApp 1.6.0	Doncheva et al., 2019	https://apps.cytoscape.org/apps/stringapp
Other		
Eclipse Ti inverted fluorescence microscope	Nikon	N/A

MATERIAL AND METHODS

Cell lines and cell culture

Validated primary patient-derived melanoma cell lines M000921 and MM121224 were given by M.P. Levesque, University Hospital Zurich, Zurich, Switzerland, through the university of Zurich biobank program in accordance with the ethical approval numbers 647 and 800. Cell lines were isolated as previously established[102] and have been regularly tested negatively for mycoplasm contamination. Both melanoma lines were cultured in growth RPMI-1640 medium formulated with 2 mM L-glutamine (Sigma-Aldrich/Merck) and supplemented with 10% fetal bovine serum (FBS; Sigma-Aldrich/Merck), 1% of 100 mM sodium pyruvate solution, 200U/mL penicillin and 200 µg/mL streptomycin. Stable cell lines with H2B-miRFP703, ERK-KTR-mScarlet, and Akt-KTR-mNeonGreen were generated by transfection with FuGENE (Promega) according to the manufacturer's protocol and antibiotic selection with Blasticidin, Hygromycin, and Puromycin, respectively. Unless differently specified, all the experiments were carried out in starvation medium, which differs from the complete medium by the absence of 10% FBS. Starvation was achieved by removing the growth medium followed by 2 washes in starvation medium, a final replacement with again starvation medium, and an incubation time of about 6h before the execution of the experiments.

Plasmids

All the plasmids used in the present study were available in our research group. Briefly, as previously described[103], the nuclear marker H2B-miRFP703[104] was subcloned in the PiggyBac plasmid pPBbSr2-MCS, and Akt-KTR-mNeonGreen was generated by fusing the green fluorescent protein mNeonGreen CDS (Shaner et al., 2013)[30] with the 1-1188 portion of the human forkhead box 03 a (FoxO3a) CDS. Akt-KTR-mNeonGreen was cloned in the PiggyBac plasmid pSB-HPB (gift of David Hacker, Lausanne)[105]. ERK-KTR[27]-mScarlet[29] sequence was ordered (Biomatik) and cloned in the PiggyBac plasmid pBr-HPB. The PiggyBac plasmids were co-transfected with the Super Piggybac Transposase Expression Vector to facilitate the integration of the genes of interest into the genome at TTAA sites[106].

Live imaging

M000921 cells were seeded on 96-well 1.5 glass bottom plates (Cellvis) coated with 50 µL of a 50 µg/mL PBS solution of type I collagen from bovine skin (Sigma-Aldrich) at a density of 2.8×10^3 cells/well one day before the experiment. MM121224 cells were seeded at a density of 3.6×10^3 cells/well instead. Both cell lines reached a confluency of about 60-70% before the starvation protocol performed 6h before the experiment. Epifluorescence live imaging was performed on an Eclipse Ti inverted microscope (Nikon) run by NIS-Elements (Nikon) with a Plan Apo air 20x (NA 0.8). Temperature (37°C) was kept with a temperature

control system, humidity (100%) and CO2 (~5%) with a gas mixer (both from Life Imaging Services). Focus drift was prevented by the equipped Perfect Focus System (Nikon). An Andor Zyla 4.2 plus camera acquired 16-bit depth images. The optical configurations of the acquisition channels were the following (all filters from Chroma): far red: 640 nm excitation filter and ET705/72m emission filter; Scarlet: 575nm, ET652/60m; Alexa 546: 555nm, ET652/60m;NeonGreen: 508nm, ET605/52; Alexa488: 470nm, ET525/36m; DAPI: 410nm, ET460/50.

Compounds

Dabrafenib and Cobimetinib were obtained from Sigma-Aldrich/Merck. MK2206, SCH772984, Bemcentinib, Defactinib, Ruxolitinib, FRAX486 and Centrinone were obtained from MedChem. All drugs were dissolved in DMSO to stock solutions (5, 10, or 20 mM) aliquoted in screw cap vials and preserved at -80°C to avoid thaw/freeze cycles. Across experiments, drug treatments were standardized to contain the 0.1% control concentration of DMSO.

Cell viability assay

2.9×10^3 cells/well for M000921, or 3.6×10^3 cells/well for MM121224 were seeded on 96-well 1.5 glass bottom plates (Cellvis) coated with collagen to achieve 60-70% confluency the day after. Cells were starved for 6 hours and then treated with different concentrations of either a BRAF inhibitor (Dabrafenib), a MEK inhibitor (Cobimetinib), an Akt inhibitor (MK2206), or inhibitors of the protein targets identified from the kinome siRNA screen (AXL, FAK, JAK1, PAK3, PLK4, were inhibited by Bemcentinib, Defactinib, Ruxolitinib, FRAX486. Centrinone, respectively). Combination of BRAF inhibitor with either of the above-mentioned drugs were performed as appropriately indicated. After 72 hours of treatment, cells were fixed with 4% PFA at 37°C for 20 minutes and washed 3x5min with PBS. Between 20 and 25 field of views (FOVs) per well (Plan Apo air 20x) were imaged, and nuclei of living cells were segmented and counted. Normalized number of cells/FOV was calculated against the median number of cells/FOV of the control wells. In Fig.3, control corresponds to DMSO treatment. In Fig.6, control corresponds to DMSO treatment for drug monotherapies, whereas for combination therapies (with Dabrafenib 4µM) the control corresponds to Dabrafenib 4 µM monotherapy. The percentage of living cells/FOV compared to control is shown as mean and 95% confidence interval of the mean.

Immunocytochemistry

Wild-type cells fixed in 4% PFA and washed 3x5min in PBS were permeabilized for 20 min with PBS containing 0.1% Triton X-100 (PanReac AppliChem ITW Reagents) and washed again 3x5min. Blocking was performed with 2% BSA, 22.52 mg/mL glycine in PBST (PBS + 0.1% Tween 20) for 30min and then

cells were incubated with the primary antibodies in 0.1% BSA in PBST overnight at 4°C. The day after, cells were washed 3x5min with PBS and then incubated 1 hour at room temperature with the secondary antibodies in 0.1% BSA in PBST. Cells were washed again 3x5min, counterstained with DAPI for 5min, and rinsed with PBS. Cells were then imaged.

Image analysis

For live imaging movies, and images of fixed nuclei from cell viability assays, the primary segmentation of the nuclei was achieved in two steps. The first step was to run a random forest classifier implemented in Ilastik software[99] to generate nuclear probability maps (as 16-bit TIF images). The classifier was manually trained to discern nuclear pixels (30-40 annotations), background, or artifact pixels in the raw 16-bit TIF images based on multiple pixel features available in Ilastik. The second step was to use CellProfiler 3.0[98] to segment nuclei using thresholding technique on these nuclear probability maps. For images of fixed cells produced from short-term experiments (< 24 hours) – in which cell death and resulting artifacts are not expected – nuclear segmentation was immediately achieved with a threshold-based segmentation of the nuclear channel (H2B-miRFP703 or DAPI) using CellProfiler 3.0.

The secondary segmentation of the entire cell shape was performed on a merged 16-bit TIF image made as the pixel-based sum of the rescaled images of ERK-KTR-mScarlet and Akt-KTR-mNeonGreen channels, or of the relevant channels of wild-type immunostained cells. Rescaling gave comparable weight to the two channels and prevented unstable segmentation of the cell boundaries in case either of the ERK or Akt biosensors was predominantly in the nucleus. Finally, expansion of nuclear objects along the boundaries of the cellular objects up to a predefined number of pixels gave us a ring-shaped area which corresponded to the proximal portion of the cytosol. The proximal portion of the cytosol guaranteed a robust quantification of cytosolic pixel intensities by excluding the distal portion of the cytosol which becomes thinner and dimmer with increasing distance from the nucleus. Cytosolic/nuclear ratio (C/N ratio) resulted from the division of the median cytosolic pixel intensities by the median nuclear pixel intensities. Quality control was performed on nuclear and cytosolic morphological features (compactness, form factor, eccentricity, area) and pixel intensity-based features (median intensity and texture) to remove artifacts not compatible with quantifiable cells (e.g. mitotic cell rounding). Single-cell "tracking-by-assignment" (i.e. on pre-detected objects) was performed on Ilastik 1.3.3.

Alternative KTR ratios

C/N ratio is used as a proxy for ERK and AKT activities. Inactive cells have C/N ratios that can theoretically reach a lower bound of 0, whereas active cells have C/N ratios that can increase indefinitely. C/N ratio is a simple and preferred measure for translocation phenotypes in cells that turn from inactive to active or viceversa. However, fluctuations in C/N ratios for cells that have high ERK/Akt activities are visually

overestimated for active cells that have very low KTR signals in the nucleus, in which minor frame-to-frame changes in nuclear signals (due to minor cell movements, or noise of the measurements) originate big variability in C/N ratios. To reduce this visual bias in the interpretation of C/N ratios in single-cell trajectories, we measure ERK/AKT activities as min-max normalized C/(C+N) ratio. C = cytosolic median intensity; N=nuclear median intensity. C/(C+N) ratio ranges between 0 and 1. Then, for both M000921 cells and MM121224 cells, a min-max normalization of the C/(C+N) ratio is performed. In Figure 2A-B and Figure S2A-B, a C/(C+N) value of 0 corresponds to the median C/(C+N) ratio of over 200 trajectories of M000921 cells maximally inhibited with a MEK inhibitor for ERK activity, and with an Akt inhibitor for Akt activity; a C/(C+N) value of 1 corresponds to the median C/(C+N) ratio of over 200 trajectories of M000921 cells in control condition.

Data Analysis

Single-cell ERK/Akt activities of fixed cells and living cells (time-series) were analyzed and visualized with custom R scripts.

RNAi screen

The kinome screen was performed at the Advanced Light Microscopy Facility (ALMF) at the European Molecular Biology Laboratory (EMBL), We used the Ambion™ Silencer™ Select Human Kinase siRNA Library V3 mapped against the 2019 human genome (ENSEMBL V95). The kinase library consists of three distinct siRNAs for each one of the 710 known and putative human kinome genes. The 2130 siRNAs were divided in 7 unique 384-well plate format layouts (A1, A2, A3, B1, B2, C1, C2) and delivered using a solid-phase reverse transfection technique (with minor modifications from the previously described protocol[40] in 384-well 1.5 glass bottom plates (Cellvis). Each layout generated up to 16 replica plates "ready to transfect" and suitable for long-term storage in dry conditions at room temperature. To quality control the transfection efficiency and specificity, the two rightmost columns of the 7 layouts were used for control siRNAs. In more details, screen 1 and 2 contained 12 wells with the XWNeg9 siRNA (negative control; Ambion), 8 wells were empty (negative control), 4 wells contained the AURKB siRNA s17612 (transfection efficiency control; Ambion), 4 wells contained the MAPK1 s11139 siRNA (Ambion) and 4 wells contained the MAPK3 s11140 siRNA (Ambion). *AURKB* KD leads to mitotic slippage and subsequent polyploidy, and the characteristic phenotype, as previously documented[41], was seen in all cases with good or complete penetrance. *MAPK1 KD* gave the expected heterogenous decrease of ERK activity.

Liquid handling and automation system

The delivery of the siRNAs into 384-well plates required the use of several liquid-dispensing devices, i.e. Viaflo 384 (Integra) and Rainin Liquidator™ 96 (Mettler-Toledo). Cells were seeded in 50uL/well of growth

medium using a Multidrop Reagent Dispenser (Thermo Scientific). M000921 cells were seeded at a density of 500 cells/well, whereas MM121224 at a density of 650 cells/well. Screen 1 on M000921 and screen 2 on MM121224 required the replacement of the growth medium with starvation medium 66h after seeding. Screen 3 required the replacement of the growth medium with 3µM of Dabrafenib in starving medium 52h after seeding. To preserve cells from detachment during the starvation procedure (reduction of the FBS content from 10% to 0.1% or less), wells with growth medium were first diluted 4 times with starvation medium, then the whole plates were tilted and given a firm blow over multiple layers of absorbing paper to empty the wells (we observed that a thin layer of medium at the bottom of the wells protected cells from detachment when this starvation procedure was done with an FBS content above ~2%). Wells were then immediately filled with starvation medium and rinsed with starvation medium (screen 1 and 2) to reduce the FBS content below 0.1%, or starvation medium containing Dabrafenib (screen 3) to achieve a final concentration of 3 µM in the treated wells. After 72 hours from seeding, cells were fixed in 4% PFA (room temperature, 20min; Electron Microscopy Sciences), rinsed 3 times with PBS and counterstained with DAPI (20min) for a better compatibility of the nuclear channel with the optical configuration of the automated imaging solution at ALMF compared to the genetically encoded H2B-miRFP703.

Fixed cells microscopy

Automated wide-field fluorescence microscopy was performed on a Nikon Ti-E inverted screening microscope equipped with a robotic plate loader (Prior) and controlled by NIS-Elements (Nikon). The microscope mounted a 20x, 0.75 NA CFI P-Apo Lambda air objective (Nikon), a Sola SE II 365 light source (Lumencor), a DS-Qi2 camera (7.3 um pixel size; Nikon). The optical configurations were the following: Scarlet: 562/40 EX, 640/75 EM; NeonGreen: 482/35 EX, 536/40 EM; DAPI: 377/50 EX, 447/60 EM. Nine positions per well were acquired as 16-bit TIF images (2048x2048 pixels).

Screen image analysis

16-bit TIF images of the screen were processed on a HPC cluster with an automatic image analysis pipeline run on CellProfiler 2.2. Minor adaptations of the pipeline were manually curated on occasion. Nuclear segmentation was achieved with a threshold-based segmentation of the nuclear channel (DAPI) and the secondary and tertiary segmentations were performed as described in the "image analysis" section. The extracted intensities and morphological features generated the primary data.

Data analysis and hit selection

Quality control was first achieved by visual inspection of the images of control wells, then by comparing heat maps of the 384-well showing the image-based median ERK/Akt activities per well (9 positions) between duplicates, via the shinyHTM software (https://github.com/embl-cba/shinyHTM). At the single-cell level, miss detected object were removed by gating on nuclear and cytosolic morphological features (compactness, form factor, eccentricity, area) and pixel intensity-based features (median intensity and

texture) not compatible with quantifiable cells (e.g. mitotic cell rounding, cell debris, others). Images with less than 5 quantifiable cells and wells with less than 15 quantifiable cells were discarded. Linear correlation of the scatterplots of ERK/Akt signals between duplicates (Fig. S2C) confirmed the high reproducibility of the screen. Plate-by-plate robust normalization of single-cell ERK/Akt activities as reported by the C/N ratio was performed against the median of the XWNeg9 negative control. Criteria for gene hit selection were the phenotype penetrance for at least 2 out of 3 siRNAs per gene and the penetrance in both duplicates. Stringent thresholds for hit selection were applied on normalized ERK/Akt C/N ratios and were chosen to reflect the desired visible phenotype. In details, the threshold for ERK activity inhibition was set to 0.84 for screen 1 and screen 2; the threshold for Akt activity inhibition was set to 0.65 for screen 1, and 0.68 for screen 2 and screen 3. The ranked hitlists were sorted first on the amount of effective siRNAs (either 2 or 3 effective siRNAs per gene), and second on the average of the well-based median values of ERK/Akt C/N ratios of effective siRNAs across duplicates.

Network visualization

Protein-protein interaction (ppi) networks shown in Fig.4 and Figure S3 and S4 were elaborated with an automated pipeline for Cytoscape 3.8[101] written on a custom R script loaded with the RCy3 package (R library leveraging the CyREST API). The pipeline first generated and imported ppi networks via stringApp[107] out of the hit list of the indicated screen condition and phenotype of interest. The lists of hits fed to stringApp were complemented by a set of core components of ERK/Akt pathways to shown potential interactions with these two networks, and complemented by a minimum of 1 and a maximum of 3 additional interactors (based on the size of the particular hit list) evaluated by string based on significancy of interaction with the input nodes. Then, the interaction knowledge was sorted to only include curated databases, experiments, and text mining, with edge (interaction) scores at medium confidence. A force-directed layout was applied, and the final position of the nodes was manually adjusted to improve consistency of visualization across networks. Color-code representation of the nodes and the edges is indicated in the figure legend.

Supplementary material:

Exploring Signaling Mechanisms regulating genetic and non-genetic Drug Resistance in Melanoma

Alberto Mattei [1], Maciej Dobrzyński [1], Beate Neumann [2], Mitchell P. Levesque [3], Olivier Pertz [1,4]*

[1] Institute of Cell Biology, University of Bern, Baltzerstrasse 4, 3012 Bern, Switzerland

[2] EMBL Heidelberg, Meyerhofstrasse 1, 69117 Heidelberg, Germany

[3] Department of Dermatology, University of Zurich Hospital, Gloriastrasse 31, 8091 Zurich, Switzerland
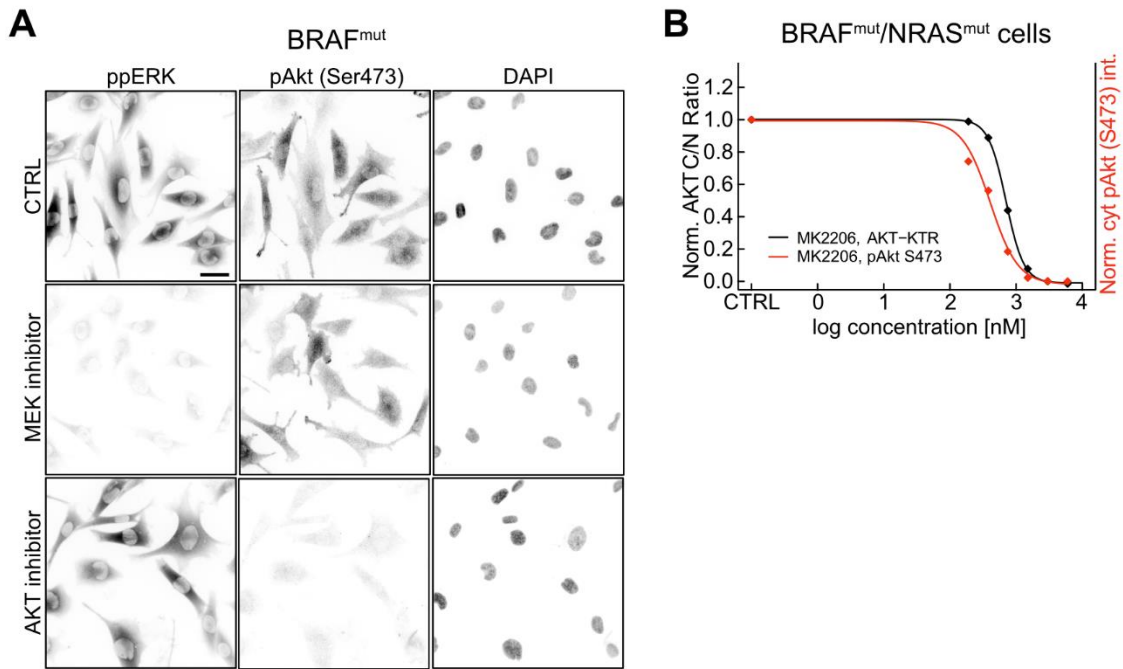
[4] Lead contact

Figure S1

Figure S1 (relative to main figure 1): immunostaining of pERK and pAkt Ser473 as validation of ERK/Akt biosensors. (A) Representative micrographs of pERK and pAkt Ser473 signals in BRAF[V600E] cells that do not express the biosensors in presence of Akt or MEK inhibition. Scale bar = 50 µm. **(B)** Dose-response curves of an Akt inhibitor as fitted from biosensor measurements (black lines) and from average cytosolic intensities of pAkt S473 immunostaining data (red lines) measured in the same BRAF[V600E]/NRAS[Q61K] cells. Data were min-max normalized between the 3rd quartile of inhibited cells (value= 0) and the median of the control (value=1). Symbols indicate median values.

Figure S2

A BRAF^mut

B BRAF^mut/NRAS^mut

C BRAF^mut
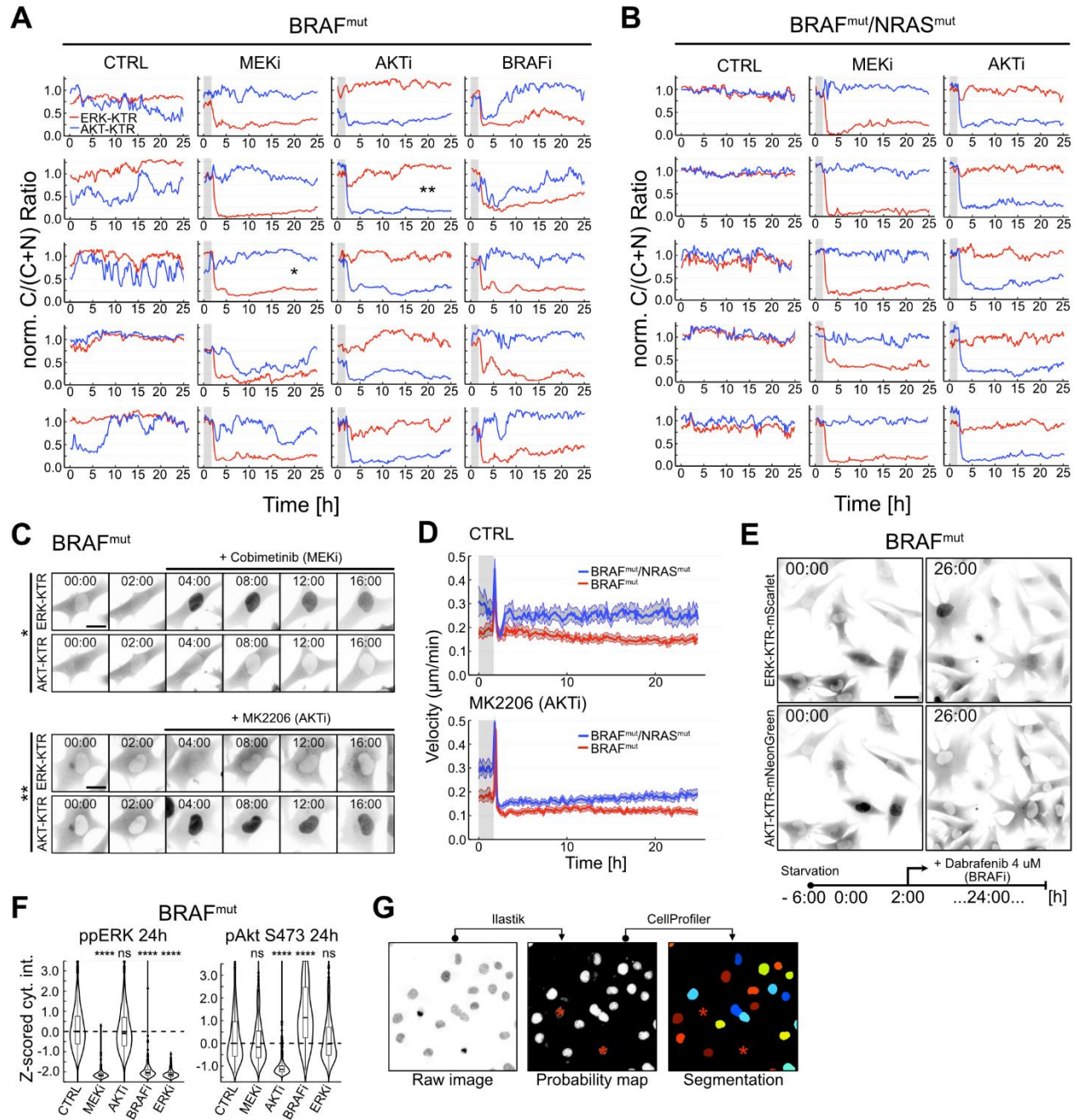
D

E BRAF^mut

F BRAF^mut

G

Figure S2 (relative to main figure 2): BRAF inhibition converts fluctuating Akt activity in BRAF^{V600E} to sustained activity. (A,B) Representative single-cell trajectories of ERK/Akt activities in BRAF^{V600E} cells (A) and BRAF^{V600E}/NRAS^{Q61K} cells (B) for the indicated treatments. ERK/Akt activities are reported here as min-max normalized cytosolic/(cytosolic+nuclear) fluorescence ratio of ERK/Akt KTR biosensors (details in

90

material and methods). Asterisks refer to the corresponding micrographs in (C). Gray areas indicate the first 2h of baseline before drug addition. **(C)** Micrographs of ERK-KTR and Akt-KTR signals relative to the trajectories labeled with asterisks in BRAF^{V600E} cells in (A), in presence of MEK (top) or Akt (bottom) inhibition. T: hours:minutes; scale bar = 25 µm. **(D)** Population medians of cellular velocity (µm/min) are shown for controls and treatment with MK2206 (2 µM). Abrupt increase of velocity immediately after addition of DMSO/drug in starvation medium at 2 hours is an artifact of liquid pipetting under the microscope. Gray areas indicate the 95% confidence interval of the population medians (N > 300 cells for every group). Gray areas indicate the first 2 hours of baseline before the drug addition. **(E)** Representative ERK/Akt KTR images before and 24 hours after dabrafenib treatment. Scale bar = 50 µm. **(F)** Violin plots that show normalized Z-scored mean cytosolic intensities of pERK (left) and pAkt Ser473 (right) against control in BRAF^{V600E} cells after 24 hours of incubation with the indicated treatments. Boxplots inside the violins indicate median and interquartile range. The horizontal dashed lines indicate the control at Z-score=0. N=200 cells per group. Significance was obtained with a non-parametric Mann-Whitney U test. *, P <0.05; ****, P < 0.0001. **(G)** Schematic of the pipeline to identify nuclei of living cells (details in material and methods). Red asterisks indicate the position of objects in the raw images correctly evaluated as not healthy nuclei. MEKi = 0.2 µM Cobimetinib; Akti = 2 µM MK2206; BRAFi = 4 µM Dabrafenib; ERKi = 0.2 µM of SCH772984.

Figure S3
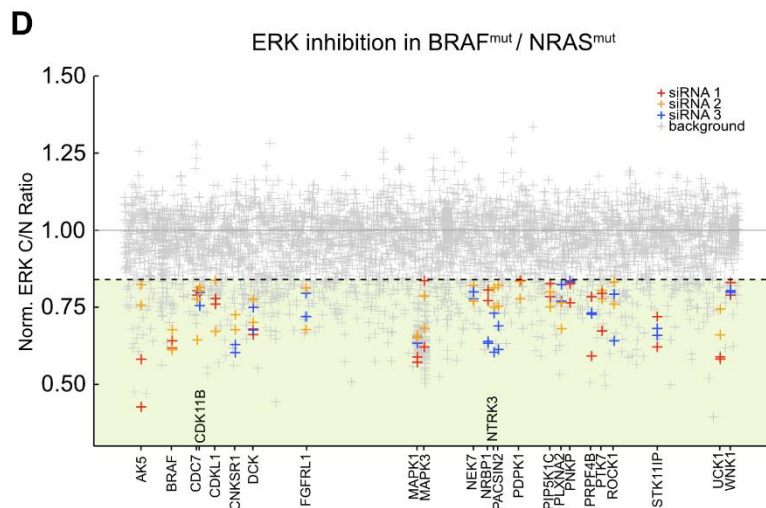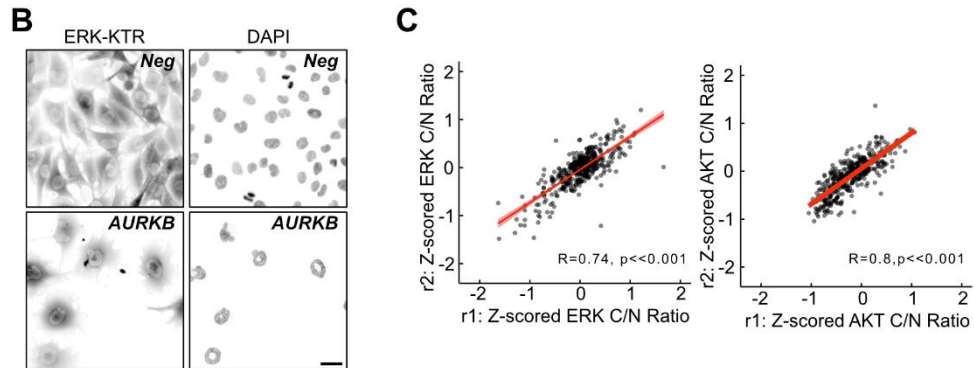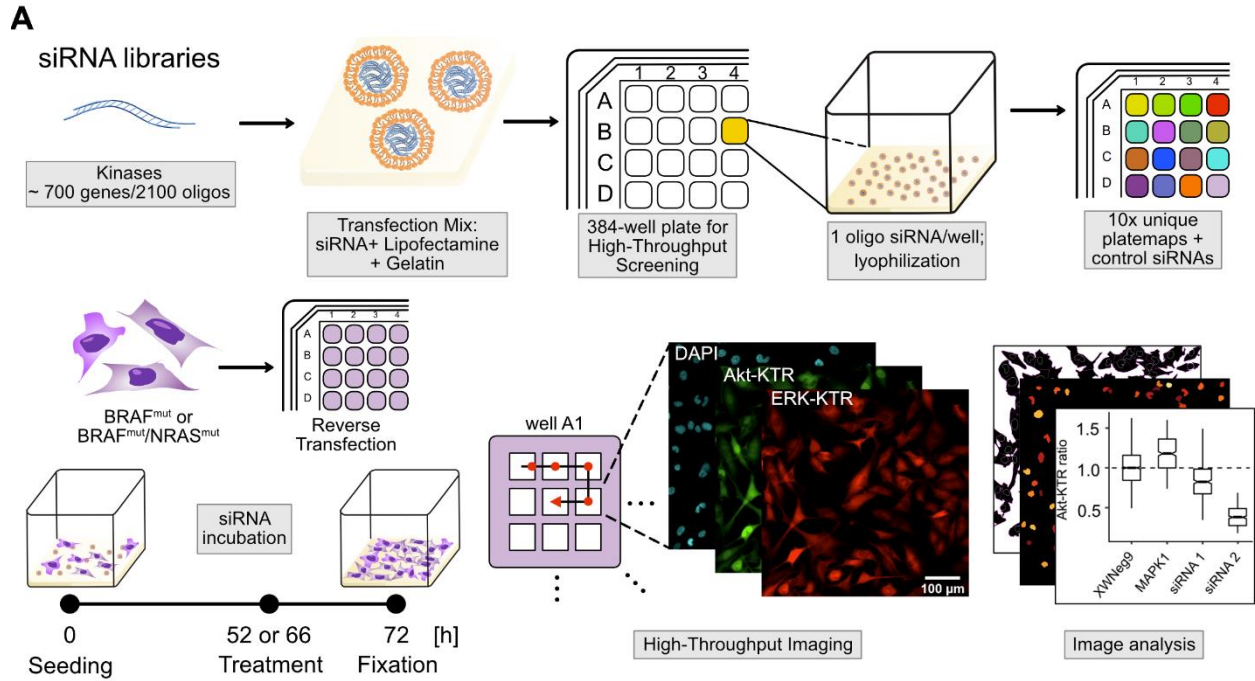
Figure S3 (relative to main figure 3): High-throughput setting for siRNA screening on BRAF^{V600E} and BRAF^{V600E}/NRAS^{Q61K} cells. (A) Ambion™ Silencer™ Select Human Kinase siRNA Library V3 (3 oligo siRNAs per gene) are first mixed with Lipofectamine 2000 and gelatin, then diluted with water, and finally distributed into 10 unique 384-well plate layouts (platemaps) to be lyophilized and stored dry for years. Up to 16 replicates of a single layout can be produced at a time (upper panels). Melanoma cells are reverse transfected upon seeding on lyophilized screen plates in complete medium. In screen 1 and screen 2 complete medium is replaced with starving medium (SM) after 66 hours to allow cells to starve for a period of 6 hours before fixation. In screen 3 complete medium is replaced with 3 µM of Dabrafenib in starving medium after 52 hr. After 72 hours of total siRNA incubation, cells are fixed and imaged with a high-throughput automated microscope equipped with a robotic well plate loading system. The siRNA screens are performed in duplicates. **(B)** Representative micrographs of ERK-KTR signal and nuclear signal in cells transfected with *AURKB* siRNA, our transfection efficiency control. Scale bar = 50 µm **(C)** Scatterplots of Z-scored ERK- (left) and Akt- (right) KTR C/N ratios across duplicates show high correlation (Spearman's Rank Sum Correlation Test). **(D)** Scatterplot that shows the effect of the hits identified in screen 2 for KDs that downregulate ERK activity. X-axis is the list of all the kinase genes sorted in alphabetical order. X-axis labels are present only for hits. Y-axis shows the magnitude of the effect on ERK activity as reported by normalized C/N ratios per plate. Red, orange, and blue crosses correspond to the first, second and third siRNA of a particular gene. Highlighted are siRNAs that showed the desired phenotype in both replicates. Grey crosses correspond to the siRNAs that do not display the desired phenotype. For details on the data processing and analysis of kinome siRNA screens refer to the material and methods section. Green area indicates the phenotype space beyond the threshold (at C/N ratio = 0.84).

Figure S4

A — AKT inhibition in BRAF^mut

B — AKT inhibition in BRAF^mut / NRAS^mut

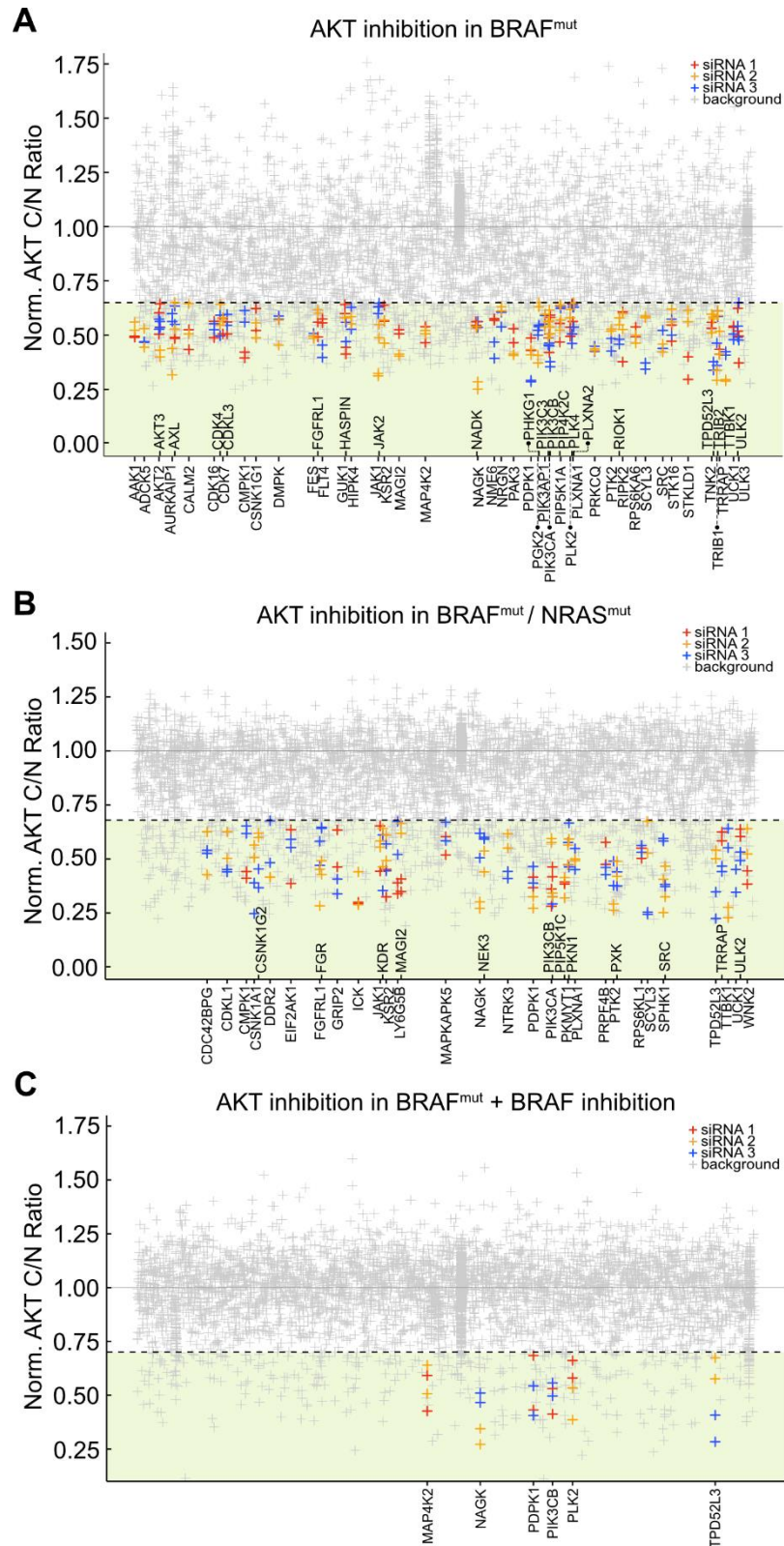**C** — AKT inhibition in BRAF^mut + BRAF inhibition

Figure S4 (relative to main figure 3): Hit spaces composed of kinase KDs that downregulated Akt activity in screen 1-2-3. (A,B,C) Scatterplot that shows the effect of the hits identified in screen 1 (A), screen 2 (B), and screen 3 (C) for KDs that downregulate Akt activity. X-axis is the list of all the kinase genes sorted in alphabetical order. X-axis labels are present only for gene hits. Y-axis shows the magnitude of the effect on Akt activity as reported by normalized C/N ratios per plate. Red, orange, and blue crosses correspond to the first, second and third siRNA of a particular gene. Highlighted are siRNAs that showed the desired phenotype in both replicates. Grey crosses correspond to the siRNAs that do not display the desired phenotype. For details on the data processing and analysis of kinome siRNA screens refer to the material and methods section. Green area indicates the phenotype space beyond the threshold (at C/N ratio = 0.65 for screen A, 0.70 for screen 2, and 0.7 for screen 3).
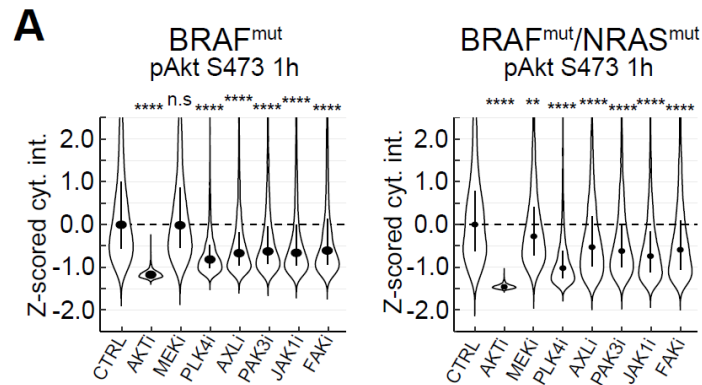
Figure S5

Figure S5 (relative to main figure 5): immunostaining of pAkt Ser473 validates kinase targets as Akt pathway interactors. (A) Violin plots that show normalized Z-scored mean cytosolic intensities of pAkt Ser473 against control in BRAF[V600E] cells after 1 hour of incubation with the indicated treatments. Boxplots inside the violins indicate median and interquartile range. The horizontal dashed lines indicate the control at Z-score=0. N=200 cells per group. Significance was obtained with a non-parametric Mann-Whitney U test. n.s., not significant; *, P <0.05; ****, P < 0.0001.

5.Additional Results

5.1 Phosphatome-wide siRNA Sscreens

5.1.1 Introduction

Cell signaling is dominated by phosphorylation and dephosphorylation events. Phosphatases negatively regulate protein phosphorylation and they can act on several timescales, i.e. with immediate or delayed activity. The interplay between kinase and phosphatase activities creates spatiotemporal phosphorylation patterns flowing through a signaling network that finally shape the overall kinetics of activation of the downstream kinase effector of a signaling pathway. Signal transduction through a wired network can therefore be attenuated or terminated by phosphatase activity, often within seconds or minutes. In other words, induced phosphatase activities create negative feedback loops that impact on signaling dynamics[76]. The importance of phosphatases in cell signaling makes them attractive targets for drug development. However, investigation of the regulation of phosphatases has been a challenge for two main reasons. First, to study a given phosphatase function *in vitro* the relevant substrate need to be first phosphorylated by the relevant kinase. Second, the almost impossible development of specific small molecule inhibitors due to the highly conserved, shallow active site.

Here, we performed phosphatome-wide siRNA screens targeting each three oncogenic signaling paradigms to identify relevant players that act as positive or negative regulators of ERK and Akt aberrant activities.

As presented in the manuscript in chapter 4 (Results), the three oncogenic signaling paradigms, corresponding to screen 1, screen 2, and screen 3, are:

1) Sustained ERK activity and Akt activity that fluctuates on timescales of hours in BRAF^{V600E} cells,
2) Sustained ERK and Akt activity in BRAF^{V600E}/NRAS^{Q61K} cells,
3) Sustained Akt activity in BRAF^{V600E} cells mediated by dabrafenib BRAF^{V600E} inhibition over timescales of hours.

In the future, such systemic knowledge might provide new possibilities of research to tackle the problem of drug resistance in melanoma.

5.1.2 Material and methods

Phosphatome-wide RNAi screens were performed as described in the Material and Methods section of the manuscript. Differences are briefly described here.

1) We used the Ambion™ Silencer™ Human Phophatase siRNA Library mapped against the 2019 human genome (ENSEMBL V95). The kinase library consists of three distinct siRNAs for each one of the 298 known and putative human phosphatome genes. The 894 siRNAs were divided in 3 unique 384-well plate format layouts (A1, B1, C1).

2) Screen 1 and Screen 2 (BRAF^{V600E} line and BRAF^{V600E}/NRAS^{Q61K} line in starvation, respectively) were performed in triplicates, while screen 3 in duplicates (BRAF^{V600E} cells treated with the BRAF^{V600E} inhibitor dabrafenib).

3) Criteria for hit selection were the phenotype penetrance for at least 2 out of 3 siRNAs per gene and the penetrance in at least 2 out of 3 replicates. Stringent thresholds for hit selection were applied on normalized ERK/Akt C/N ratios and were chosen to reflect the desired visible phenotype.

4) As for the kinome screens, the threshold for ERK activity inhibition was set to 0.84 for screen 1 and screen 2; the threshold for Akt activity inhibition was set to 0.65 for screen 1, and 0.68 for screen 2 and screen 3. Additionally, the threshold for ERK activity upregulation was set to 1.15 for screen 1 and screen 2, and 1.3 for screen 3; the threshold for Akt activity upregulation was set to 1.2 for screen 1, and 1.15 for screen 2 and screen 3.

5.1.3 Results

Tables that list the hits that we found are presented below. The ranking reflects the penetrance of the phenotype. Genes in bold characters are shared between either two or three of the screens.

List 1 **Hits that led to loss of ERK activity**.

Rank	Screen 1	Screen 2	Screen 3
1	*PPA1*	*DUSP13*	-
2		*DUSP5*	

List 2 **Hits that led to gain of ERK activity**.

Rank	Screen 1	Screen 2	Screen 3
1	***PPP2R2A***	***PPP2CA***	***PPP6C***
2	*CTDP1*	***PPP6C***	
3	*PPP2R1A*	*PPP2CB*	
4	*PPP1R14C*	***PPP2R2A***	
5	*FIG4*		
6	*PALD1*		
7	*MTMR9*		
8	*PTP4A3*		
9	***PPP2CA***		

List 3 **Hits that led to loss of Akt activity**.

Rank	Screen 1	Screen 2	Screen 3
1	*G6PC*	***ACP7***	*ACP5*
2	*PTPRZ1*	***PLPP3***	*INPP5K*
3	*DUSP1*	*ALPI*	
4	*LOC441868*		
5	***ACP7***		
6	*PPP2R5B*		
7	***PLPP3***		
8	*PDXP*		
9	*PPP1R11*		
10	*FIG4*		
11	*ENTPD3*		
12	*PPP1R16B*		
13	*INPP5A*		
14	*PTPRA*		
15	*PPP1R14A*		
16	*ACYP1*		

List 4 **Hits that led to gain of Akt activity**.

Rank	Screen 1	Screen 2	Screen 3
1	***INPPL1***	*PPP1R3A*	*PTPRC*
2	*PPP2CB*		*ATP6V0E1*
3	*PPP2R1A*		***INPPL1***
4	*DUSP2*		
5	*ANP32A*		

Phosphatases are crucial regulators of cell signaling dynamics. We identified relevant phosphatases that contribute to each three oncogenic signaling paradigms. We focused not only on phosphatase KDs that led to a loss of ERK/Akt activities, but also to an upshoot of ERK/Akt activities, as phosphatases are better known as negative regulators of phosphorylation events. To add some context, compared to the 518 kinases found in the human genome, grouped in 90 tyrosine (Tyr) kinases and 428 serine/threonine (Ser/Thr) kinases, there are 107 putative protein Tyr phosphatases (PTPs) and only around 30 protein Ser/Thr phosphatases (PSPs). Thus, PSPs are over 10 times fewer than Ser/Thr kinases. However, PSPs holoenzymes are formed by the combination of a shared catalytic subunit and a large number of regulatory subunits[77]. PSPs are further divided in three major families: phosphoprotein phosphatases (PPPs), metal-dependent protein phosphatases (PPMs), and the aspartate-based phosphatases (FCP/SCP). Representative PPPs are PP1, PP2A, PP2B (known as calcineurin), PP4, PP5, PP6, and PP7. Both genes of catalytic and regulatory subunits occur among the hits that we found in our RNA screens.

Figure 10 depicts a visual overview of the hits that we found and the robustness of the phenotype across different siRNAs and replicates for screen 1 and screen 2. Differently from our kinome screens, phosphatome screens 1 and 2 were performed in triplicates, so that the criteria for hit selection was the observed phenotype in at least 2 out of 3 replicates for each one of the three siRNAs of a specific gene. Hence, a third replicate of an siRNA that did not cross the threshold for hit selection is visible in this figure. As for the kinome RNAi screens, we again found that ERK network is built to be robust against perturbations, in particular to perturbations that lead to loss of ERK activity. We identified only *PPA1* for BRAF[V600E] line, *DUSP13* and *DUSP5* for BRAF[V600E]/NRAS[Q61K] line (List 1). ERK activity is self-limiting by the rapid ERK-mediated negative feedbacks and the delayed induction of dual specificity MAP kinase phosphatases (MKP2/DUSPs). In contrast with our findings, it has been shown that *DUSP5* deletion causes BRAF[V600E]-mediated ERK hyperactivation[78]. To explain that, DUSP5 has been shown to inactivate and anchor ERK in the nucleus, but to paradoxically increase cytoplasmic ERK activity. We speculate that the additional NRAS[Q61K] mutation adds an oncogene-specific role for DUSP5 in controlling ERK signaling. PPA1 and DUSP13 have not been sufficiently studied with respect to their interaction with the MAPK-ERK pathway.

ERK activity upshoot is a phenotype that we identified in phosphatome screens and that underscores the incomplete, yet sustained, baseline ERK activity in our melanoma cell

lines. ERK activity upshoot was observed with *PPP2CA* and *PPP2R2A* KDs (List 2), encoding for the catalytic and a regulatory subunit of PP2A respectively, in starved BRAF^{V600E} and BRAF^{V600E}/NRAS^{Q61K} cells. PP2A is a known negative regulator of ERK signaling[79], and therefore the KDs we identified might be considered as control genes. Strikingly, *PPP6C*, that encodes for the catalytic subunit of PP6, was the only gene identified in dabrafenib-treated BRAF^{V600E} cells, a finding that suggests that PP6C negatively regulates ERK pathway downstream of BRAF. Very recently, PPP6C has been indeed shown to dephosphorylate MEK and to sensitize melanoma cells to MEK inhibitors, while loss of PPP6C caused ERK hyperactivation in cells harboring BRAF and RAS mutations[80]. Moreover, *PPP6C* was identified as a recurrently mutated gene in whole-exome sequencing studies in melanoma[16].

We then identified the very interesting case of *FIG4* KD, that led to loss of Akt activity but upshoot of ERK activity in BRAF^{V600E} line. This finding is unreported in literature. FIG4 is a poly-phosphoinositide phosphatase that dephosphorylate PI3,5P$_2$ to PI3P and then to PI. AKT activity loss might me therefore explained by impaired PI3K activation at the membrane, although implications for ERK activity can be only speculative. Of note, *G6PC* KD led to the most prominent Akt activity loss in BRAF^{V600E} line, a finding that corroborate how nutrient metabolism modulates Akt activity in cells, similarly to the *NAGK* KD in kinome screens that also led to a very robust inhibition of Akt output. Finally, we observed that BRAF^{V600E}/NRAS^{Q61K} cells displayed a very high robustness of Akt network against genetic perturbations, possibly due to the activating NRAS^{Q61K} mutation. However, in the kinome screens many hits led to loss of Akt activity. We hypothesize that the broad substrate specificity of phosphatases is associated with redundancy of functions and thus the KD of one phosphatase can be partially compensated by other phosphatases.

In summary, we applied a systemic approach to identify crosstalks between phosphatases activities and ERK/Akt nerworks. Unfortunately, research on regulation of phosphatases is slowed down by the absence of specific small molecule inhibitors coupled with the broad substrate specificity of many phosphatases. However, the future looks brighter as at least six phosphatase inhibitors are now in the clinic, and allosteric drug discovery looks on track to change the stigma of undruggability of phosphatases[81].
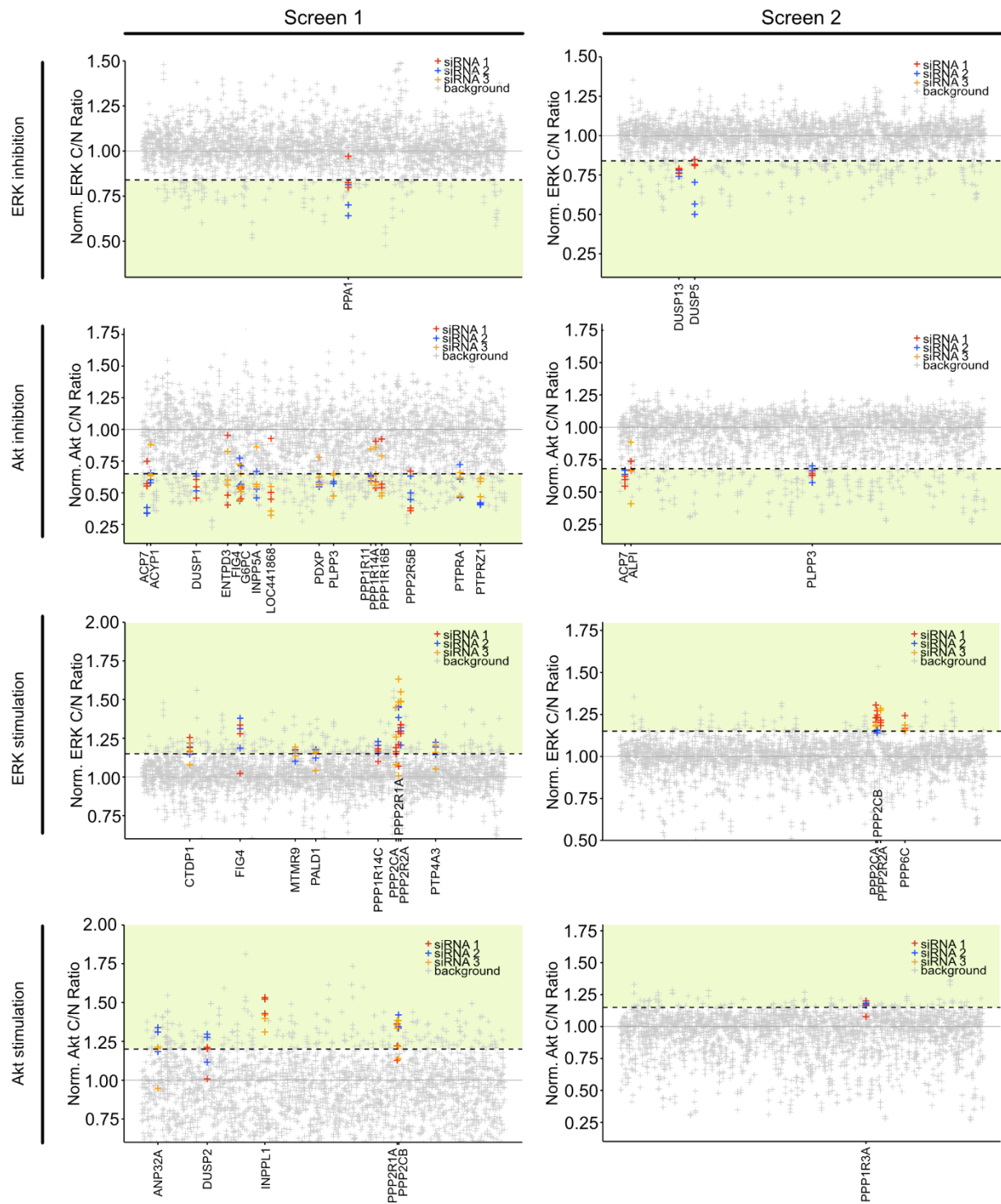
Figure 10 Overview of phosphatome RNAi screens on BRAF^{V600E} cells and BRAF^{V600E}/NRAS^{Q61K} cells. Scatterplots that show the effect of the hits identified in screen 1 (left) and screen 2 (right) for four phenotypes of interest: ERK activity downregulation/upregulation, Akt activity downregulation/upregulation. X-axis is the list of all the phosphatase genes sorted in alphabetical order. X-axis labels are present only for gene hits. Y-axis shows the magnitude of the effect on ERK/Akt activities as reported by normalized C/N ratios per plate. Red, blue, and orange crosses correspond to the first, second and third siRNA of a particular gene. Highlighted are siRNAs that showed the desired phenotype in at least two out of three replicates. Grey crosses correspond to the siRNAs that do not display the desired phenotype. Green area indicates the phenotype space beyond the threshold.

6.Discussion

In this project, I aimed to provide new insights into the pathological signaling network states that regulate genetic and non-genetic drug resistance in primary patient-derived melanoma cells. As more and more studies demonstrated that signal transduction dynamics encode information and might determine cell fates in single cells, and even survival in melanoma cells, we tackled the challenge to investigate how aberrant oncogenic signaling fuels resistance in our short-term (dabrafenib-treated BRAF[V600E] cells), and genetic (BRAF[V600E]/NRAS[Q61K] cells) drug resistance cell systems. It has been previously shown that pulsatile ERK activity in single cells appear within hours of a BRAF[V600E] inhibition regimen, and that this drives tumor drug resistance, both in cell cultures[82] and in organoid models from tumor samples[56]. However, this is possibly the first study that shows how Akt signaling in single cells promotes non-genetic and genetic drug-resistance in two relevant low-passage primary melanoma cell lines that have been successfully isolated from native biopsies and that have been extensively characterized by exome-sequencing and verified to harbor relevant mutations[83]. We also carried for the first time high-throughput kinome- and phosphatome-wide RNAi screens that looked systemically and simultaneously at the interactions with both ERK and Akt oncogenic activities.

6.1 Technical considerations and limitations of the thesis

The possibility to exploit fluorescent biosensors to track ERK and Akt activities in thousands of individual cells comes with a cost. Tracking cells over prolonged time still remains a difficult task also in 2D cell cultures, as events such as mitosis, apoptosis due to drug treatments, cell movement trajectories that overlap, cells moving in and out of the field-of-views, phototoxicity, represent a considerable challenge to track individual cells. In this study, we generally limited our time-lapse acquisition to less than 30 hours, and we never exceeded a confluency of the cells beyond 70% in the acquired field-of-views to facilitate tracking. Even in these conditions, the state-of-the-art high-throughput technology in the lab was limited by the semi-automatic use of multiple software that required constant manual training to achieve optimal segmentations of nuclei in living and moving cells, and by the extensive post-processing quality control of the extracted trajectories. Streamlining the process into a single automatic pipeline that is robust enough to minimize user-input and that tackles the challenge of confluency of cells and cell fate detection remains an unsolved issue in time-lapse technology. Such a pipeline

might open a new era in time-lapse imaging to explore rare signaling phenotypes that might appear under prolonged drug treatment in confluent settings.

BRAF^{V600E} inhibition led to pulsatile reactivation of MAPK/ERK pathway in cell systems that were completely confluent in 2D, or in systems that were in 3D and *in vivo*. In the timespan of our acquisitions, we did not observe pulsatile ERK activity and in general a significant rebound of ERK activity. We hypothesize that growing cells at confluency enables mechanisms of drug resistance that remained undetected in our cell systems. Instead, we observed oncogenic Akt activities that were associated with enhanced survival. However, we relied on classical readouts for survival, i.e. 72 hours viability assays evaluated at the population level. Tracking cells in time-lapse microscopy for 72 hours would rather provide an explicit correlation between oncogenic signaling and cell fate decision (apoptosis, mitosis). Moreover, in the time constraints of this study, a systematic cell-cycle analysis was not performed. Ideally, cell lines expressing the ERK- and Akt-KTRs biosensors, a nuclear marker, and a cell cycle marker such as geminin, might provide direct correlations between ERK/Akt activities, cell-cycle stage, and, with the possibility of tracking cells and cell fates for 72 hours, also to cell death and proliferation. Our findings on the role of sustained Akt activity in non-genetic and genetic drug resistance still needs to be validated on additional primary cell lines. However, suitability of cell lines to imaging might represent an issue. Not shown, additional primary melanoma cell lines tested in the lab did not suit criteria for robust imaging. In general, these cell lines had very elongated and thin morphologies and displayed the tendency to grow in confluent clusters with cells organized in multiple overlapping layers, which would make robust quantification of cytosolic and nuclear KTR (but also immunostaining) intensities really challenging.

Finally, our model systems come from different patients with different genetic substrate beyond the secondary activating NRAS^{Q61K} mutation. If this diversity underscores relevant tumor biology, it also prevents to isolate the effect of the NRAS mutation. For example, BRAF^{V600E}/NRAS^{Q61K} cells showed enhanced survival upon BRAF^{V600E} inhibition compared to BRAF^{V600E} cells, and we showed that sustained Akt activity in the former line fuels this resistance. Whether this resistance stems exclusively from the signaling influenced by the additional NRAS mutation is speculative, we rather think that NRAS^{Q61K} is a fundamental genetic factor in drug resistance that led to multiple phenotypic adaptations that together promoted survival in the treated patient. Reverting

the NRAS^{Q61K} mutation to its wildtype form might provide additional insights into its specific role in genetic drug resistance, but this involves many genetic manipulations that require time and that might introduce artifacts in low-passage patient-derived cells. As a second example, we showed with kinome screens that MAPK network displays robustness against genetic perturbations in BRAF^{V600E} cells, as only 6 kinase KDs led to loss of ERK activity, and that, in marked contrast, BRAF^{V600E}/NRAS^{Q61K} cells were more sensitive to perturbations (24 hits). We argue that the NRAS^{Q61K} mutation restores some signaling inputs and crosstalks to the MAPK cascade, making it more sensitive to perturbations. This result needs to be further validated in additional BRAF mutated and BRAF/NRAS double mutated cell lines to exclude cell line-specific causes.

6.2 Mechanisms of non-genetic and genetic drug resistance

We showed that BRAF^{V600E} cells display heterogeneous single-cell Akt activity states that fluctuate on timescales of hours, which then switch to sustained Akt activity upon BRAF^{V600E} inhibition with dabrafenib on a timescale of 6-24 hours. In BRAF^{V600E}/NRAS^{Q61K} cells, Akt activity is sustained both in presence and absence of dabrafenib. PI3K-mediated activation of Akt can be elicited by three main players: RTKs-mediated inputs, GPCRs-mediated inputs, and from RAS GTPases activity (Figure 11). In BRAF^{V600E} cells, we reasoned that BRAF^{V600E} inhibition with dabrafenib resulted in the relief of profound ERK-mediated upstream negative feedbacks to RTKs, which in turn led to RTKs-induced activation of RAS[48]. In this setting, we speculate that active RAS plays the same role in both cell lines: promoting a sustained Akt activation that enhances survival. The same mechanisms in both non-genetic and genetic drug resistance underscores the striking plasticity of oncogenic signaling in melanoma cells and the important role that PI3K/Akt pathway plays in promoting drug resistant states. Of importance, a major difference between the two cell lines comes from the mechanism of RAS activation. If in one case we speculate that is due to the activating NRAS mutation, in BRAF^{V600E} cells is thought to be RTKs-mediated. However, which ligand(s) induces RTK activity is unknown. Experiments were carried on starvation medium, which indicates that the ligand might be secreted by the cells. Many studies showed that secreted ligands from fibroblasts and macrophages of the tumor microenvironment can induce RTKs activity and mediate drug resistance in melanoma cells[84,85]. Melanoma cells were also shown to secrete factors in response to BRAF or MEK inhibition, such as FGF1, that stimulate fibroblasts to secrete HGF, which in turn leads to RTKs signaling in melanoma[86].

Some studies provided evidence for therapy-induced secretomes that promote drug resistance in isolated melanoma cell lines. Here, BRAF inhibition led to downregulation of the transcription factor Fra1, an effector of ERK, that in turn led to a complex network of secreted signals able to hyperactivate several signaling pathways, most prominently the Akt pathway[87]. Hence, testing the effect of several RTK inhibitors (e.g. ErbBi, FGFRi, METi) on dabrafenib treated BRAF^{V600E} cells might partially elucidate the role of RTKs in the observed Akt upshoot.

It is further unclear what causes heterogeneous single-cell Akt activity states that fluctuate on timescales of hours in BRAF^{V600E} cells. Kinome screens revealed an extended network of kinases that sustain Akt activity in both cell lines. Among these kinases, AXL and VEGFR3 receptor tyrosine kinases KDs led to loss of Akt activity in BRAF^{V600E} cells, and KD of kinases involved in nutrient sensing and cell motility downregulated Akt output in both cell lines. As exposed in the manuscript Discussion section, we think that this heterogeneous Akt activity might be explained by cellular motility cues and metabolic cues to PI3K/Akt pathway. The tight connection of the PI3K/Akt network with cellular motility is well documented in literature and is corroborated by the Akt-dependent high motility of BRAF^{V600E}/NRAS^{Q61K} cells. Importantly, Figure 11 highlights how Akt pathway can be activated by at least three independent mechanisms, and a clear distinction between the contribution of each mechanisms remains elusive. In fact, even in BRAF^{V600E}/NRAS^{Q61K} cells, which carry an activating *NRAS* mutation, several kinase KDs upstream of PI3K led to loss of Akt activity (the receptors *NTRK3*, *PLXNA1*, *DDR2*, *KDR*).
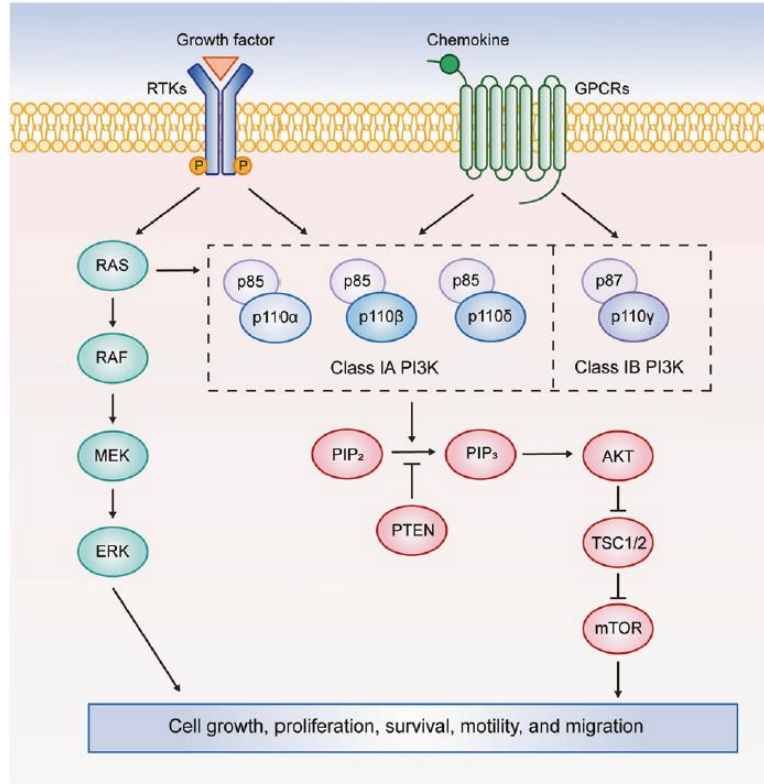
Figure 11 **Activation of the PI3K/AKT/mTOR signaling pathway.** Class IA PI3Ks can be activated by RTKs, GPCRs, RAS and other adapter proteins, while class IB PI3K is exclusively activated by GPCRs. Activated PI3/Akt signaling promotes growth, survival, motility, and migration. (Sun and Meng, 2020)[88]

6.3 Open questions and outlook

Over the last years, pioneering studies opened the era of single-cell quantifications of signaling dynamics into the field of cancer biology. Nowadays, population-averaged assays are still the gold-standard techniques, but the increasingly recognized role of signaling dynamics in encoding the specification of cell fates promises to bring single-cell technologies at the core of cancer research. If single-cell omic techniques are already established in cancer research, techniques to investigate single-cell signaling suffer from the high technological burden that they require, and the know-how needed to mine meaningful data from very large datasets. This work brings recent progresses on single-cell technologies for the quantification of cell signaling, with the simultaneous

quantification of the two most important signaling pathways in melanoma: MAPK/ERK and PI3K/Akt pathways.

While we document oncogenic signaling states in our non-genetic and genetic drug resistance 2D model systems, drivers of resistance in a tumor *in vivo* might significantly differ. We observed very robust oncogenic states that occurred across the entire population of monoclonal cells, but melanoma tumors are vastly heterogeneous. What we observed in our cells might not be the elective mechanism of resistance in other BRAF^{V600E} and BRAF^{V600E}/NRAS^{Q61K} subpopulation of cells within even the same tumor. It is therefore of crucial importance to identify novel drug targets that can help the fight against tumor heterogeneity. We provided our small contribution in the identification of possible kinases that might sustain oncogenic signaling with an innovative RNAi screening. However, validation of our hits as candidate drug targets needs to be formally proven with rescue of knockdown phenotypes in 2D, and experiments *in vivo*.

Moreover, despite the recognized importance of kinases, about 50% of kinases are largely uncharacterized and many of them have completely unknown function[89]. The availability of a broader panel of kinase inhibitors with high specificity is a forced step to validate drug targets in pre-clinical research. Progresses were made in the development of isoform specific drugs (e.g. PI3Ki) or even mutation-specific drugs (EGFRi, BRAFi, KRASi). In the future, such drugs might lead to a deeper understanding of cancer biology and to highly targeted therapies.

In summary, we provided a rationale for the investigation of selected signaling pathways that might sustain oncogenic activities (such as PLK4 and PAK3 networks interacting via direct crosstalks with Akt network), and the integration of single-cell signaling and omic data might promote a more holistic comprehension of drug-induced kinome remodeling in pathological signaling states.

7.References

1. Ferlay, J. *et al.* Cancer incidence and mortality patterns in Europe: Estimates for 40 countries in 2012. *European Journal of Cancer* **49**, 1374–1403 (2013).

2. Minini, R., Rohrmann, S., Braun, R., Korol, D. & Dehler, S. Incidence trends and clinical–pathological characteristics of invasive cutaneous melanoma from 1980 to 2010 in the Canton of Zurich, Switzerland. *Melanoma Research* **27**, 145–151 (2017).

3. Kinderkrebsregister, S. Current situation and developments. 144.

4. Cancer Facts & Figures 2021. 72 (1930).

5. Markovic et al. - Malignant Melanoma in the 21st Century, Part 1 Ep.pdf.

6. Markovic, S. N. *et al.* Malignant Melanoma in the 21st Century, Part 1: Epidemiology, Risk Factors, Screening, Prevention, and Diagnosis. *Mayo Clin Proc.* 18.

7. Lazovich, D. *et al.* Association Between Indoor Tanning and Melanoma in Younger Men and Women. *JAMA Dermatol* **152**, 268 (2016).

8. Rastrelli, M., Tropea, S., Rossi, C. R. & Alaibac, M. Melanoma: Epidemiology, Risk Factors, Pathogenesis, Diagnosis and Classification. *in vivo* 7 (2014).

9. Bevona, C. Cutaneous Melanomas Associated With Nevi. *Arch Dermatol* **139**, 1620 (2003).

10. Olsen, C. M., Carroll, H. J. & Whiteman, D. C. Estimating the Attributable Fraction for Cancer: A Meta-analysis of Nevi and Melanoma. *Cancer Prev Res* **3**, 233–245 (2010).

11. Goldstein, A. M. *et al.* High-risk Melanoma Susceptibility Genes and Pancreatic Cancer, Neural System Tumors, and Uveal Melanoma across GenoMEL. *Cancer Res* **66**, 9818–9828 (2006).

12. Tsao, H. & Niendorf, K. Genetic testing in hereditary melanoma. *Journal of the American Academy of Dermatology* **51**, 803–808 (2004).

13. Titus-Ernstoff, L. *et al.* Pigmentary characteristics and moles in relation to melanoma risk. *Int. J. Cancer* **116**, 144–149 (2005).

14. Davies, H. *et al.* Mutations of the BRAF gene in human cancer. *Nature* **417**, 949–954 (2002).

15. Milagre, C. *et al.* A Mouse Model of Melanoma Driven by Oncogenic KRAS. *Cancer Res* **70**, 5549–5557 (2010).

16. Akbani, R. *et al.* Genomic Classification of Cutaneous Melanoma. *Cell* **161**, 1681–1696 (2015).

17. Bernards, A. & Settleman, J. GAPs in growth factor signalling. *Growth Factors* **23**, 143–149 (2005).

18. Davis, E. J., Johnson, D. B., Sosman, J. A. & Chandra, S. Melanoma: What do all the mutations mean?: Mutations in Melanoma. *Cancer* **124**, 3490–3499 (2018).

19. Dankort, D. *et al.* BrafV600E cooperates with Pten loss to induce metastatic melanoma. *Nat Genet* **41**, 544–552 (2009).

20. Ming, M. & He, Y.-Y. PTEN: New Insights into Its Regulation and Function in Skin Cancer. *Journal of Investigative Dermatology* **129**, 2109–2112 (2009).

21. Kuryk, L. *et al.* From Conventional Therapies to Immunotherapy: Melanoma Treatment in Review. *Cancers* **12**, 3057 (2020).

22. Rebecca, V. W., Sondak, V. K. & Smalley, K. S. M. A brief history of melanoma: from mummies to mutations. *Melanoma Research* **22**, 114–122 (2012).

23. Ascierto, P. A. *et al.* Update on tolerability and overall survival in COLUMBUS: landmark analysis of a randomised phase 3 trial of encorafenib plus binimetinib vs vemurafenib or encorafenib in patients with BRAF V600–mutant melanoma. *European Journal of Cancer* **126**, 33–44 (2020).

24. Wang, L. *et al.* An Acquired Vulnerability of Drug-Resistant Melanoma with Therapeutic Potential. *Cell* **173**, 1413-1425.e14 (2018).

25. Du, Z. & Lovly, C. M. Mechanisms of receptor tyrosine kinase activation in cancer. *Mol Cancer* **17**, 58 (2018).

26. Chiasson-MacKenzie, C. & McClatchey, A. I. Cell–Cell Contact and Receptor Tyrosine Kinase Signaling. *Cold Spring Harb Perspect Biol* **10**, a029215 (2018).

27. Plotnikov, A., Zehorai, E., Procaccia, S. & Seger, R. The MAPK cascades: Signaling components, nuclear roles and mechanisms of nuclear translocation. *Biochimica et Biophysica Acta (BBA) - Molecular Cell Research* **1813**, 1619–1633 (2011).

28. Pearson, G. *et al.* Mitogen-Activated Protein (MAP) Kinase Pathways: Regulation and Physiological Functions. **22**, 31 (2001).

29. Lavoie, H., Gagnon, J. & Therrien, M. ERK signalling: a master regulator of cell behaviour, life and fate. *Nat Rev Mol Cell Biol* (2020) doi:10.1038/s41580-020-0255-7.

30. Yoon, S. & Seger, R. The extracellular signal-regulated kinase: Multiple substrates regulate diverse cellular functions. *Growth Factors* **24**, 21–44 (2006).

31. Hübner, A., Barrett, T., Flavell, R. A. & Davis, R. J. Multisite Phosphorylation Regulates Bim Stability and Apoptotic Activity. *Molecular Cell* **30**, 415–425 (2008).

32. Treisman, R. Regulation of transcription by MAP kinase cascades. *Current Opinion in Cell Biology* **8**, 205–215 (1996).

33. Murphy, L. O., MacKeigan, J. P. & Blenis, J. A Network of Immediate Early Gene Products Propagates Subtle Differences in Mitogen-Activated Protein Kinase Signal Amplitude and Duration. *Mol Cell Biol* **24**, 144–153 (2004).

34. Manning, B. D. & Cantley, L. C. AKT/PKB Signaling: Navigating Downstream. *Cell* **129**, 1261–1274 (2007).

35. Arozarena, I. & Wellbrock, C. Overcoming resistance to BRAF inhibitors. *Ann. Transl. Med.* **5**, 387–387 (2017).

36. Shi, H. *et al.* Acquired Resistance and Clonal Evolution in Melanoma during BRAF Inhibitor Therapy. *Cancer Discovery* **4**, 80–93 (2014).

37. Allen, E. M. V. *et al.* The Genetic Landscape of Clinical Resistance to RAF Inhibition in Metastatic Melanoma. 17.

38. Manning, B. D. & Toker, A. AKT/PKB Signaling: Navigating the Network. *Cell* **169**, 381–405 (2017).

39. Fruman, D. A. *et al.* The PI3K Pathway in Human Disease. *Cell* **170**, 605–635 (2017).

40. Sarbassov, D. D. Phosphorylation and Regulation of Akt/PKB by the Rictor-mTOR Complex. *Science* **307**, 1098–1101 (2005).

41. Levine, J. H., Lin, Y. & Elowitz, M. B. Functional Roles of Pulsing in Genetic Circuits. *Science* **342**, 1193–1200 (2013).

42. Lake, D., Corrêa, S. A. L. & Müller, J. Negative feedback regulation of the ERK1/2 MAPK pathway. *Cell. Mol. Life Sci.* **73**, 4397–4413 (2016).

43. Sagner, A. & Briscoe, J. Morphogen interpretation: concentration, time, competence, and signaling dynamics: Morphogen interpretation. *WIREs Dev Biol* **6**, e271 (2017).

44. Day, E. K., Sosale, N. G. & Lazzara, M. J. Cell signaling regulation by protein phosphorylation: a multivariate, heterogeneous, and context-dependent process. *Current Opinion in Biotechnology* **40**, 185–192 (2016).

45. Shain, A. H. *et al.* The Genetic Evolution of Melanoma from Precursor Lesions. *N Engl J Med* **373**, 1926–1936 (2015).

46. Avruch, J. Ras Activation of the Raf Kinase: Tyrosine Kinase Recruitment of the MAP Kinase Cascade. *Recent Progress in Hormone Research* **56**, 127–156 (2001).

47. Berk-Krauss, J., Stein, J. A., Weber, J., Polsky, D. & Geller, A. C. New Systematic Therapies and Trends in Cutaneous Melanoma Deaths Among US Whites, 1986–2016. *Am J Public Health* **110**, 731–733 (2020).

48. Lito, P. *et al.* Relief of Profound Feedback Inhibition of Mitogenic Signaling by RAF Inhibitors Attenuates Their Activity in BRAFV600E Melanomas. *Cancer Cell* **22**, 668–682 (2012).

49. Montagut, C. *et al.* Elevated CRAF as a Potential Mechanism of Acquired Resistance to BRAF Inhibition in Melanoma. *Cancer Res* **68**, 4853–4861 (2008).

50. Villanueva, J. *et al.* Acquired Resistance to BRAF Inhibitors Mediated by a RAF Kinase Switch in Melanoma Can Be Overcome by Cotargeting MEK and IGF-1R/PI3K. *Cancer Cell* **18**, 683–695 (2010).

51. Yen, I. *et al.* ARAF mutations confer resistance to the RAF inhibitor belvarafenib in melanoma. *Nature* **594**, 418–423 (2021).

52. Gerosa, L. *et al.* Receptor-Driven ERK Pulses Reconfigure MAPK Signaling and Enable Persistence of Drug-Adapted BRAF-Mutant Melanoma Cells. *Cell Systems* S2405471220303707 (2020) doi:10.1016/j.cels.2020.10.002.

53. Straussman, R. *et al.* Tumour micro-environment elicits innate resistance to RAF inhibitors through HGF secretion. *Nature* **487**, 500–504 (2012).

54. Fedorenko, I. V., Wargo, J. A., Flaherty, K. T., Messina, J. L. & Smalley, K. S. M. BRAF Inhibition Generates a Host–Tumor Niche that Mediates Therapeutic Escape. *Journal of Investigative Dermatology* **135**, 3115–3124 (2015).

55. Wang, T. *et al.* BRAF Inhibition Stimulates Melanoma-Associated Macrophages to Drive Tumor Growth. *Clin Cancer Res* **21**, 1652–1664 (2015).

56. Hirata, E. *et al.* Intravital Imaging Reveals How BRAF Inhibition Generates Drug-Tolerant Microenvironments with High Integrin β1/FAK Signaling. *Cancer Cell* **27**, 574–588 (2015).

57. Levy, C., Khaled, M. & Fisher, D. E. MITF: master regulator of melanocyte development and melanoma oncogene. *Trends in Molecular Medicine* **12**, 406–414 (2006).

58. Ferrao, P. T. Phenotype switching in melanoma: implications for progression and therapy. *Frontiers in Oncology* 7.

59. Dummer, R. & Flaherty, K. T. Resistance patterns with tyrosine kinase inhibitors in melanoma: new insights. *Current Opinion in Oncology* **24**, 150–154 (2012).

60. Bai, X., Fisher, D. E. & Flaherty, K. T. Cell-state dynamics and therapeutic resistance in melanoma from the perspective of MITF and IFNγ pathways. *Nat Rev Clin Oncol* **16**, 549–562 (2019).

61. Grzywa, T. M., Paskal, W. & Włodarski, P. K. Intratumor and Intertumor Heterogeneity in Melanoma. *Translational Oncology* **10**, 956–975 (2017).

62. Villanueva, J. *et al.* Acquired Resistance to BRAF Inhibitors Mediated by a RAF Kinase Switch in Melanoma Can Be Overcome by Cotargeting MEK and IGF-1R/PI3K. *Cancer Cell* **18**, 683–695 (2010).

63. Irvine, M. *et al.* Oncogenic PI3K/AKT promotes the step-wise evolution of combination BRAF/MEK inhibitor resistance in melanoma. *Oncogenesis* **7**, 72 (2018).

64. Caporali, S. *et al.* Targeting the PI3K/AKT/mTOR pathway overcomes the stimulating effect of dabrafenib on the invasive behavior of melanoma cells with acquired resistance to the BRAF inhibitor. *International Journal of Oncology* **49**, 1164–1174 (2016).

65. Johannessen, C. M. *et al.* COT drives resistance to RAF inhibition through MAP kinase pathway reactivation. *Nature* **468**, 968–972 (2010).

66. Amaral, T. *et al.* The mitogen-activated protein kinase pathway in melanoma part I – Activation and primary resistance mechanisms to BRAF inhibition. *European Journal of Cancer* **73**, 85–92 (2017).

67. Ryu, H. *et al.* Frequency modulation of ERK activation dynamics rewires cell fate. *Mol Syst Biol* **11**, 838 (2015).

68. Rosenbloom, A. B. *et al.* β-Catenin signaling dynamics regulate cell fate in differentiating neural stem cells. *Proc Natl Acad Sci USA* **117**, 28828–28837 (2020).

69. Harvey, C. D. *et al.* A genetically encoded fluorescent sensor of ERK activity. *Proceedings of the National Academy of Sciences* **105**, 19264–19269 (2008).

70. Ryu, H. *et al.* Integrated Platform for Monitoring Single-cell MAPK Kinetics in Computer-controlled Temporal Stimulations. *Sci Rep* **8**, 11126 (2018).

71. Regot, S., Hughey, J. J., Bajar, B. T., Carrasco, S. & Covert, M. W. High-Sensitivity Measurements of Multiple Kinase Activities in Live Single Cells. *Cell* **157**, 1724–1734 (2014).

72. Regot, S., Hughey, J. J., Bajar, B. T., Carrasco, S. & Covert, M. W. High-Sensitivity Measurements of Multiple Kinase Activities in Live Single Cells. *Cell* **157**, 1724–1734 (2014).

73. Maryu, G., Matsuda, M. & Aoki, K. Multiplexed Fluorescence Imaging of ERK and Akt Activities and Cell-cycle Progression. *Cell Struct. Funct.* **41**, 81–92 (2016).

74. Kudo, T. *et al.* Live-cell measurements of kinase activity in single cells using translocation reporters. *Nat Protoc* **13**, 155–169 (2018).

75. Maryu, G. *et al.* Live-cell Imaging with Genetically Encoded Protein Kinase Activity Reporters. *Cell Struct. Funct.* **43**, 61–74 (2018).

76. Nguyen, L. K., Matallanas, D., Croucher, D. R., von Kriegsheim, A. & Kholodenko, B. N. Signalling by protein phosphatases and drug development: a systems-centred view: Phosphatases and drug development: a systems-centred view. *FEBS Journal* **280**, 751–765 (2013).

77. Shi, Y. Serine/Threonine Phosphatases: Mechanism through Structure. *Cell* **139**, 468–484 (2009).

78. Kidger, A. M. *et al.* Dual-specificity phosphatase 5 controls the localized inhibition, propagation, and transforming potential of ERK signaling. *Proc Natl Acad Sci USA* **114**, E317–E326 (2017).

79. Yu, L.-G., Packman, L. C., Weldon, M., Hamlett, J. & Rhodes, J. M. Protein Phosphatase 2A, a Negative Regulator of the ERK Signaling Pathway, Is Activated by Tyrosine Phosphorylation of Putative HLA Class II-associated Protein I (PHAPI)/pp32 in Response to the Antiproliferative Lectin, Jacalin. *Journal of Biological Chemistry* **279**, 41377–41383 (2004).

80. Cho, E., Lou, H. J., Kuruvilla, L., Calderwood, D. A. & Turk, B. E. PPP6C negatively regulates oncogenic ERK signaling through dephosphorylation of MEK. *Cell Reports* **34**, 108928 (2021).

81. Mullard, A. Phosphatases start shedding their stigma of undruggability. *Nat Rev Drug Discov* **17**, 847–849 (2018).

82. Gerosa, L. *et al. Sporadic ERK pulses drive non-genetic resistance in drug-adapted BRAF* ^{V600E} *melanoma cells*. http://biorxiv.org/lookup/doi/10.1101/762294 (2019) doi:10.1101/762294.

83. Raaijmakers, M. I. G. *et al.* A new live-cell biobank workflow efficiently recovers heterogeneous melanoma cells from native biopsies. *Exp Dermatol* **24**, 377–380 (2015).

84. Almeida, F. V., Douglass, S. M., Fane, M. E. & Weeraratna, A. T. Bad company: Microenvironmentally mediated resistance to targeted therapy in melanoma. *Pigment Cell Melanoma Res* **32**, 237–247 (2019).

85. Straussman, R. *et al.* Tumour micro-environment elicits innate resistance to RAF inhibitors through HGF secretion. *Nature* **487**, 500–504 (2012).

86. Grimm, J. *et al.* BRAF inhibition causes resilience of melanoma cell lines by inducing the secretion of FGF1. *Oncogenesis* **7**, 71 (2018).

87. Obenauf, A. C. *et al.* Therapy-induced tumour secretomes promote resistance and tumour progression. *Nature* **520**, 368–372 (2015).

88. Sun, P. & Meng, L. Emerging roles of class I PI3K inhibitors in modulating tumor microenvironment and immunity. *Acta Pharmacol Sin* **41**, 1395–1402 (2020).

89. Fedorov, O., Müller, S. & Knapp, S. The (un)targeted cancer kinome. *Nat Chem Biol* **6**, 166–169 (2010).

8.Acknowledgements

First, I want to thank Prof. Olivier Pertz for the invaluable opportunity of working in his lab and pursue my PhD studies in an innovative and challenging environment. The support, mentorship, but also lessons learned from him meant a lot for me, and in particular his structured thinking and simple, yet effective, way to approach problems have been inspiring over the years. What I learned from Olivier is not only science-related but is also very transferable and valuable for my future personal development.

I also want to thank the other members of my thesis committee, Prof. Mitchell Levesque, Prof. Mario Tschan and Prof. Curzio Ruegg for the time they invested in my project.

I especially want to thank Dr. Beate "Faba" Neumann of the Advanced Light Microscopy Facility at EMBL (Heidelberg) for the constant support she gave me during my months of work in Germany, and for her always positive attitude that meant a lot for me. Beside Faba, all the other members of the ALMF have been part of my short life abroad and they provided me with a very stimulating environment in a top european institution. This gave me perspective on how research in Europe is a living network that connects amazing researchers and students from all over the world. Sometimes I forgot that aspect throughout my PhD studies.

My thanks also to all the visitor students at ALMF that I had the pleasure to meet; I made new friends and with each one of them I had precious discussions on each other's project. In particular, Vitali Vistunou is now a special connection and friend who shared the office with me and who supported my work with his programming tips and tricks that made my life easier.

I also want to thank all of my colleagues in the lab and at the institute for sharing part of their life with me: your help and support was invaluable! I experienced a stimulating and fun environment that I will never forget. A special mention to Dr. Paolo Gagliardi, who speaks my mother tongue and spent many hours in providing me with conceptual inputs, and Judith Trüb, a real asset of the lab as a lab manager and technician.

9.Curriculum Vitae

Alberto Mattei

Birth date: September 03, 1991

Nationality: Swiss

Address: Weissensteinstrasse 32

3008 Bern, Switzerland

+41 78 610 3749

alberto.mattei@izb.unibe.ch

Education

2016 – 2021:
University of Bern, Institute of Cell Biology, 3012 Bern
PhD in Cell Biology at the graduate School for Cellular and Biomedical Sciences
Dissertation: **Exploring Signaling Mechanisms regulating genetic and non-genetic Drug Resistance in Melanoma** supervised by Prof. Dr. Olivier Pertz

2014 – 2016:
University of Bern, Institute of Cell Biology, 3012 Bern
M.Sc. in Biomedical Sciences
Final Grade: Insigni cum laude (average: 5.5/6 (max)), CSL Behring 3rd prize for best degree
Thesis: **Influence of electrotonic interactions on cardiac action potential propagation** supervised by Prof. Dr. med. Jan Kucera

2011 – 2014:
University of Fribourg, 1600 Fribourg
B.Sc. in Biomedical Sciences
Major in Biomedical sciences 120 ECTS; Minor in Advanced biomedical sciences 30 ECTS; Minor in Applied biomedical sciences 30 ECTS

2006 – 2010:
Maturità Liceo Lugano 2, 6942 Savosa

Publications

Mattei, A., Dobrzyński, M., Neumann, B., Levesque, M.P, Pertz, O. (2021). Exploring Signaling Mechanisms regulating genetic and non-genetic Drug Resistance in Melanoma.
In preparation.

Contributions to meetings and conferences

GCB Symposium 2020. Bern, Switzerland, January 2020. Oral presentation: Signaling mechanisms of non-genetic cancer drug resistance in melanoma.

2nd CORBEL Service Operator and User Meeting. Heidelberg, Germany, October 2019. Oral presentation: Targeting Aberrant ERK/AKT Signaling in Melanoma using genetic and chemical screens.

Declaration of Originality

Last name, first name:

Matriculation number:

I hereby declare that this thesis represents my original work and that I have used no other sources except as noted by citations.

All data, tables, figures and text citations which have been reproduced from any other source, including the internet, have been explicitly acknowledged as such.

I am aware that in case of non-compliance, the Senate is entitled to withdraw the doctorate degree awarded to me on the basis of the present thesis, in accordance with the "Statut der Universität Bern (Universitätsstatut; UniSt)", Art. 69, of 7 June 2011.

Place, date

Signature